DISSERTATION

ELUCIDATING THE MECHANISMS OF VASCULAR DYSFUNCTION IN OBESITY AND TYPE 2 DIABETES: THE ROLE OF THE GUT MICROBIOTA

Submitted by

Dustin Michael Lee

Department of Food Science and Human Nutrition

In partial fulfillment of the requirements

For the Degree of Doctor of Philosophy

Colorado State University

Fort Collins, Colorado

Summer 2019

Doctoral Committee:

Advisor: Christopher L Gentile

Tiffany L Weir
Sarah A Johnson
Adam J Chicco

ABSTRACT

ELUCIDATING THE MECHANISMS OF VASCULAR DYSFUNCTION IN OBESITY AND TYPE 2 DIABETES: THE ROLE OF THE GUT MICROBIOTA

One of the key processes that links both obesity and type 2 diabetes (T2D) to cardiovascular disease (CVD) is the development of vascular dysfunction, characterized by arterial stiffness and endothelial dysfunction. Vascular dysfunction occurs prior to overt CVD, and the development of vascular dysfunction in obesity and T2D strongly predicts future cardiovascular events and mortality. While the mechanisms of vascular dysfunction continue to be fully elucidated, an abundant body of research suggests that the gut microbiota mediate many cardiometabolic diseases. Disturbances to microbial equilibrium, broadly termed gut dysbiosis, have been implicated in numerous metabolic disorders. In a proof of concept study, our lab has previously demonstrated that suppression of gut dysbiosis reverses vascular dysfunction. Thus, further identifying useful and cost effective treatments that beneficially target the gut microbiota in obesity or T2D to prevent or reverse vascular dysfunction remains an important area of research.

The goals of this dissertation research were to 1) examine the underlying causes of vascular dysfunction in models of obesity and T2D and 2) identify novel strategies to prevent or attenuate the development of vascular dysfunction in both obesity and T2D. To investigate the aforementioned, we conducted three separate preclinical studies utilizing a mouse model of T2D, diet-induced obesity, and gut microbiota transplantation. In these studies, we measured aortic pulse wave velocity and endothelium-dependent dilation to examine arterial stiffness and endothelial dysfunction, respectively. Both of these techniques are clinically relevant. We also

employed several biochemical techniques to examine the mechanisms by which obesity and T2D lead to vascular dysfunction in our models.

In the first study (Chapter 2), we explored epidemiological data suggesting that the antidiabetic drug class, sodium glucose cotransporter 2 inhibitors (SGLT2i), have beneficial effects on cardiovascular outcomes. Utilizing a genetic model of T2D to examine the vascular effects of SGLT2i, we found that treatment with dapagliflozin significantly improved both arterial stiffness and endothelial function. These changes were accompanied by decreased circulating inflammation and subtle alterations to the gut microbiota. In the second study (Chapter 3), we examined the effect of a gut microbiota-derived tryptophan metabolite on cardiometabolic outcomes. Mice fed a western diet displayed increased body weight, arterial stiffness and elevated markers of liver inflammation. Supplementation with the tryptophan metabolite, indole-3-propionic acid, had no effect on these outcomes. Finally, in the third study (Chapter 4) we examined whether human gut dysbiosis represents a causal factor in obesity-related vascular dysfunction. Utilizing human fecal samples from lean and obese subjects, we found that mice colonized with an obese gut microbiota displayed endothelial dysfunction independent of body weight changes.

Collectively, these studies provide evidence that 1) SGLT2i-related cardiovascular protection is in part mediated by improvements in vascular dysfunction, 2) gut microbial metabolites have differing effects on host physiology, and 3) the obese human microbiota promotes endothelial dysfunction independent of body weight. Future studies should examine more mechanistic contributions of the gut microbiota that mediate vascular dysfunction in obesity and type 2 diabetes.

DEDICATION

To my wife, Skye, my parents, Terri and Donald, my sister, Allison, my in-laws, Gae and Tom, for their indefatigable support, encouragement, and love. Additionally, to those that have played significant roles as mentors in my professional and academic career.

TABLE OF CONTENTS

CHAPTER 1: INTRODUCTION

Cardiovascular disease (CVD) continues to be the leading cause of death both in the United States (US) and worldwide (16). It is estimated that CVD accounts for approximately 1 in every 3 deaths in the US, which shockingly equates to one death every 38 seconds (16). Although significant advancements in medicine and science have been made, CVD remains a significant health issue both at the cost of lives and healthcare expenses. Deaths and direct costs from CVD are projected to increase such that by 2035, direct costs from CVD will increase to $749 billion (16). Two major and well established risk factors for CVD are obesity and type 2 diabetes (T2D). It is not surprising that the rates of obesity and T2D are also on the rise. Thus, elucidating the mechanisms by which obesity and T2D lead to the development of CVD and identifying cost effective treatments remain a critical component of biomedical research.

Obesity and Type 2 Diabetes Statistics in Relation to Cardiovascular Disease

Obesity, as defined by a body mass index (BMI; kg/m^2) of greater than or equal to 30, has become an epidemic over the past few decades. Starting in 1960, obesity rates in adult men and women have risen from ~10-15% to well over 30% (62). This statistic also plagues children and adolescents whereby roughly one-third of this population is overweight or obese (16, 62). The cost of obesity is also an economic burden given that individuals with obesity paid on average 42% more for health care costs than their normal weight counterparts (59). Furthermore, escalations and progressions in BMI categories (overweight to obese to morbidly obese) increase lifetime risk of CVD mortality (85). Considering the close link between obesity and CVD, this is particularly concerning as the rates of obesity are projected to further increase in the coming years such that by 2030 it is estimated that 51% of the population will be obese (58). While there is a close relationship between obesity and CVD, obesity is also associated with risk of T2D whereby increasing risk of T2D closely mirrors increases in BMI (1).

Statistics from the American Diabetes Association and Centers for Diseases Control and Prevention show that in 2015, 30.3 million Americans or 1 in 10 individuals had diabetes and an estimated 1.5 million Americans are newly diagnosed each year (128). The economic burden of diabetes is estimated at $327 billion dollars per year and similar to obesity, average health care costs for individuals with diabetes were 2.3 times higher than those without diabetes (7). Furthermore, diabetes accounted for 80,058 US deaths in 2016 and is the 7th leading cause of death (128). Strikingly, 84.1 million or 1 in 3 Americans have prediabetes and the prevalence of diabetes is expected to rise by 54% to more than 54.9 million Americans between 2015 and 2030 (139). The aforementioned statistics include both type 1 and type 2 diabetes, although T2D alone accounts for 90-95% of all diabetes cases (139). As previously mentioned, increased BMI is closely and independently related to risk of T2D (64). Additionally, individuals with diabetes are at heightened risk for developing CVD (106) and individuals with T2D are 2-4 times more likely to develop CVD compared to individuals without T2D (107). CVD is estimated to account for at least half of the mortality observed in T2D (52) and risk of CVD increases continually with increases in fasting plasma glucose levels (157).

Two key features linking obesity and T2D to CVD are the development of 1) arterial stiffness (increased pulse wave velocity) and 2) endothelial dysfunction (impaired endothelium-dependent dilation), collectively termed vascular dysfunction (37, 93, 94, 163). Vascular dysfunction observed in obese and T2D individuals precedes overt CVD and is strongly predictive of future cardiovascular events and mortality (116, 182, 185). Taken together, vascular dysfunction is an important target in the prevention of obesity and T2D associated CVD. However, limited treatments exist for the vascular dysfunction observed in obese and T2D individuals and thus, there is an urgent need to identify new novel and cost-effective treatments to enhance quality and duration of life in this ever-growing population.

Vascular Dysfunction: Arterial Stiffness and Endothelial Function

The circulatory system was previously thought of as a passive conduit for the transport of blood to peripheral tissues. Indeed, the circulatory system plays a crucial role in the transport of dissolved gases and other molecules to tissues and organs for nutrition, maintenance, growth, and repair (18). Additional roles of the circulatory system include transporting hormones and neurotransmitters, distributing heat to the surface and peripheral body, and mediating inflammation and defense responses against invading microorganisms (18). However, it is now known and well established that the arterial system plays a significant role in many pathophysiological processes, including the development of CVD (126). Prior to overt CVD, deleterious changes to the vasculature occur characterized by arterial stiffening and endothelial dysfunction, collectively termed vascular dysfunction.

Conduit arteries such as the aorta serve to deliver oxygenated blood from the heart to the periphery. One major role of this centrally located vessel is to provide biomechanical buffering given its elastic properties to oppose the pulsatile nature of cardiac blood flow. During one cardiac cycle, blood leaves the left ventricle in systole during which a compliant aorta expands to accommodate the bolus of blood. In diastole, the expanded aorta then recoils to prevent drops in arterial pressure and buffer the pulsatile flow. A compliant aorta also minimizes pulse pressure. However, arterial stiffening can occur over time as is the case with ageing and various diseases (61, 122, 193). Arterial stiffness is defined as a decrease in compliance of the vasculature and can be measured by the speed at which the pulse wave travels through an artery or, pulse wave velocity (PWV), where a higher PWV is indicative of stiffer arteries. PWV can be measured both in clinical (human) and preclinical (rodent) models and is the gold standard for assessing arterial stiffness. Increased arterial stiffness is observed in obese humans and a linear relationship exists between BMI and PWV (37, 147). Similarly, individuals with T2D also exhibit increased PWV (77, 145) and this arterial stiffening in both obesity and T2D strongly predicts future cardiovascular events and all-cause mortality (182).

Multiple factors can influence the development of arterial stiffness. Both inflammation and oxidative stress can lead to structural and regulatory alterations that ultimately lead to arterial stiffness. One structural change that influences arterial stiffness is the amount or proportion of collagen and elastin, and long-term oxidative stress leads to aortic stiffening through increased collagen deposition and decreased elastin within the vasculature (197). Certain enzymes such lysyl oxidase (LOX) or matrix metalloproteases (MMP) can alter the content of collagen and elastin and thus an appropriate balance of enzyme activity is critical to maintain vascular compliance (110, 133, 181). Along with the increase in PWV observed in individuals with obesity or T2D, deleterious alterations in structure and enzyme (i.e. LOX or MMP) (37, 40, 131) play a critical role in the arterial stiffness observed in these populations. Attenuating oxidative stress reverses collagen deposition and decreases arterial stiffness in rodent models (60). In addition to structural remodeling, alterations in smooth muscle tone can greatly influence arterial stiffness. Endothelial cells produce nitric oxide (NO) which generally leads to vascular smooth muscle cell relaxation. However, in a state of inflammation and oxidative stress such as obesity or T2D, the bioavailability of NO is decreased (197) which can ultimately lead to arterial stiffness.

The vascular endothelium is a single cell monolayer that lines the internal surface of the entire cardiovascular system, including arteries. In addition to serving as a critical barrier between circulating blood and underlying tissues, the endothelium acts as a first responder by modulating vascular tone, permeability, and interacting with circulating molecules to maintain cardiovascular homeostasis (126). A healthy endothelium is capable of quickly responding to perturbations in homeostasis by generally promoting an anti-inflammatory environment, vasodilatory phenotype, anti-coagulation, and suppression of smooth muscle cell proliferation (26, 46). Conversely, a prolonged and sustained disruption in the balance of homeostasis can lead to vascular dysfunction characterized by a pro-inflammatory environment, vasoconstrictive

phenotype, coagulative, and proliferative phenotype (46). One commonly used assessment of endothelial function or dysfunction is the surrogate measurement endothelium-dependent dilation (EDD), whereby impairments in EDD represent endothelial dysfunction. Under certain conditions, this altered phenotype of the endothelium can ultimately lead to CVD.

Broadly, endothelial dysfunction is an imbalance between vasodilatory and vasoconstrictive substances. As with many disease processes, inflammation and oxidative stress play a major role in the development of endothelial dysfunction similar to the aforementioned mechanisms involved in arterial stiffness. Oxidative stress influences functional properties of the endothelium in which endothelium-dependent dilation is improved with the attenuation of oxidative stress (60). This is in part due to improving NO bioavailability, the main vasodilatory compound produced by the endothelial cells (177). NO is primarily derived from endothelial nitric oxide synthase (eNOS) although two additional isoforms exist, inducible NOS and neuronal NOS. While the posttranslational modifications and signaling of eNOS are beyond the scope of this research, both inflammation and oxidative stress can contribute to the uncoupling of eNOS (a shift from the production of NO to more superoxide whereby eNOS is no longer coupled to the formation of NO) leading to reduced NO-bioavailability and impaired endothelial function (36, 86, 132). Additionally, inflammation and oxidative stress as seen in obesity and T2D can reduce the expression of eNOS (47). The aforementioned mechanisms contributing to vascular dysfunction observed in obesity and T2D have been extensively studied, but the upstream or initial sources of this oxidative stress and inflammatory signaling are still unclear.

The Gut Microbiota as a Mediator of Vascular Dysfunction

The gut microbiota consists of commensal bacteria which reside within the intestinal tract and have emerged as critical regulators of host physiology (120). Gut bacterial cells were initially thought to outnumber human cells at a ratio of 10:1 (108) but more recent analyses

suggest this ratio is closer to 1:1 (150). Regardless, this massive number of microbes play a key role in host health and the extent to which these microbes influence disease processes has only begun to emerge. In addition to the impressive number of bacteria residing in the gut, these microbes carry a diverse set of genes roughly 150-fold higher than the number of genes in the human genome (129). This massive repertoire of genes correlates with health status, whereby the richness in genes positively correlates with healthy metabolic status. Indeed, individuals with obesity or T2D have lower bacterial gene richness (42, 96) which can potentially alter the metabolites produced by the gut microbiota (31, 124) and alter host metabolism (136). These detrimental alterations to the gut microbiota, broadly termed gut dysbiosis, have been suggested to drive cardiometabolic diseases (71). A few factors that can affect the composition and function of gut microbes include disease state (i.e. obesity and T2D) as previously mentioned, diet (i.e. western diet), and xenobiotics (i.e. drugs).

One of the major influences on gut microbiota composition and activity is dietary intake, (43) and deleterious changes secondary to a high-fat or Western (high fat, high sugar) diet have been implicated in the development of several cardiometabolic alterations (22). In a seminal paper, Cani et al. showed that obesity related gut dysbiosis in high-fat fed mice leads to “metabolic endotoxemia” responsible for the deleterious metabolic alterations observed in this model (29). In support of this, previous data from our own lab suggests that suppression of gut dysbiosis in western diet-fed mice reverses vascular dysfunction (12). Many dietary components and their subsequent metabolites have been implicated in host health. By cataloging various genes that aid in metabolism of these dietary components, the gut microbiota is capable of producing a diverse set of metabolites that affect the host (31). Exogenous sources from the diet can serve as substrates for the gut microbiota. For example, indoles are metabolites of bacterial tryptophan metabolism and have recently been implicated in numerous physiological roles (3). Another emerging factor effecting gut microbiota composition is xenobiotics and specifically, non-antibiotic drugs (109). For example, the commonly prescribed antidiabetic drug Metformin

has been shown to mediate its effects through the gut microbiota by affecting functional pathways in two different phyla (188). In support of this gut microbiota-mediated mechanism, metformin is more active when consumed orally compared to intravenous delivery (164). As new drugs enter the market (i.e. sodium glucose cotransporter 2 inhibitors), their effects on the gut microbiota or metabolism by the gut microbiota, collectively drug-microbiota interactions, should be characterized.

Given the alterations in the gut microbiota that occur in obesity (102) and T2D (130) and the metabolic disruptions in these disease states, research has begun to focus on the gut microbiota as critical mediators of host health and disease (120). Furthermore, emerging research has identified the gut microbiota to play a central role in obesity-related vascular dysfunction. Two studies published around the same time provided the first evidence that the gut microbiota can mediate endothelial function (83, 178). Vikram et al. demonstrated that microRNA-204 is remotely regulated by the gut microbiota and impairs aortic endothelial function by downregulating Sirtuin 1. Additionally, elimination of gut dysbiosis in a high-fat diet model partially restored endothelial function and rescued NO bioavailability by downregulating microRNA-204 (178). Around the same time, Karbach et al. demonstrated that the gut microbiota is required for angiotensin-II-induced endothelial dysfunction, whereby germfree mice lacking commensal gut microbiota are protected from dysfunction (83). We recently showed that western diet (WD)-induced obesity led to both endothelial dysfunction and aortic stiffness. Suppression of gut dysbiosis in WD-fed mice (12) or older mice (25) reversed vascular dysfunction, suggesting that the gut microbiota are critical regulators of obesity-related vascular dysfunction (13). Unpublished data from our lab utilizing gut microbiota transplants also suggests that the obese gut microbiota can induce arterial stiffness in lean mice. These data from our lab compliment and extend the evidence for the role of the gut microbiota in vascular dysfunction. To the best of our knowledge, we were the first to show that the gut microbiota can

mediate arterial stiffness and our data confirms findings linking the gut microbiota to endothelial function.

Collectively, these studies provide evidence for the critical role of the gut microbiota in mediating obesity and T2D-related pathologies such as vascular dysfunction and provide a foundation for future studies examining the role of the gut microbiota in obesity-related vascular dysfunction. However, published studies have utilized preclinical models to demonstrate the role of the gut microbiota in obesity-related vascular dysfunction and no current evidence exists for the role of the human gut microbiota in regulating vascular function.

Research Objectives

The goal of this dissertation research was to investigate some of the underlying causes of vascular dysfunction in obesity and T2D. In three studies, we utilized models of T2D, diet-induced obesity, and gut microbiota transplants and measured both arterial stiffness and endothelial function during and/or immediately after experimental interventions. First (chapter 2), we treated T2D mice with the sodium glucose cotransporter 2 inhibitor, dapagliflozin, to examine the effects of this new class of antidiabetic drugs on vascular dysfunction. Second (chapter 3), we treated western diet-fed, obese mice, with the gut microbial metabolite of tryptophan metabolism, indole-3-propionic acid, to examine the cardiometabolic effects of this bioactive metabolite in a prevention study design. Third (chapter 4), we collected stool from lean and obese human subjects, without and with vascular dysfunction, respectively. We then colonized germ-free mice with the gut microbiota of lean and obese female subjects to determine if the gut microbiota has a causal role in the development of vascular dysfunction.

CHAPTER 2: SGLT2 INHIBITION VIA DAPAGLIFLOZIN IMPROVES GENERALIZED VASCULAR DYSFUNCTION AND ALTERS THE GUT MICROBIOTA IN TYPE 2 DIABETIC MICE[1]

Summary

Background: Type 2 diabetes (T2D) is associated with generalized vascular dysfunction characterized by increases in large artery stiffness, endothelial dysfunction, and vascular smooth muscle dysfunction. Sodium glucose cotransporter2 inhibitors (SGLT2i) represent the most recently approved class of oral medications for the treatment of T2D, and have been shown to reduce cardiovascular and overall mortality. Although it is currently unclear how SGLT2i decrease cardiovascular risk, an improvement in vascular function is one potential mechanism. The aim of the current study was to examine if dapagliflozin, a widely prescribed STLT2i, improves generalized vascular dysfunction in type 2 diabetic mice. In light of several studies demonstrating a bi-directional relation between orally ingested medications and the gut microbiota, a secondary aim was to determine the effects of dapagliflozin on the gut microbiota. *Methods*: Male diabetic mice (Db, n = 24) and control littermates (Con; n = 23) were randomized to receive either a standard diet or a standard diet containing dapagliflozin (60 mg dapagliflozin/kg diet; 0.006%) for 8 weeks. Arterial stiffness was assessed by aortic pulse wave velocity; endothelial function and vascular smooth muscle dysfunction were assessed by dilatory responses to acetylcholine and sodium nitroprusside, respectively. *Results*: Compared to untreated diabetic mice, diabetic mice treated with dapagliflozin displayed significantly lower

[1] This is the peer reviewed but unedited manuscript version of the following article: Lee, Dustin M., Micah L. Battson, Dillon K. Jarrell, Shuofei Hou, Kayl E. Ecton, Tiffany L. Weir, and Christopher L. Gentile. "SGLT2 inhibition via dapagliflozin improves generalized vascular dysfunction and alters the gut microbiota in type 2 diabetic mice. Cardiovascular diabetology. 2018. 17(1) 62. (doi: 10.1186/s12933-018-0708-x.). The final published version is available at https://cardiab.biomedcentral.com/articles/10.1186/s12933-018-0708-x

arterial stiffness (Db = 469 cm/s vs. Db + dapa = 435 cm/s, $p < 0.05$), and improvements in endothelial dysfunction (area under the curve [AUC] Db = 57.2 vs. Db + dapa = 117.0, $p < 0.05$) and vascular smooth muscle dysfunction (AUC, Db = 201.7 vs. Db + dapa = 285.5, $p < 0.05$). These vascular improvements were accompanied by reductions in hyperglycemia and circulating markers of inflammation. The microbiota of Db and Con mice were distinctly different, and dapagliflozin treatment was associated with minor alterations in gut microbiota composition, particularly in Db mice, although these effects did not conclusively mediate the improvements in vascular function. *Conclusions*: Dapagliflozin treatment improves arterial stiffness, endothelial dysfunction and vascular smooth muscle dysfunction, and subtly alters microbiota composition in type 2 diabetic mice. Collectively, the improvements in generalized vascular function may represent an important mechanism underlying the cardiovascular benefits of SGLT2i treatment.

Introduction

Type 2 diabetes (T2D) affects nearly 30 million individuals in the US and over 350 million individuals worldwide (41). Among the myriad health consequences of T2D, cardiovascular disease (CVD) is the most common and critical. Individuals with T2D are more than twice as likely as individuals without diabetes to develop CVD during their lifetime; and CVD is the most common cause of hospitalization and death in people with diabetes, accounting for nearly 70% of diabetes-related fatalities (107). Although there is a strong correlation between the magnitude of hyperglycemia and CVD event rates among people with diabetes (63, 66), the cardiovascular benefits of successful glucose control are unclear, and there remains considerable uncertainty as to whether current anti-diabetic medications reduce CVD risk (69, 158). As such, identification of novel anti-diabetic therapies with substantiated CVD risk reduction properties is a top clinical priority.

Sodium glucose cotransporter 2 inhibitors (SGLT2i) represent the most recently approved class of oral medications for the treatment of T2D. Early modeling data predicted that,

unlike other classes of antidiabetic medications, SGLT2i may have significant beneficial effects on cardiovascular outcomes (51). Results from the EMPA-REG OUTCOME trial support these predictive data, and found that SGLT2i in patients with T2D reduced cardiovascular mortality by 38%, sudden death by 31%, and hospitalizations for heart failure by 35% (199). These data have prompted tremendous interest in identifying the underlying physiological changes that mediate the beneficial cardiovascular effects of SGLT2i (75, 142). One potential but understudied mechanism that may explain the beneficial CV effects of SGLT2i is an improvement in vascular function. Indeed, vascular dysfunction is a hallmark of T2D and may explain much of the heightened CVD risk in people with diabetes (44, 176). Among the various features of vascular dysfunction, three components in particular contribute to diabetes-related CVD: 1) arterial stiffness, 2) endothelial dysfunction and 3) vascular smooth muscle dysfunction. Arterial stiffness and endothelial dysfunction are well characterized features of T2D, and both precede clinical manifestations of CVD, and are independent predictors of future cardiovascular events in people with diabetes (44, 185). Vascular smooth muscle dysfunction, as determined by reductions in endothelium-independent dilation (EID), has received considerably less focus in regards to its prognostic potential. However, numerous studies have demonstrated that reductions in EID are commonly observed in T2D (15, 111) and predict cardiovascular complications and mortality (76, 143). Importantly, few studies have assessed the effects of SGLT2i on vascular dysfunction in people with diabetes. Among the existing studies, variable results have been reported, and no studies have comprehensively examined the effects of chronic SGLT2i on vascular function in type 2 diabetes (38, 151, 160, 196). In light of these data, it is conceivable that the cardio-protective effects of SGLT2i treatment are mediated by improvements in generalized vascular dysfunction.

The intestinal microbiota has emerged as a critical regular of human physiology and disease processes (19), and data from our laboratory (12) and elsewhere (25, 178) indicate that

the gut microbiota is an important regulator of vascular function. Previous studies have also shown that there is a bi-directional interaction between various orally ingested (non-antibiotic) medications and the gut microbiota (i.e. the microbiota affects medication activity; certain medications can affect microbiota composition). For example, various drug classes have been shown to profoundly alter gut microbiota composition (32, 117); and the gut microbiota can alter drug absorption and metabolism or mediate some of the physiological effects of T2D medications (109, 117). Importantly, this bi-direction relation extends to various medications for CVD and T2D whose primary site of action is outside of the intestines. Thus, there is tremendous clinical relevance in determining the interaction between the gut microbiota and SGLT2i, although to date, no studies have done so.

With this background, the purpose of the present study was to examine the effects of dapagliflozin, a selective SGLT2i approved for use in treating T2D, on arterial stiffness, endothelial dysfunction, and vascular smooth muscle cell dysfunction in male T2D mice, and to characterize the effects of SGLT2i on the gut microbiota.

Methods

Eight-week old diabetic mice homozygous for a point mutation in the leptin receptor gene (C57BLKS/J-lepr^{db}/lepr^{db}) and age- and gender-matched heterozygous littermates (C57BLKS/J-lepr^{db}/+) were obtained from the Jackson Laboratory (Bar Harbor, ME). Mice were housed in a temperature and humidity controlled environment on a 12h:12h light-dark cycle. Prior to initiating experimental procedures, mice were acclimatized to the housing conditions for 2 weeks. All animal procedures were reviewed and approved by the Colorado State University Institutional Animal Care and Use Committee. Following acclimatization, control (n=23) and diabetic (n=24) mice were randomized to receive one of two diets for 8 weeks: 1) standard diet (D111122001, Research Diets, Inc., New Brunswick, NJ) consisting of 15% fat, 65% carbohydrate, and 20% protein, or 2) standard diet containing dapagliflozin (Farxiga) (60mg dapagliflozin/kg diet;

0.006%) (D06081805, Research Diets). This resulted in the following four groups: 1) control mice receiving a standard diet (Con; n=11), 2) control mice reviving standard diet containing dapagliflozin (Con+dapa; n=12), 3) diabetic mice receiving standard diet (Db; n=12) and, 4) diabetic mice receiving standard diet containing dapagliflozin (Db+dapa; n=12). Mice were cohoused according to treatment group. The Con groups were cohoused 4 mice/cage while the Db groups were cohoused 2 mice/cage given the polyuria accompanied by this phenotype. Mice were allowed free access to food and water for the duration of the 8-week intervention; and body weight and food intake were measured weekly.

***Fasting Glucose*.** Fasting blood glucose was determined after a 6 hour fast from tail vein blood using a glucometer (AlphaTRAK, Abbott Laboratories, Abbott Park, IL) at weeks 0, 2, 4, and 8.

Aortic Pulse Wave Velocity (aPWV). Large elastic artery stiffness was determined by aPWV at baseline and following the 8-week intervention as previously described (12, 97). Briefly, mice were anesthetized using 2% isoflurane and oxygen at 2L per minute, placed supine on a heating board with legs secured to ECG electrodes, and maintained at a target heart rate of ~450 bpm by adjusting isoflurane concentration. Doppler probes (20MHz) (Mouse Doppler data acquisition system; Indus Instruments) were placed on the transverse aortic arch and abdominal aorta and the distance between the probes was determined with precision calipers. Pre-ejection time, the time between the R-wave of the ECG and the foot of the Doppler signal, was determined for each site. aPWV was calculated by dividing the distance (cm) between the probes by the difference in pre-ejection times (seconds) of the thoracic and abdominal regions.

Animal Termination and Tissue Collection. Mice were anaesthetized with isoflurane and euthanized by exsanguination via cardiac puncture. Blood was collected with an EDTA-coated syringe and immediately centrifuged at 1,000 rcf for 10min at 4°C to obtain plasma. Second-order mesenteric arteries were excised in ice-cold physiologic saline solution (PSS: 0.288g NaH_2PO_4, 1.802g glucose, 0.44g sodium pyruvate, 20.0g BSA, 21.48g NaCl, 0.875g KCl,

0.7195g MgSO4 7H20, 13.9g MOPS sodium salt, and 0.185g EDTA per liter solution at pH 7.4) and cannulated for vascular reactivity experiments (see below). Adipose tissue depots (subcutaneous, epididymal, and mesenteric depots) were excised and weighed.

Vascular Reactivity. Vascular function was determined as previously described (11, 97). Briefly, second-order mesenteric arteries were placed in pressure myograph chambers (DMT Inc., Atlanta, GA) containing warm PSS, cannulated onto glass micropipettes and secured with suture. Arteries were equilibrated for 1 hour at 37°C and an intraluminal pressure of 50 mmHg. Arteries were constricted with increasing doses of phenylephrine (PE: 10^{-9} to 10^{-5} M) followed immediately by a dose-response with endothelium-dependent dilator acetylcholine (ACh: 10^{-9} to 10^{-4} M). We have previously established that arteries maintain constriction to PE for the duration of experiments and that dilation is not spontaneous. If arteries do spontaneously dilate during the constriction period (i.e. 5-12 minutes), data are not included. After a washout period, a dose-response to endothelium-independent dilator sodium nitroprusside (SNP: 10^{-10} to 10^{-4} M) was obtained after pre-constriction to PE (10^{-5} M). Percent dilation was calculated based on the maximal luminal diameter of each artery.

Circulating Inflammatory Cytokines. Plasma was analyzed in duplicate on a single plate to determine the concentration of circulating inflammatory markers interleukin [IL] -1β, IL-6, IL-10, IL17, monocyte chemoattractant protein-1 (MCP-1), and chemokine ligand 5 (CCL5) using a multiplex assay (MCYTOMAG-70K; EMD Millipore, Billerica, MA, USA). Intra-assay variability (<5%) was within the normal limits reported by the manufacturer.

Intestinal Microbiota Characterization. Feces were collected fresh from individual animals prior to termination and flash frozen in liquid nitrogen. DNA was extracted using the PureLink Microbiome DNA Purification Kit (A29790, Invitrogen, Carlsbad, CA). The 16s rRNA gene was amplified for sequencing following the Earth Microbiome Project 16s protocol utilizing 515F-806R primer set (forward: 5'GTGYCAGCMGCCGCGGTAA 3'; reverse 5'

GGACTACNVGGGTWTCTAAT 3') (33). Unique 12bp error correcting barcodes were included in the construct of the forward primer. Cycling conditions using the Biorad CFX96 thermal cycler were as follows: 94°C for 3min and then 35 cycles of 94°C 45s, 50°C 60s, 72°C 90s followed by 72°C for 10min. Paired-end sequencing libraries of the V4 region were then constructed by purifying amplicons using AmPure beads and quantifying and pooling equimolar ratios of each sample library. The pooled library was quantified by qPCR and sequenced on an Illumina MiSeq at the Next-Generation Sequencing Facility at Colorado State University. Paired-end sequence reads were concatenated and all combined 16s sequences were filtered, trimmed and processed with the DADA2 (R bioconductor package (27)) implementation included in the open source bioinformatics tool myPhyloDB version 1.2.1 (www.myphylodb.org/). Briefly, all primers were removed from each sequence using the open source Python program Cutadapt (113) and sequence variants were inferred using the default pipeline in DADA2. Each sequence variant identified in DADA2 was classified to the closest reference sequence contained in the Green Genes reference database (Vers. 13_5_99) using the usearch_global option (minimum identity of 97%) contained in the open source program VSEARCH (138). After processing, data were normalized by rarefaction consisting of Laplace smoothing followed by sub-sampling with replacement. Data were rarefied to 12,629 sequence reads with 100 iterations. ANCoVA analysis was conducted in myPhyloDB (112), and MicrobiomeAnalyst (48) was used to calculate alpha diversity scores, Bray-Curtis distances, and LEfSe. The raw sequencing data and associated metadata will be made available upon request.

Statistics. Data are expressed as mean ± SEM. Statistical analysis was performed using one-way ANOVA with LSD post hoc test (SPSS for Windows, release 11.5.0; SPSS, Chicago, IL, USA). A mixed model ANOVA (within factor, time; between factor, treatment group) was used for variables measured over time (i.e. body weight and blood glucose). A p-value of <0.05 was considered statistically significant. Microbial community α and β–diversity were calculated using

Chao1 and Shannon indices (α-diversity) and Bray-Curtis distances (β–diversity**)** visualized by Principle Coordinates Analysis (PCoA). Non-parametric Mann-Whitney/Kruskil-Wallace tests were used to determine statistical significance of α-diversity measures and permutational MANOVA was used to determine differences in β–diversity. Microbial markers based on differential abundance among the treatment groups were identified using ANCoVA with post hoc Tukey method for multiple comparisons ($p<0.05$) and Linear Discriminate Analysis Effect Size (LEfSe) with an LDA>1 and $q<0.05$ (149). Pearson's correlations were conducted between taxa selected as biomarkers in LEfSe and metadata for endothelial-dependent dilation, endothelial-independent dilation, and aortic pulse wave velocity.

Results

Animal characteristics are shown in Table 2.1. As expected, both groups of diabetic mice (Db and Db+dapa) consumed significantly more food and generally displayed higher body weight (Fig. 2.1a) and indices of body fat than non-diabetic mice (Con and Con+dapa). Db mice lost weight during the intervention, which is commonly observed in this strain as the diabetic condition advances (105, 148). Conversely, all other groups significantly gained weight during the intervention. At the end of the 8-week intervention, body weight and indices of body fat were generally higher in Db+dapa compared to all other groups (Table 2.1). Dapagliflozin treatment did not significantly affect body weight and indices of body fat in Con+dapa mice.

At baseline, fasting blood glucose was closely matched between mice of the same genotype randomized to receive dapagliflozin-supplemented or non-supplemented diet; and as expected, fasting blood glucose was markedly higher in both diabetic groups compared to controls (Fig. 2.1b). Db mice experienced significant worsening of hyperglycemia during the intervention period. In contrast, blood glucose significantly decreased over time in Db+dapa such that levels were significantly lower than (and approximately half of) Db mice at weeks 2, 4

and 8 (Fig. 2.1b). No effect of time or dapagliflozin treatment were observed in the two Con groups.

Endothelium-dependent dilation (EDD) was markedly impaired in both diabetic groups compared to non-diabetic mice. Dapagliflozin treatment improved EDD in Db+dapa mice such that dilation was modestly and significantly increased at several doses of acetylcholine (ACh) (Fig. 2.2a), and total area under the curve (AUC) was more than doubled (Fig. 2.2b). Endothelium-independent dilation in Db was significantly impaired and AUC was approximately 50% compared to both Con groups (Fig. 2.2c and 2.2d). Dapagliflozin treatment significantly improved EID in Db+dapa mice such that AUC and dilation to most doses of sodium nitroprusside (SNP) was significantly higher in Db+dapa compared to Db (Fig. 2.2c and 2.2d). The improvement in EID in Db+dapa was such that final dilation to SNP was restored to levels observed in Con+dapa, although AUC remained significantly lower in Db+dapa compared to both non-diabetic groups (Fig. 2.2d). Neither endothelium-dependent nor -independent dilation differed between Con and Con+dapa, and constriction responses to phenylephrine (PE) did not differ among any groups (data not shown). Aortic stiffness, measured by pulse wave velocity, was significantly higher only in Db, and levels in Db+dapa were similar to Con mice at 8 weeks (Fig. 2.3).

Given the close association between vascular dysfunction and chronic inflammation (50, 192), we measured several circulating inflammatory markers. MCP-1, IL-1β and IL-6 were all significantly elevated in Db mice and significantly attenuated in Db+dapa mice. IL-17, CCL5, and the anti-inflammatory marker IL-10, were only detected in Db mice and were below detectable limits in all other groups (Fig. 2.4).

To examine the effects of SLGT2i on the gut microbiota, we used 16s sequencing to analyze fecal samples from each mouse. PCoA and hierarchical clustering by Ward's linkage of these visualizations suggest clustering of microbiota based on mouse genotype (Con vs Db

groups), with the Db+dapa animals clustering as a subset within the Db group (Fig. 2.5a; PCoA: R2=0.27488; p<0.001). Hierarchical clustering of the Db and Db-dapa groups was incomplete, with one sub-cluster containing animals from both groups, suggesting that there were responders and non-responders in this population (Fig. 2.5b). There was also a subtle, but significant interaction between genotype and dapagliflozin treatment for OTU richness and diversity (Chao1: p=0.00245; Shannon: p=0.00832), with significantly reduced richness and diversity in the Db+dapa group compared to Con and Con+dapa groups (Fig. 2.5c-d). Using ANCoVA for phyla-level taxonomic comparisons among groups, we identified Actinobacteria, Bacteroidetes, Firmicutes, Proteobacteria, and Verrucomicrobia significantly differed among treatment groups (Table 2.2). Although most of these differences were associated with diabetes status, Bacteroidetes and Proteobacteria also appeared to be influenced by dapagliflozin treatment in a subset of the Db-dapa animals (Fig. 2.6, Table 2.2). Calculating the ratio of Firmicutes:Bacteroidetes (F:B) showed that Db+dapa animals had a significantly lower ratio than the other treatment groups (Fig. 2.6f).

Using LEfSe, we found the abundance of several taxa differed among the experimental groups. For example, the composition of *Akkermansia muciniphila* was significantly decreased in Db compared to Con; *Oscillospira* was significantly reduced in the Db+dapa compared to all other groups; *Enterococcus* was significantly elevated in the Db group compared to all other groups; and *Lactobacillus* was significantly higher in the Con group compared to all other groups (Fig. 2.7a-d). Using Pearson's correlation analysis, significant correlations were found between *A. muciniphila* and vascular function (Fig. 2.8a-c). Additionally, Proteobacteria, Firmicutes, and F:B ratio significantly correlated with vascular outcomes (Fig. 2.8d-f).

Discussion

The primary findings of the present study were that diabetic mice treated with dapagliflozin for 8 weeks displayed significantly lower arterial stiffness, and improvements in

endothelial dysfunction and vascular smooth muscle dysfunction compared to non-treated diabetic mice. These vascular improvements were accompanied by dramatic improvements in hyperglycemia and reductions in circulating markers of inflammation. Dapagliflozin also altered microbial diversity in diabetic animals but had little effect on control animals. Several specific taxa changes were also associated with dapagliflozin treatment in diabetic but not control animals, although the relevance of these changes to treatment efficacy remains unclear.

Arterial stiffness, as measured by aPWV, predicts cardiovascular events in patients with T2D and other populations at elevated CVD risk (39, 155). We found that aPWV was significantly elevated in Db mice, but not Db mice consuming dapagliflozin. These results extend two published reports which found that SGLT2i reduced pulse pressure, an indirect marker of arterial stiffness (38, 125). Solini found that acute (48h) dapagliflozin treatment reduced PWV in patients with type 2 diabetes (160). Therefore, the current results extend these existing studies by demonstrating that chronic SGLT2i reduces arterial stiffness in T2D mice.

We also found that EDD, another strong predictor of cardiovascular outcomes in patients with T2D (155, 176), was modestly and significantly improved in diabetic mice following dapagliflozin treatment. These data are consistent with those by Solini et al., who found an improvement in flow mediated dilation (FMD) following acute (48h) administration of dapagliflozin (160). Conversely, Shigiyama found no change in FMD following chronic (16wk) SGLT2i (151). Lin et al., reported modest improvements in EDD after 10 weeks of empagliflozin treatment in diabetic mice (105). EDD in the current study was measured in mesenteric arteries whereas Lin et al., reported changes in the aorta; thus, collectively, the two studies suggest that SGLT2i elicits favorable effects on endothelial function in both large elastic and smaller resistance arteries. These broad improvements across the vascular tree may enhance the clinical relevance given the relative importance of larger and smaller arteries on atherogenesis and blood pressure regulation. Despite significant improvements in EDD in Db+dapa compared

to Db, values remained significantly lower compared to both control groups. The inability of SGLT2i to return EDD values closer to control levels may have been due to the incomplete resolution of hyperglycemia in the Db+dapa group. However, Lin et al., used a higher dose of SGLT2i and consequently observed a much greater reduction in blood glucose levels, but the improvements in EDD were still modest and similar to those in the current study. Another possibility is that other factors, either independent or downstream of hyperglycemia, may mediate a portion of the endothelial dysfunction but are not affected by SGLT2i.

Similar to aPWV and EDD, vascular smooth muscle dysfunction, as determined by reductions in EID, is common in T2D and predicts cardiovascular complications and mortality (76, 143). We found that EID was significantly improved following SGLT2i. Several studies that examined the effects of SGLT2i on endothelial function did not report results on EID (151, 160). Among the studies that did report EID, results have been somewhat conflicting. Han et al., demonstrated that SGLT2i had negative, neutral, or positive effects on EID depending on the vessel type and the method of drug delivery (74). However, similar to the current study, Lin et al., found that EID was improved following SGLT2i in diabetic mice (105). Given that dilation to ACh (EDD) ultimately requires smooth muscle cell relaxation, it is possible that the reductions in EDD and EID commonly observed in T2D mainly reflect dysfunction at the level of the smooth muscle cell rather than the endothelium. Regardless of the relative contribution of the two cell types, the current data indicate that dapagliflozin has pronounced effects on EID that may contribute to the reduction in CVD risk.

Compared to control mice, diabetic animals exhibited marked dysbiosis, which has been associated with numerous aspects of metabolic dysfunction (57, 154). Treatment with dapagliflozin appeared to have little effect on the microbiota in control mice, but did cause subtle alterations in the richness and diversity of microbial communities in diabetic animals. Specifically, richness and diversity were reduced in Db+dapa, although the response seemed to

be driven by minor differences across phyla rather than significant increases or decreases in specific bacterial taxa. Db+dapa-associated differences in Bacteroidetes and Proteobacteria might be partially responsible for global differences observed; however, there appear to be responder/non-responder animals, confounding biological interpretation of these changes. Overall, the ratio of Firmicutes:Bacteriodetes was reduced in Db+dapa animals compared to other groups. Higher levels of Bacteroidetes and a reduced Firmicutes:Bacteroidetes (F:B) ratio have been associated with a lean phenotype in previous studies (82). In this case, the reduced F:B was not associated with a lean phenotype in the current study, as Db+dapa mice displayed significantly increased body weight compared to Db. Ussar et al. recently suggested that these simplified metrics are not reliable predictors of metabolic outcomes, but rather are more reflective of varying environments interacting with genotypes (174). In either case the increase in body weight in this group may have been protective, as Db mice tend to lose weight as the severity of diabetes progresses, and medications that improve health outcomes in Db mice have been shown to preserve or increase body weight (105, 148).

Finally, at the species level, we also observed a trend for increased *Akkermansia muciniphila* in the Db+dapa group relative to Db. *A. muciniphila* has been shown to improve metabolic outcomes, including vascular function (56, 104, 153). Furthermore, increases in *A. muciniphila* have recently been demonstrated following Metformin administration in diabetic individuals and mice, and have been suggested to mediate some of the protective effects of the drug (98, 153). *Akkermansia* exclusively feeds off of the intestinal mucosa, therefore future studies are necessary to confirm whether SGLT2i administration is associated with an increase in *Akkermansia* and whether this might be the result of reductions in intestinal inflammation and an increase in protective mucosal secretions.

Chronic low-grade inflammation plays an important role in the cardio-metabolic consequences of gut dysbiosis (53). Chronic inflammation is also an established mediator of

vascular dysfunction (50, 192) and has been shown to explain much of the excess cardiovascular mortality in individuals with T2D (44). We therefore determined several circulating markers of inflammation and found that all factors were markedly increased in Db mice and decreased by SGLT2i. These results are similar to those by Leng and colleagues, who reported that dapagliflozin reduced circulating levels of NLRP3, IL1β, and IL-18 in diabetic apoE$^{-/-}$ mice (100). In type 2 diabetic mice, Tahara et al., found that SGLT2i reduced serum levels of several of the same markers of inflammation determined in the current study, including IL-6 and MCP-1 (167). Collectively, these data indicate that SGLT2i reduce systemic inflammation, although future studies in patients with T2D are necessary to determine the clinical relevance of these animal studies.

Conclusions and Limitations

Several limitations to the current study should be noted. First, although the db/db model used in the current study is the most widely used mouse model of T2D, and db/db mice do display gut dysbiosis (195), the monogenetic underpinnings of the model are not an exact representation of T2D in humans. Second, the current study was not designed to determine whether the improvements in vascular function were mediated by direct effects of SGLT2i on the vasculature or by indirect effects such as reductions in blood glucose. *In vitro* studies have indicated that SGLT inhibition may have direct effects within endothelial cells (103), but future studies are needed to directly address this issue. Similarly, although the vascular parameters measured in the current study are independent predictors of cardiovascular events in patients with T2D, we cannot state with any certainty that improvements in these parameters underlie the broader cardiovascular protection of SGLT2i observed in clinical trials. Lastly, fecal samples for gut microbiota analysis were only collected at the end of the study. Although consistencies in diet and housing conditions across all animals helped minimize fluctuations in gut microbiota

composition, pre and post measures of the gut microbiota would have strengthened the study design.

In conclusion, the current data suggest that improvements in generalized vascular dysfunction may underlie the beneficial cardiovascular effects of SGLT2i. Furthermore, in diabetic animals, SGLT2i was associated with subtle alterations in microbial richness and diversity which appear to be mainly due to the accumulation of non-significant variations across multiple taxa. The extent to which these alterations mediate the beneficial effects of SGLT2i on vascular function are unclear. Future studies utilizing co-administration of antibiotics or intravenous administration of SGLT2i are necessary to comprehensively address this issue.

Figures and Tables

Table 2.1 General and metabolic characteristics

VARIABLE	**Con**	**Con+dapa**	**Db**	**Db+dapa**
Weekly Food Intake, g	20.6±0.3	23.9±0.2	37.6±1.7#†	49.8±2.4*
Weight Gain, g	3.8±0.4	2.5±0.4	-5.2±1.4*	5.4±0.8‡†
Subcutaneous Fat, g	906±70	938±111	3415±339*	4357±204*
Epididymal Fat, g	1055±63	1117±119	2085±211#†	2442±102#†
Mesenteric Fat, g	541±35	581±44	957±123*	1331±92*
PVAT, g	30±2	26±2	36±5	47±5*

Values are mean ± SEM; *PVAT* perivascular adipose tissue, n=11-12/group; *p<0.05 vs all other groups, #p<0.05 vs Con, †p<0.05 vs Con+dapa, ‡p<0.05 vs Db

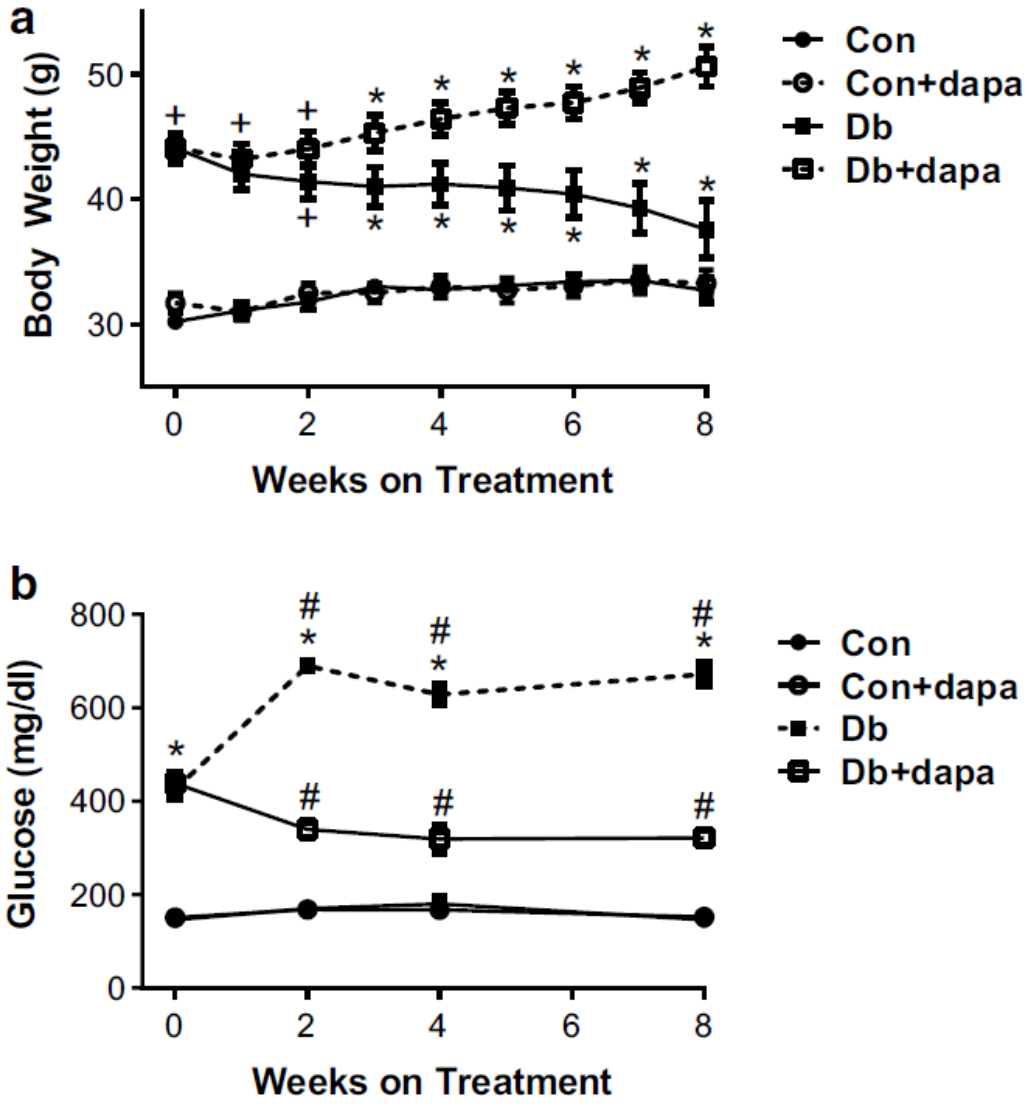

Figure 2.1. The effects of dapagliflozin on body weight and fasting (6 h) blood glucose. a Changes in body weight from weeks 0 to 8; **b** 6 h fasted blood glucose levels from 0 to 8 weeks. Data are expressed as mean ± SEM; *p < 0.05 vs all other groups at the same time point; +p<0.05 vs both Con groups at same time point; #p < 0.05 from week 0 within the same treatment group; n = 11–12/group

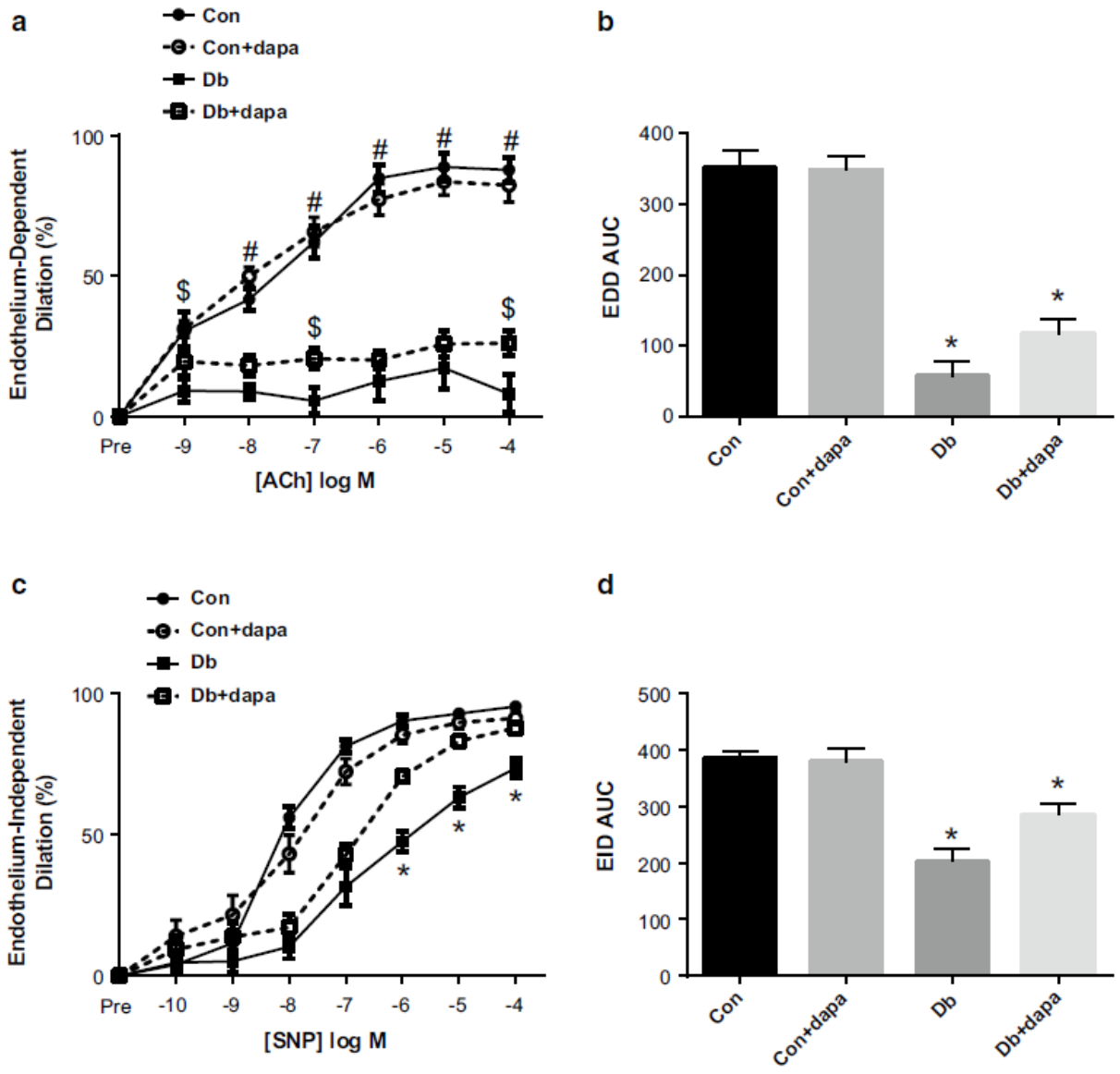

Figure 2.2. The effects of dapagliflozin on endothelium dependent- and -independent dilation. **a** Endothelium-dependent dilation; **b** area under of the curve for endothelium-dependent dilation (EDD); **c** endothelium-independent dilation; **d** area under of the curve for endothelium-independent dilation (EID). Data are expressed as mean ± SEM; *p < 0.05 vs, all other groups; #p < 0.05 vs both Db groups; $p < 0.05 vs Db group; n = 10–12/group

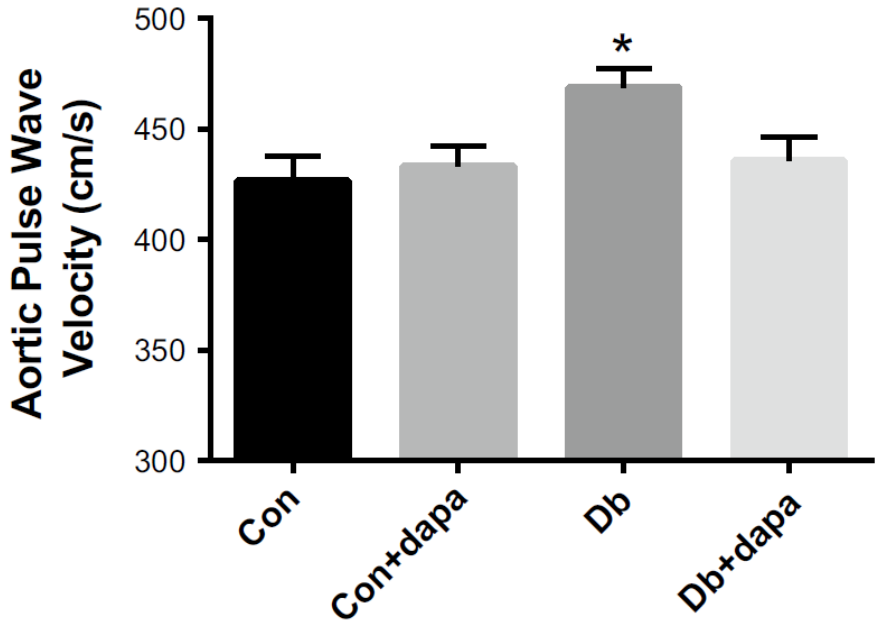

Figure 2.3. The effects of dapagliflozin on aortic pulse wave velocity (aPWV). aPWV after 8 weeks of dapagliflozin treatment. Data are expressed as mean ± SEM; *p < 0.05 vs all other groups; n = 10–12/group.

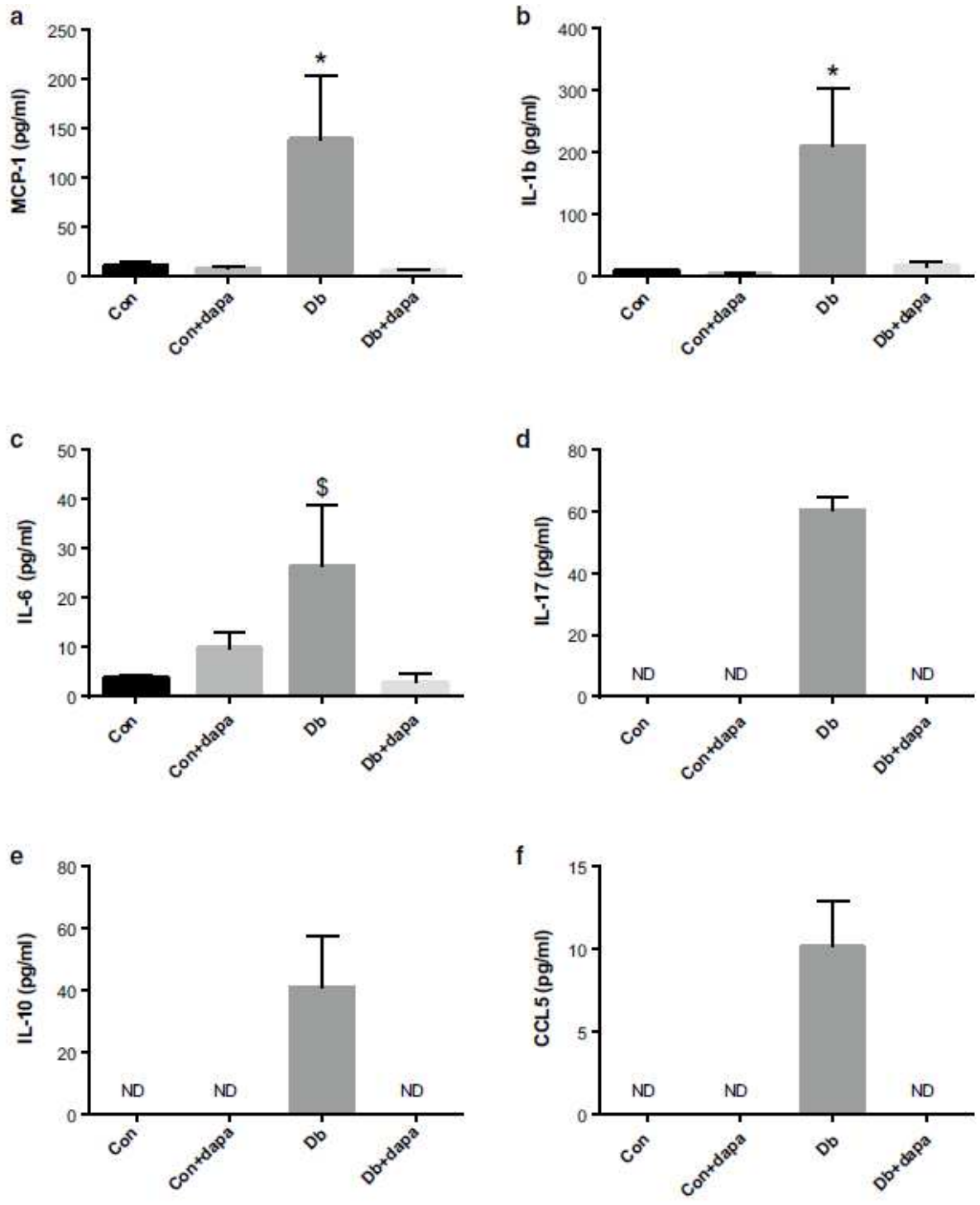

Figure 2.4. The effects of dapagliflozin on circulating markers of inflammation. a Monocyte chemoattractant protein-1 (MCP-1); **b** interleukin-1 beta (IL-1β); **c** interleukin-6 (IL-6); **d** interleukin-17 (IL-17); **e** interleukin-10 (IL-10); **f** chemokine ligand 5 (CCL5). Data are expressed as mean ± SEM; *p < 0.05 vs all other groups; $p < 0.05 vs Con and Db + dapa; n = 3–8/group. *ND* below detectable limits.

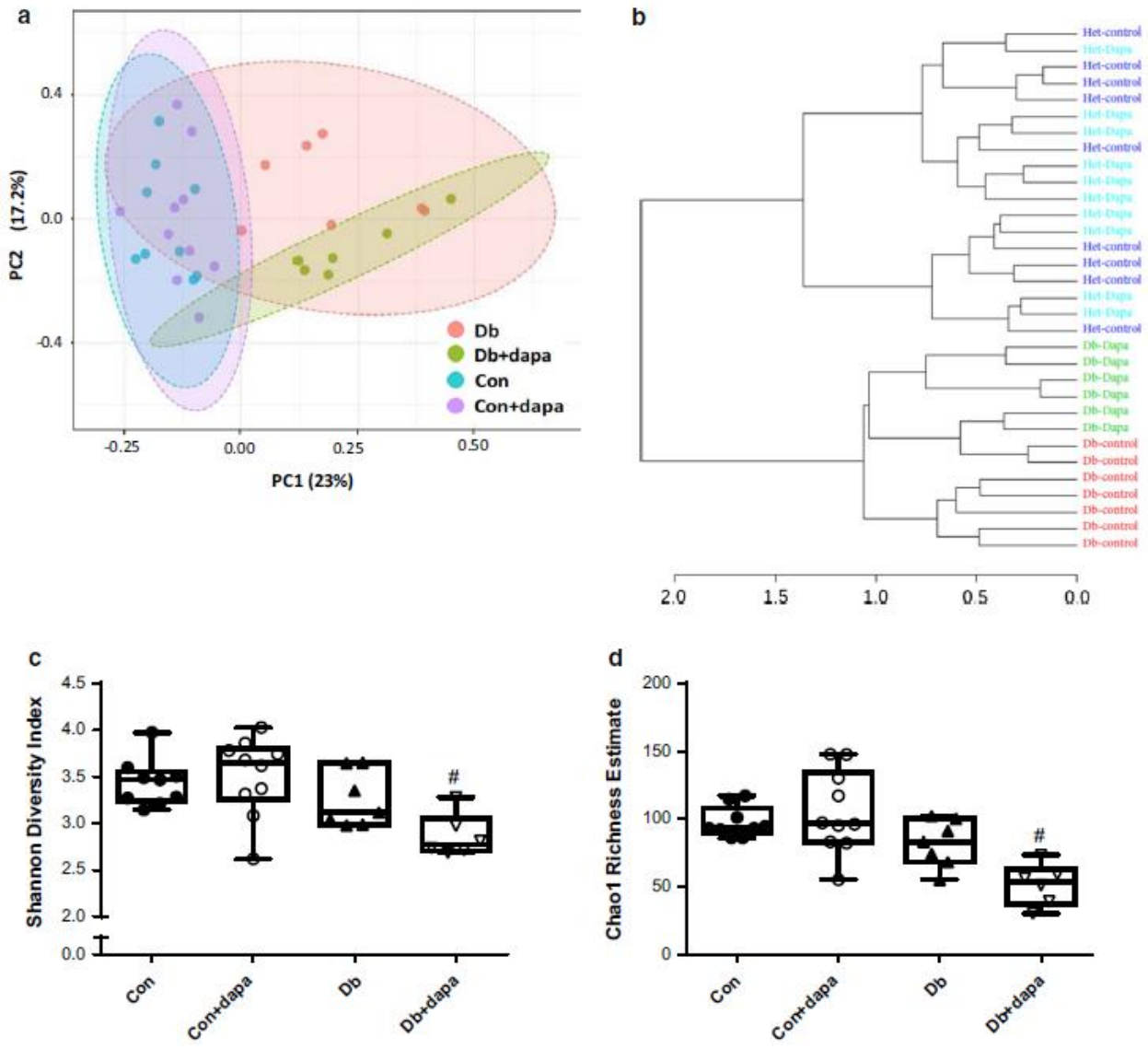

Figure 2.5. Microbiota characteristics of beta- and alpha-diversity after 8 weeks of treatment with dapagliflozin. a PCoA of OTU-level Bray–Curtis; **b** hierarchical clustering of OTU-level Bray–Curtis distances using Ward's linkage; **c** Shannon diversity measures; and **d** Chao1 richness estimates of fecal samples across treatment groups OTU. Box represents 25th–75th percentiles, median values are represented by boxplot internal line and ranges by whiskers; #p < 0.05 vs both Con groups; n = 6–10/group

Table 2.2: Phyla Level ANCOVA Analysis of Microbiota Characteristics

Phyla	Db (all) vs Con (all)	Db (no dapa) vs Con (no dapa)	Db vs Db+Dapa	Con+Dapa vs Db+Dapa
Actinobacteria	0.0431 (0.0007)	NS	NS	NS
Bacteroidetes	0.001 (0.0359)	0.0484 (0.0496)	NS	0.0053 (0.0519)
Firmicutes	0.0319 (0.0443)	NS	NS	NS
Proteobacteria	0.0006 (0.0015)	NS	NS	0.0069 (0.0022)
Verrucomicrobia	0.0494 (0.0333)	NS	NS	NS

Data are expressed as p-value (SE), NS indicates non-significant; n=6-10/group. “Db (all) vs Con (all)” indicates interaction between the genotype of Db (diabetic $db^{+/+}$) and Con (heterozygous $db^{+/-}$) mice, irrespective of drug treatment; “no dapa” indicates only those mice not receiving the drug within the genotype.

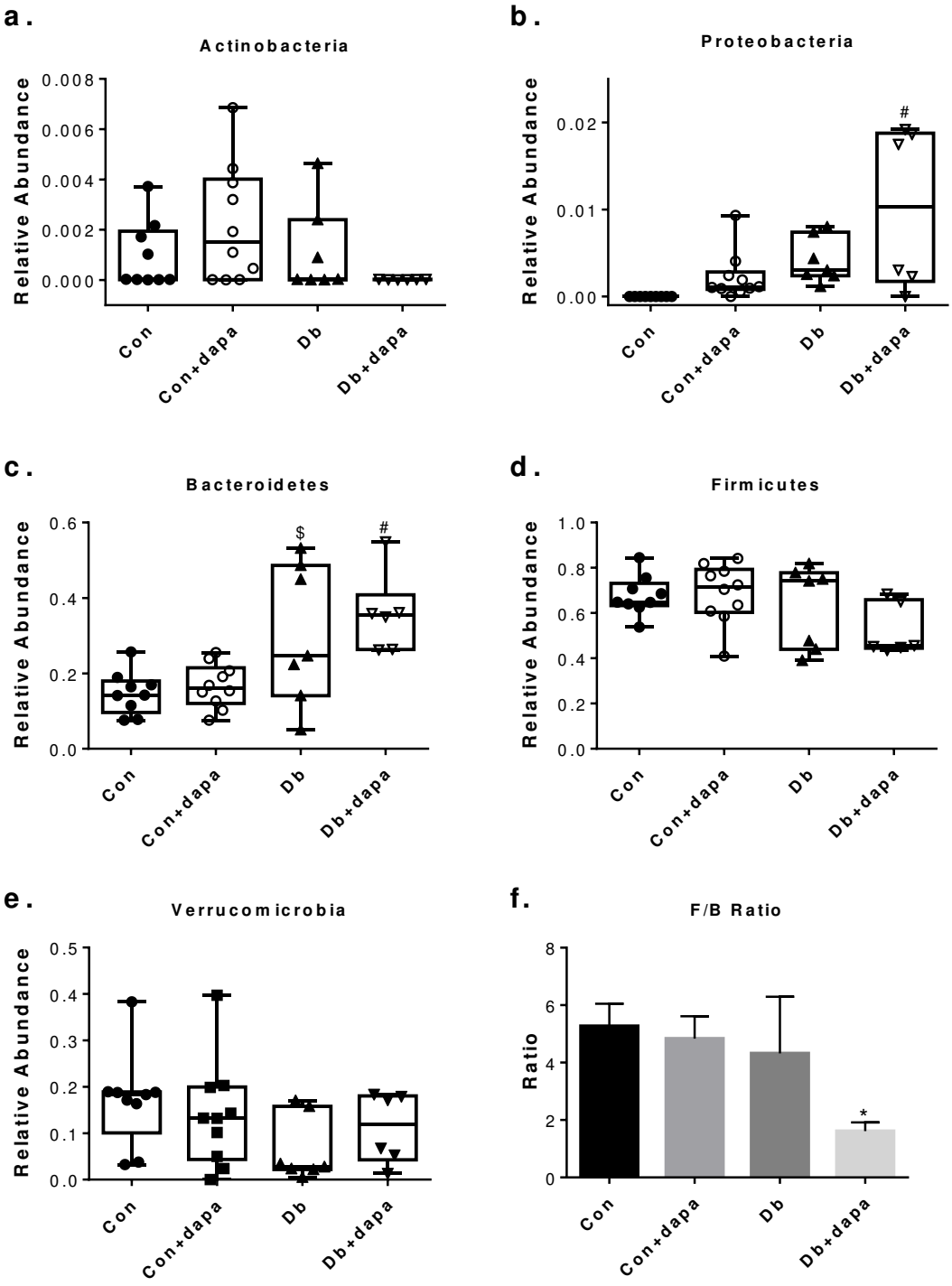

Figure 2.6. Phyla level characteristics of the microbiota. Relative abundance of **a** Actinobateria; **b** Proteobateria; **c** Bateriodetes; **d** Firmicutes; **e** Verrucomicrobioa; **f** Firmicutes:Bacteriodetes ratio. Box represents 25th–75th percentiles, median values are represented by boxplot internal line and ranges by whiskers; *p < 0.05 vs all other groups, #p < 0.05 vs Con groups, $p < 0.05 vs Con; n = 6–10/group

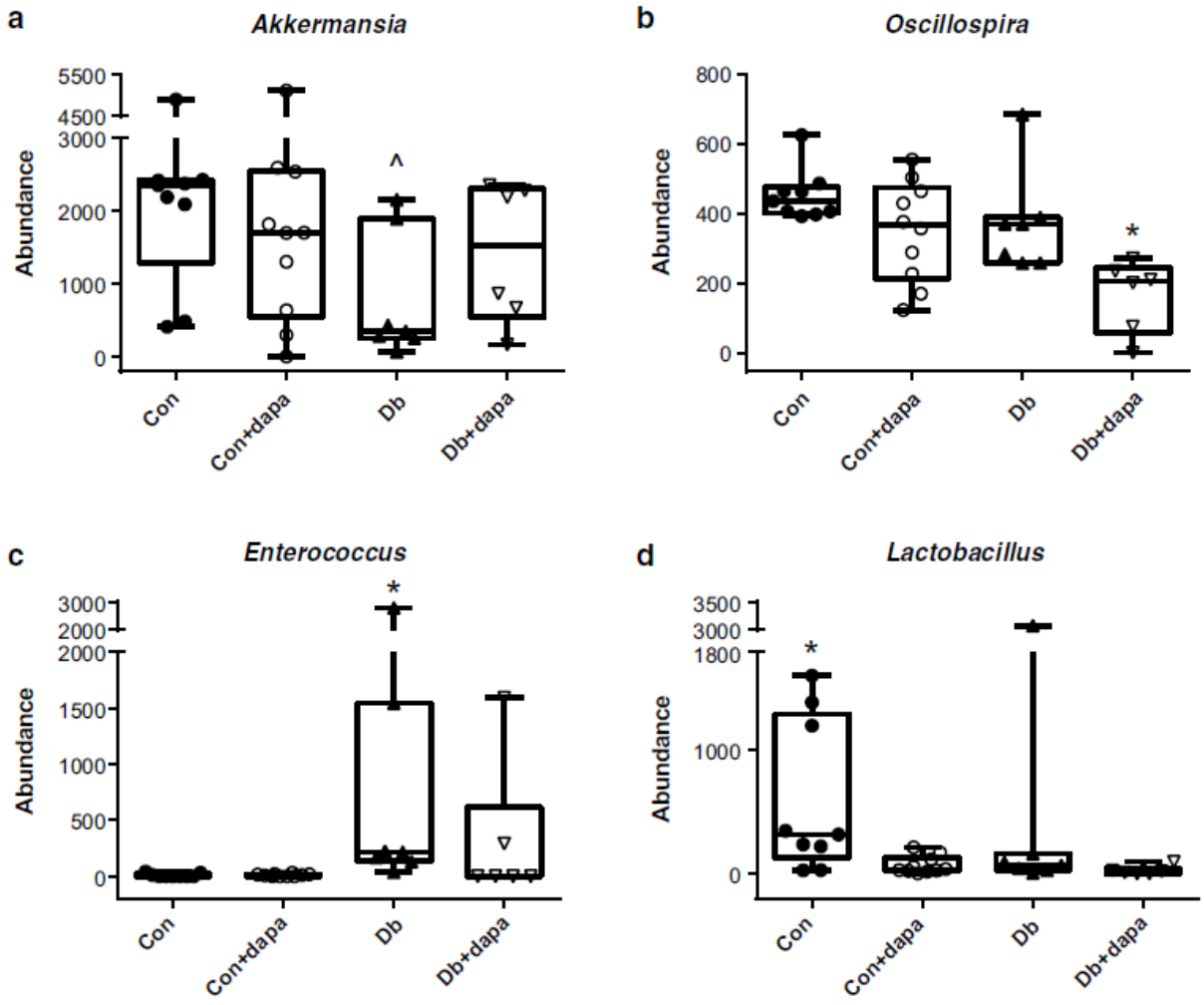

Figure 2.7. Species level characteristics of the microbiota. Abundance of **a** Akkermansia; **b** Oscillispira; **c** Enterococcus; **d** Lactobacillus. Box represents 25th–75th percentiles, median values are represented by boxplot internal line and ranges by whiskers; ^p < 0.05 vs Con; *p < 0.05 vs all other groups, #p < 0.05 vs both Con groups; n = 6–10/group

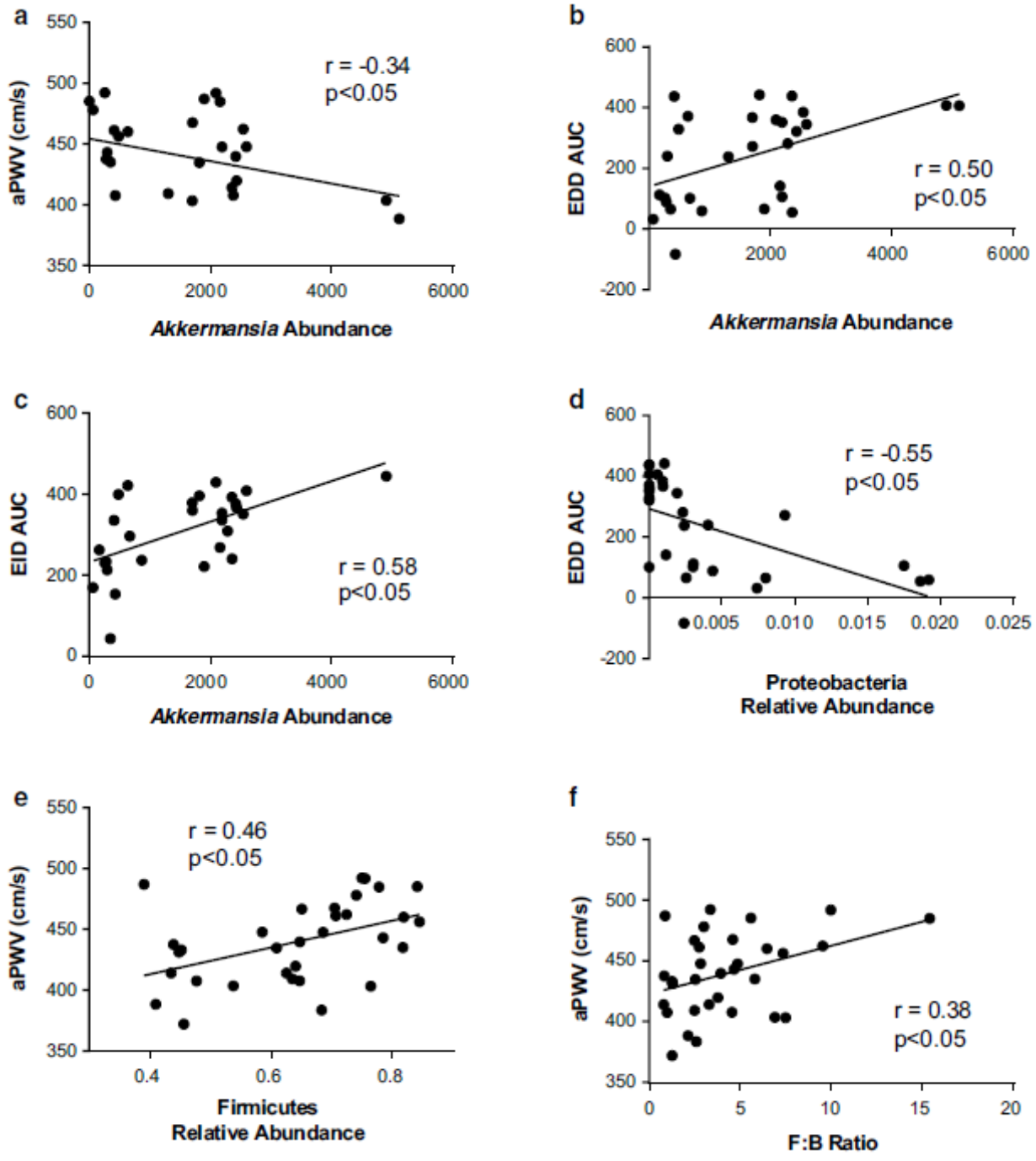

Figure 2.8. Correlations between microbiota and vascular outcomes. a aPWV and *Akkermansia* abundance; **b** EDD AUC and *Akkermansia* abundance; **c** EID AUC and *Akkermansia* abundance; **d** EDD AUC and Proteobacteria relative abundance; **e** aPWV and Firmicutes relative abundance; **f** aPWV and F:B ratio. r and p values are given following Pearson's correlation test. n = 6–10/group

CHAPTER 3: EFFECTS OF INDOLE-3-PROPIONIC ACID ON CARDIOMETABOLIC PARAMETERS IN WESTERN DIET-FED MICE.

Summary

Background/Aims: Our lab has recently reported that the gut microbiota helps regulate vascular dysfunction. However, the specific mechanisms by which microbes regulate host physiology remain obscure. Indoles are products of bacterial tryptophan metabolism and have been shown to exert various physiological effects on the host. In the current study, we examined the effects of indole-3-propionic acid (IPA) on cardiometabolic outcomes in western diet-fed mice. *Methods*: Male C57BL/6J mice were fed either a standard diet (SD) or western diet (WD) for 5-months (mo). Two additional groups were fed the same diets and supplemented with IPA (SD+IPA and WD+IPA) in autoclaved drinking water (0.1mg/ml) for the duration of the dietary intervention. Arterial stiffness was assessed by aortic pulse wave velocity (aPWV). Intestinal permeability was assessed with FITC-dextran. Glucose tolerance was assessed after a 6 hour fast followed by intraperitoneal injection of 2g/kg glucose solution. Feces were collected for gut microbiota characteristics. *Results:* Both WD-fed groups displayed significantly higher body weight compared to SD and SD+IPA ($p<0.05$) with no effect of IPA supplementation. At 5mo, aPWV was significantly higher in WD and WD+IPA compared to SD (WD: 485.7±6.7 & WD+IPA: 492.8±8.6 vs SD: 436.9±7.0 cm/s, $p<0.05$), but not SD+IPA (SD+IPA: 468.1±6.6 vs WD groups, $p>0.05$). Supplementation with IPA in the SD+IPA group significantly increased glucose AUC compared to SD mice (SD+IPA: 1763.3±92.0 vs SD: 1397.6±64.0, $p<0.05$) and no significant differences were observed with either WD or WD+IPA groups (WD: 1623.5±77.3 & WD+IPA: 1658.4±88.4, $p>0.05$). No significant differences were observed between groups with regard to intestinal permeability. The gut microbiota clustered by diet with little effect of IPA supplementation. *Conclusions:* Supplementation with IPA in WD-fed mice did not affect arterial

stiffness, glucose tolerance, or intestinal permeability but could be potentially deleterious in SD-fed mice. Future analyses will determine other cardiometabolic effects and further characterize the gut microbiota.

Introduction

The mammalian gastrointestinal tract contains trillions of microorganisms collectively referred to as the gut microbiota. The gut microbiota confers many metabolic and biological functions for human health (120). While these microorganisms play a critical role in host physiology and health, deleterious changes have been linked to various diseases including cardiometabolic disease (29). Diet is one of the most important determinants to changes or alterations in the gut microbiota environment (43) and deleterious changes secondary to a high-fat or Western (high fat, high sugar) diet have also been implicated in the development of several cardiometabolic alterations (22).

The gut microbiota is able to adapt to changes in their environment (i.e. diet) by cataloging various genes that aid in metabolism and fermentation of numerous energy sources. The extremely diverse set of metabolites produced from exogenous (i.e. dietary) and endogenous components include but are not limited to short chain fatty acids (89), bile acids (162), trimethylamine-N-oxide (TMAO) (88, 169), and nitric oxide (170). These metabolites act as messengers of host-microbiota crosstalk and have been implicated in host health and disease. Many of the well-studied bacterial metabolites originate from degradation of fiber or conversion of bile acids, but much less is known regarding metabolites from bacterial proteolysis. A recent study identified a gut bacterial pathway that can metabolize aromatic amino acids into bioactive compounds (49).

Tryptophan is one of four aromatic amino acids and can be metabolized by gut bacteria into bioactive compounds (49). Indoles are a class of compounds produced by the gut microbiota from tryptophan and have been shown to effect host physiology (3). The majority of

dietary protein (i.e. tryptophan) (90-95%) is absorbed in the small intestine and endogenously metabolized by the host (55). However, the gut microbiota is capable of directly utilizing tryptophan and approximately 4-6% can be metabolized to various compounds including indoles (65, 190). While bacterial protein degradation products have generally been considered harmful to host health (123), specific tryptophan metabolites may be important to host health and research is only beginning to understand this relationship.

Dietary tryptophan can be directed to three main pathways including the serotonin (5HT), kynurenine/IDO, and indole/AhR pathways (3). While some steps of the kynurenine/IDO pathway can be directed by microbial enzymes, the indole/AhR pathways is dependent solely upon microbial metabolism of tryptophan. A variety of indole compounds are produced through microbial metabolism and serve as ligands for the aryl hydrocarbon receptor (AhR) (78, 191). Activation of AhR via indole compounds can have a variety of effects on the host (137) including the modulation of inflammatory responses (92) and regulation of intestinal immunity (144). Given the many AhR ligands in addition to indole compounds, a layer of complexity is added to teasing out the specific effects of individual ligands beyond general AhR activation.

Epidemiological data have correlated circulating indoles with type 2 diabetes (T2D) and atherosclerosis whereby higher levels of indolepropionic acid were inversely associated with incidence of T2D (172); and lower levels of tryptophan, indole, and other indole-derived metabolites were significantly correlated with atherosclerosis (34). A translational study identified indole-3-propionic acid (IPA) to promote human and murine intestinal homeostasis via regulation of the IL-10 receptor (5). While some data surrounding indoles have shown positive correlations to host health, other research has suggested the opposite. In contrast to low levels of tryptophan, Wang et al. found high levels of tryptophan to be predictive of future development of T2D (184), although these data do not specifically link microbial tryptophan metabolism to T2D. Preclinical data suggests that indole negatively impacts emotional behavior in rats (81).

Additionally, Huc et al. showed that indole exacerbates portal hypertension in rats (79). These data providing conflicting evidence to the protective role of indoles and potentially suggest that specific tryptophan metabolites may have differing metabolic effects.

Despite these data, the effect of specific tryptophan metabolites (i.e. IPA) on cardiometabolic disease remains unknown. Therefore, the aim of the current study was to assess the cardiometabolic effects of IPA supplementation in both healthy and diet-induced obese (western diet-fed) mice and characterize the effects of IPA on the gut microbiota. We hypothesized that supplementation with IPA would improve cardiometabolic effects of diet-induced obesity given the current data supporting the role of indoles in intestinal health. Our results indicate that supplementation with exogenous IPA does not affect cardiometabolic parameters in Western diet-fed mice but may have negative effects in otherwise healthy control mice.

Methods

Experimental design. Male C57BL/6J mice were obtained from the Jackson Laboratory (Bar Harbor, ME) and acclimated for 2 weeks with *ad libitum* access to a standard diet (SD; TD.08485, Harlan Laboratories) consisting of 13% fat, 67.9% carbohydrate, and 19.1% protein calories. Mice were co-housed two per cage in a temperature- and humidity-controlled environment on a 12h:12h light-dark cycle. All animal procedures were reviewed and approved by the Colorado State University Institutional Animal Care and Use Committee. Once acclimated, 4 to 5-month-old mice were randomly assigned to a standard diet (SD; n=24) or Western diet (WD; n=24) (TD.88137, Harlan Laboratories) consisting of 42.0% fat (61.8% saturated, 27.3% monounsaturated, 4.7% polyunsaturated), 42.7% carbohydrate (80% sucrose), and 15.2% protein calories for 5 months with *ad libitum* access. Diet compositions are shown in Table 3.1. Mice were then randomly assigned to receive normal drinking water or drinking water supplemented with indole-3-propionic acid (IPA) (Sigma-Aldrich, #57400) at

0.1mg/ml as previously described (5) resulting the following groups 1) SD receiving normal drinking water, 2) WD receiving normal drinking water, 3) SD+IPA, and 4) WD+IPA each including 12 mice per group. Supplemented IPA drinking water was changed twice per week and the stability of IPA was confirmed with HPLC prior to starting the study. Body weight and food intake were recorded weekly. Fluid intake was tracked and recorded twice per week.

Arterial Stiffness. Aortic pulse wave velocity (aPWV) was measured at 0, 2 and 5 months on diet and treatment. Mice were anesthetized using 2% isoflurane and oxygen at 2L per minute, placed supine on a heating board with legs secured to ECG electrodes, and maintained at a target heart rate of ~450 bpm by adjusting isoflurane concentration. Doppler probes (20MHz) (Mouse Doppler data acquisition system; Indus Instruments, Houston, TX) were placed on the transverse aortic arch and abdominal aorta and the distance between the probes was determined simultaneously with precision calipers. At least five consecutive 2-second recordings were obtained for each mouse and used to determine the time between the R-wave of the ECG and the foot of the Doppler signal for each probe site (Δtime). aPWV (in cm/s) was calculated as aPWV = (distance between the two probes) / ($\Delta time_{abdominal}$ - $\Delta time_{transverse}$).

Glucose Tolerance Test. At month 5 on diet/treatment and 2 weeks prior to termination, mice were food fasted for 6 hours and blood glucose was determined from tail-vein blood using AlphaTRAK 2 glucose meters (Abbott Laboratories, Chicago, IL). After baseline glucose readings (time point “0”), mice received an intraperitoneal injection of 2g/kg glucose, and blood glucose levels were measured at 15, 30, 60, 90, and 120 min post injection.

***Intestinal Permeability*.** At month 5 on diet/treatment and 1 week prior to termination mice were water-fasted for 12 hours during the dark cycle prior to oral gavage with a 125mg/ml FITC-dextran (4,000 mol. wt.) (Sigma-Aldrich, #46944) solution diluted in sterile 1x PBS for a goal dose of 600mg/kg body weight of FITC-dextran. Food was removed immediately after oral gavage and blood was collected 4 hours later via tail bleed for quantification of plasma FITC-

dextran concentration. Plasma samples were diluted 1:2 in 1x PBS and fluorescence was measure on a spectrophotometer at 485/20 (excitation) and 528/20 (emissions). Plasma concentrations were calculated based on a standard curve of known FITC-dextran concentrations prepared in control plasma from untreated mice.

Animal Termination and Tissue Collection. Mice were anaesthetized with isoflurane and euthanized by exsanguination via cardiac puncture. The liver was immediately removed and flash frozen. Next, the thoracic aorta was excised and cleaned of surrounding perivascular adipose tissue (PVAT) on ice-cold physiologic saline solution (PSS: 0.288g NaH_2PO_4, 1.802g glucose, 0.44g sodium pyruvate, 20.0g BSA, 21.48g NaCl, 0.875g KCl, 0.7195g $MgSO_4$ $7H_2O$, 13.9g MOPS sodium salt, and 0.185g EDTA per liter solution at pH 7.4). A 1 mm segment of proximal aorta was frozen in optimal cutting temperature (OCT) media for later analysis. The remainder of the aorta and PVAT were flash frozen and stored at -80°C for later biochemical analyses. The gastrointestinal tract was excised and colon length recorded. Cecum, spleen, heart, and adipose tissue (subcutaneous, epididymal, and mesenteric depots) were isolated and weighed. Sections of colon and distal ileum were obtained 0.25cm away from the cecum.

Liver Triglycerides and Gene Expression. Liver was excised after termination and immediately flask frozen and stored at -80°C until biochemical analyses. For triglyceride quantification, liver was first digested with ethanolic potassium hydroxide. Liver triglycerides were quantified using a colorimetric assay kit according to the manufacturer's protocol (Cayman Chemical, Ann Arbor, MI, #10010303). Another portion of liver was partitioned for total RNA extraction using TRIzol reagent, according to the manufacturer's protocol (Invitrogen, Carlsbad, CA). For real-time PCR, reverse transcription was performed using 0.5µg of DNase-treated RNA, SuperScript II RNase H and random hexamers. PCR reactions were performed in 96-well plates using transcribed cDNA and iQ-SYBR Green master mix (Bio-Rad Laboratories, Hercules, CA). Primer sequences are provided in Table 3.2. PCR efficiency was between 90%

and 105% for all primer and probe sets and linear over five orders of magnitude. The specificity of products generated for each set of primers was examined for each amplicon using a melting curve and gel electrophoresis. Reactions were run in duplicate, and data were calculated as the change in cycle threshold (ΔCT) for the target gene relative to the ΔCT for β2-microglobulin (reference gene) similar to the methods used by Battson et al. (11). Fold change differences were calculated by $2^{\Delta\Delta Ct}$.

Plasma Indole Quantification, Instrumentation and Sample Preparation.

Sample Preparation: Plasma protein was precipitated by combining plasma (16µl) and 50% methanol (84µl) with a labeled internal standard (indole-3-propionic-2,2-d_2 acid, CDN Isotopes, #D-7686) at 0.05µg/ml final concentration, followed by incubation at room temperature for 5 minutes. Samples were then centrifuged at 12,000g x 5 min, 19°C. The subsequent supernatant (50 µl) was transferred to a clean vial (Agilent, #5190-6118) with a high recovery insert (Agilent, #5182-0549) and diluted with 50µl solvent (50% methanol in water), so that both standards and samples had the same final internal standard and plasma dilution concentrations.

Standard Preparation: Standards were prepared with blank plasma and protein was precipitated with internal standard in the same manner as described above. For the standard curve solutions, the plasma supernatant with internal standard (50µl) was added to a high recovery insert and diluted with 50µl of indole-3-propionic acid (Sigma-Aldrich, #57400) standards in 50% methanol to final concentrations of 0.07, 0.10, 0.25, 0.40, 0.55, 0.70 and 1.0µg/ml. A true blank was created with only plasma supernatant with no internal standard and solvent while a calibrant zero was created with only plasma supernatant with internal standard and solvent. Quality controls used were 0.10, 0.40, and 1.0µg/ml.

Quantification: Sample plasma IPA concentrations were determined from the standard curve generated by TargetLynx software which uses a response factor of internal standard to

calibration standards peak areas to determine calculated concentrations used in the standard curve. Any calibrator standard solutions with a known to calculated concentration percent difference of 20% or more were excluded. The standard curve had an R^2 of 0.977. Samples and standards were run in duplicate.

Materials: UPLC grade acetonitrile, formic acid, and water were purchased from Sigma-Alrdrich and solvents were filtered before use.

Instrumentation and UPLC-MS-MS Parameters: Tandem UPLC-MS-MS instrumentation included a Waters Acquity ultra performance liquid chromatography (UPLC) instrument equipped with an Acquity UPLC BEH (ethylene bridged hybrid) Amide column (1.7µm, 2.1 x 100 mm column model # 186004801) and a Waters XEVO electrospray ionization (Z-Spray ESI) triple quadrupole mass spectrometer (XEVO-TQD, QCA1088). Samples were separated on the Amide column at 3 µl aliquots at 0.4 ml/min flow rate, at 40° C, with a linear gradient of 20% to 100% Eluent A (100% acetonitrile with 0.1 % (v/v) formic acid) for 4 minutes while Eluent B was 100% water with 0.1% (v/v) formic acid. The retention time of indole-3-propionic acid was 0.86 minutes. The analyte was detected in ES positive mode (ES+) with a cone voltage of 20 V, a collision energy of 10 V and a dwell time of 0.005 s. The quantifier m/z transition for indole-3-propionic acid was 190.00 > 130.00 and the MRM daughter ion m/z transition was 190.00 > 172.00. The internal standard indole-3-propionic-2,2-d_2 acid quantifier m/z transition was 192.00 > 130.00.

Software: Waters Acquitiy Console software was used to control the UPLC and XEVO-TQD while MassLynx version 4.1 was used to control the MS and sample lists. Samples were quantified using TargetLynx tab in MassLynx.

Microbiota Characterization. Fecal material was collected fresh from individual animals, flash frozen in liquid nitrogen and stored at -80°C until later analyses. Fecal DNA was

extracted using the FastDNA® Kit (MP Biomedicals, #116540400) following manufacturers protocol. Samples were incubated in lysis buffer for 15-20 minutes before beginning the initial extraction steps to soften stool and expedite the homogenization process. Negative extraction controls, following the same protocol for stool samples but excluding the stool sample, were used to account for user error or kit contamination. Amplification of the V4 16S rRNA region via qPCR was completed following the Earth Microbiome Project protocol utilizing 515F-806R primer set (forward: 5'GTGYCAGCMGCCGCGGTAA 3'; reverse 5' GGACTACNVGGGTWTCTAAT 3') (33). Unique 12bp error correcting barcodes were included in the construct of the forward primer. Cycling conditions using the Biorad CFX96 thermal cycler were as follows: 94°C for 3min and then 35 cycles of 94°C 45s, 50°C 60s, 72°C 90s followed by 72°C for 10min. Paired-end sequencing libraries of the V4 region were then constructed by purifying amplicons using AmPure beads and quantifying and pooling equimolar ratios of each sample library. The pooled library was quantified by qPCR and sequenced on an Illumina MiSeq at the Next-Generation Sequencing Facility at Colorado State University.

Paired-end sequence reads were imported into QIIME2 version 2019.1 for analysis. Briefly, the sequence reads were demultiplexed with QIIME2's '*qiime demux'* plugin to examine the overall sequence quality. Forward and reverse reads were paired for each sample using DADA2. To preserve only reads with the highest sequence quality for downstream applications, sequences were trimmed to 250 base pairs for the forward reads and 155 base pairs for the reverse reads. A feature table was generated using a taxonomic assignment based on the GreenGenes version 13.8-reference database by training a classifier with the QIIME2 q2-feature classifier plugin. Sequences were filtered to remove any undesired mitochondrial or chloroplast DNA from the dataset. Phylogenetic trees were created using the FastTree2 method.

Alpha and beta diversity were analyzed using phylogenetic and non-phylogenetic metrics through the QIIME2 diversity plugin. Evaluations of richness and evenness in individual

samples were used for alpha diversity. Unweighted UniFrac and Bray Curtis distance measurements between samples were used for beta diversity. LEfSe analysis (Linear discriminant analysis Effect Size) was applied to examine the features most likely to elucidate the differences among classes. The QIIME2 feature table was prepared for LEfSe analysis utilizing the QIIME2 feature table plugin. LEfSe analysis was performed at http://huttenhower.sph.harvard.edu/galaxy/ utilizing the default settings. This work utilized the RMACC Summit supercomputer, which is supported by the National Science Foundation (awards ACI-1532235 and ACI-1532236), the University of Colorado Boulder, and Colorado State University. The Summit supercomputer is a joint effort of the University of Colorado Boulder and Colorado State University (8).

Statistics. Data are expressed as mean ± SEM. Statistical analysis was performed using a one-way ANOVA (SPSS for Windows, Release 25.0.0.1; SPSS, Chicago, IL). When a significant main effect was observed, Tukey's post-hoc test was performed to determine specific pairwise differences. A p-value of <0.05 was considered statistically significant. Microbial community α and β-diversity were calculated using Pielou_e and Faiths indices (α-diversity) and Bray-Curtis distances (β-diversity) visualized by principle coordinates analysis (PCoA). Non-parametric Kruskal-Wallis test was used to determine statistical significance of α-diversity measures. Microbial markers based on differential abundance among the treatment and diet groups were identified using linear discriminate analysis effect size (LEfSe) with an LDA>2 and $q<0.05$.

Results

Mice fed a WD gained significantly more weight than SD fed mice and IPA supplementation did not affect body weight at 5 months (Figure 3.1A). The change in body weight from baseline to 5 months was significantly different between the WD and WD+IPA groups, whereby WD+IPA mice gained less weight over time but weight was not different at 5-mo (Figure 3.1B). General metabolic characteristics and tissue weights are shown in Table 3.3.

Generally, fat mass differed by dietary group whereby WD-fed mice exhibited greater fat mass relative to SD-fed mice. Interestingly, cecum weight was generally lower in the WD-fed mice compared to SD-fed mice although these differences were not statistically significant. No difference was observed in colon lengths among groups. Food intake was similar among SD-fed mice but significantly greater in WD-fed mice, irrespective of IPA supplementation (Figure 3.1C). Average fluid intake over 5mo, measured twice per week, was lower in WD mice and similar among the other 3 groups (Figure 3.1D).

In line with similar average fluid intakes in both supplemented groups, SD+IPA and WD+IPA consumed similar levels of IPA (0.357±0.003 and 0.373±0.003 mg/day/mouse) although this difference was statistically significant (Figure 3.2A). We next sought to measure circulating levels of IPA given that ingestion of bioactive molecules do not always reflect levels in the plasma. Circulating levels of IPA in the plasma measured by HPLC revealed non-detectable levels in both non-supplemented control groups (WD and SD) (Figure 3.2B). However, greater plasma levels were detected in both IPA supplemented groups and a roughly 2-fold greater level was detected in SD+IPA compared to WD+IPA mice (Figure 3.2B).

We next measured arterial stiffness to gain insight in cardiovascular risk as arterial stiffness independently predicts future cardiovascular events (116). Arterial stiffness measured by aortic pulse wave velocity (aPWV) was similar among all 4 groups at baseline (Figure 3.3). Both groups of WD-fed mice displayed a progressive increase in aPWV during the 5-mo intervention with no effect of IPA supplementation. At both the 2-mo and 5-mo time points, WD and WD+IPA mice displayed a significantly higher aPWV compared to SD. Interestingly, at 2-mo of diet and treatment, SD+IPA mice began to separate from SD whereby this increase in aPWV was no longer significantly different from either WD groups. Finally, at 5-mo of diet and treatment, both groups of WD-fed mice and SD+IPA displayed a significantly higher aPWV compared to SD (Figure 3.3).

Given changes in aPWV, we next examined other features of cardiometabolic disease including glucose intolerance and intestinal permeability. Utilizing an intraperitoneal glucose tolerance test, we found that WD-fed groups tended to display impaired glucose tolerance and interestingly, IPA supplementation in SD+IPA significantly impaired glucose tolerance compared to SD (Figure 3.4A and B). To explore the potential mechanisms by which alterations to the gut lead to metabolic dysfunction, we assessed gut permeability utilizing FITC-dextran. No significant differences were observed between groups for plasma levels of FITC-dextran although IPA supplementation resulted in lower levels of FITC in both SD+IPA and WD+IPA ($p=0.10$ and $p=0.11$ vs WD, respectively) (Figure 3.5).

To further examine potential mechanisms contributing to cardiometabolic alterations, we examined lipid accumulation and markers of inflammation in liver tissue. Measurement of liver triglycerides reveled significantly higher levels in WD-fed groups compared to SD-fed groups with no effect of IPA (Figure 3.6A). In both groups of WD-fed mice the inflammatory markers TGF-b, AOAH, and NLRP3 were significantly increased compared to both SD-fed groups, with no effect of IPA supplementation (Figure 3.6B-D). Finally, expression of IL-1b tended to be higher in WD-fed mice relative to SD-fed mice, although this increase was only significant among WD+IPA (Figure 3.6E).

Finally, we characterized the gut microbiota given that indoles are bacterial metabolites and changes to the gut microbiota can drive cardiometabolic diseases. Western diet-feeding led to shifts in the gut microbiota that distinguished the two dietary groups. PCA analysis revealed a sample clustering by diet along PC1 (Figure 3.7A). Using LEfSe analysis, we found the abundance of several bacterial taxa were altered based on diet (Figure 3.7B) and some by treatment (Figure 3.7C). In particular, *Bifidobacterium* and *Akkermansia* were lower and higher, respectively, in WD-fed mice. Next we examined estimates of alpha-diversity and found that

Pielou_e evenness was higher in WD-fed animals (Figure 8A) but Faiths richness was decreased in WD-fed mice with no effect of IPA supplementation (Figure 8B).

Discussion

Recent efforts to elucidate the upstream mechanisms of cardiometabolic disease have begun to focus on the contribution of the gut microbiota. Indeed, it is now established that alterations to gut microbiota composition, termed gut dysbiosis, are associated with cardiometabolic alterations (12, 29). This gut dysbiosis, which can be characterized by an increased or decreased abundance of certain bacteria, can lead to impaired intestinal barrier function (84, 104) and increased circulating levels of lipopolysaccharide (12, 28, 29) both of which are suggested to drive development of cardiometabolic diseases (71). Given the complexity in the number of gut bacteria and metabolites they produce, understanding specific roles of these bioactive compounds and their impact on host health remain an important area of research. In the current study, we sought to characterize the cardiometabolic effects of the gut bacterial tryptophan metabolite, IPA.

The primary finding of the current study is that supplementation with IPA had no effect on WD-induced cardiometabolic outcomes. In WD-fed mice, IPA supplementation did not affect body weight, aPWV, glucose tolerance, or markers of inflammation relative to the non-supplemented WD group. Interestingly, in the SD+IPA group, glucose tolerance was significantly impaired relative to SD mice. We also observed changes in arterial stiffness in SD+IPA mice whereby aPWV began to trend upwards at 2mo and was significantly higher by 5mo compared to the non-supplemented SD group. We also found that IPA was roughly 2-fold higher in the plasma of the SD+IPA group relative to WD+IPA. While we can only speculate, it is possible that this higher circulating level of IPA may have contributed to the increase in arterial stiffness observed in this group. Collectively, our results suggest that the tryptophan metabolite,

IPA does not have a major beneficial bioactive role in the current WD-induced obesity model but may be potentially harmful at higher circulating levels as we observed in SD+IPA mice.

Converse to our findings, Cason et al. showed that indole and indole-derived metabolites were negatively associated with atherosclerosis (34). While we did not observe any cardiometabolic benefit of increasing circulating levels of IPA in our WD-fed mice, epidemiological data suggests indole-3-propionic acid specifically, to be negatively associated with ankle-brachial index, a surrogate for atherosclerosis (34). Other research surrounding indoles has suggested their role to be generally positive in relation to intestinal health. Alterations in intestinal permeability have been shown to contribute to cardiometabolic disease (29, 45, 57, 73). Indoles are suggested to be protective and important in epithelial barrier function and development (10, 49, 118, 152, 187). Utilizing an *in vitro* model with human enterocytes, Bansal et al. demonstrate that indole increased tight junction genes and attenuated markers of inflammation (10). While these data suggest indoles are important in barrier function, we did not observe any significant changes among the 4 groups with regard to intestinal permeability although the two groups supplemented with IPA tended to have improved barrier function.

Contrary to the aforementioned data, some studies have suggested indoles to be potentially harmful. A tryptophan-rich diet or intracolonic infusion of indole was found to increase portal hypertension and increase circulating levels of indoles including IPA (79). We observed higher circulating levels of IPA in the SD+IPA group who also exhibited increases in aPWV. We can only speculate, but we suspect that differences in circulating IPA levels among the supplemented groups was potentially driven by intestinal absorption given that intake was very similar among the groups and intestinal epithelial cells can serve as gatekeepers for compounds such as indole (144). Furthermore, dietary tryptophan was matched between the diets and both non-supplemented groups had circulating IPA levels that were non-detectable by our

quantification. Alternatively, it is possible that host metabolism was responsible for the differences in circulating IPA levels observed as xenobiotic metabolism can differ significantly depending on disease state (i.e. obesity or diabetes) (134). Given that indole compounds can be metabolized in the liver via microsomal cytochrome P450 enzymes (9, 137) and disease states such as obesity can alter liver xenobiotic handling (90, 121, 189), this may explain the differences we observed.

Inflammation is a key driver of cardiometabolic diseases (54) and also contributes to arterial stiffness (50). We found that WD-fed mice displayed elevated markers of liver inflammation which were not affected by IPA supplementation. This is contrary to data showing that indoles protect against liver inflammation utilizing various *in vitro*, *ex vivo*, and *in vivo* models (14, 92) and suppresses inflammation in human PBMCs in a NRF2-dependent pathway (187). The effects of indoles are mediated through their activation of the aryl hydrocarbon receptor (AhR), which can lead to several cellular responses and pathways (95). However, it appears that different indole compounds have differing effects. For example, indoleacrylic acid, but not IPA, led to reduced inflammation in human PBMCs (187). While these data support indoles protective role in intestinal health and associations with cardiometabolic diseases, specific indole compounds and their effects should be further characterized.

Given the strong link between the gut microbiota and cardiometabolic diseases, we characterized the gut microbiota of our mice. No studies have investigated the relationship between exogenous indole supplementation and alterations in the gut microbiota and to our knowledge none have characterized the gut microbiota effects of IPA supplementation. Our results indicate that the gut microbiota of mice generally clustered based on diet and some alterations in bacteria at the genus level were altered both by diet and/or treatment. We have previously shown that gut dysbiosis from WD-feeding drives vascular dysfunction and that levels of *Bifidobacterium* negatively correlated with vascular dysfunction (12). In the current study we

found that WD feeding also resulted in decreases in *Bifidobacterium*. Studies have shown that high-fat diet feeding depletes the gut microbiota of indole-3-acetate and tryptamine (92) and that humans with metabolic syndrome have impaired ability to metabolize tryptophan to indoles (118). While we observed alterations in the gut microbiota, these differences were largely driven by diet rather than treatment. We observed low bacterial richness in WD-fed animals and it has been shown that the gut microbiota of obese humans with low bacterial richness correlates with metabolic markers such as increased adiposity, insulin resistance, dyslipidemia, and an inflammatory phenotype (96).

The current study is not without limitations. We utilized a chronic model of diet and treatment lasting 5 months and did not investigate the acute effects of IPA as other studies have. We only utilized one tryptophan metabolite (IPA) and did not investigate the role of other tryptophan metabolites or indole compounds. We also did not characterize other tryptophan metabolites that could be contributing to the cardiometabolic outcomes we observed. This may be of interest given that indoles have differing effects or no effects depending on various models and factors. In conclusion, the present work adds to the understanding of indoles and their effects on host physiology. Our data suggests that the gut bacterial tryptophan metabolite, IPA, may have neutral or potentially detrimental effects on cardiometabolic outcomes depending on health status. Future studies should examine the role of other tryptophan metabolites including other indole compounds and their effects on cardiometabolic function.

Figures and Tables

Table 3.1. Diet compositions

	Standard Diet	**Western Diet**
Carbohydrate (% kcal)	67.9	42.7
Sucrose (g/kg)	120	341.46
Lipid (% kcal)	13.0	42.0
Protein (% kcal)	19.1	15.2
Tryptophan (% wt of diet)	~0.2%	~0.2%
Energy (kcal/g)	3.6	4.5

Comparisons of the Standard Diet (SD) and Western Diet (WD) used in the 5-mo experimental protocol.

Table 3.2. Sequence of qPCR primers for liver tissue

Target Gene	**Sequence**
B2M	(s) CGGTCGCTTCAGTCGTCAG (as) ATGTTCGGCTTCCCATTCTCC
AOAH	(s) TGAACCAAGAAATAGCAGGCG (as) GGGTGTGTGGTACTGGTATCT
IL-1b	(s) TCTTTGAAGTTGACGGACCC (as) TGAGTGATACTGCCTGCCTG
NLRP3	(s) AGCCTTCCAGGATCCTCTTC (as) CTTGGGCAGTTTCTTTC
TGF-b	(s) TGGACACACAGTACAGCAAGG (as) GTAGTAGACGATGGGCAGTGG

B2M, β2 microglobulin; AOAH, acyloxyacyl hydrolase; IL-1b, interleukin 1 beta; NLRP3, NLR family pyrin domain containing 3; TGF-b, transforming growth factor beta 1.

Table 3.3. General and Metabolic Characteristics

Variable	SD	WD	SD+IPA	WD_IPA
Heart (mg)	146±3.1 [a,b]	155±5.4 [a]	130±4.8 [b]	161±7.1 [a]
Spleen (mg)	109±9 [a]	139±8 [a]	100±8 [b]	138±11 [a]
Cecum (mg)	284±24 [a]	233±19 [a]	302±14 [a] p=0.057 vs WD	237±17 [a] p=0.091 vs SD+IPA
Colon Length (cm)	5.8±0.2 [a]	5.7±0.1 [a]	5.9±0.1 [a]	5.7±0.2 [a]
Epididymal Fat (mg)	1525±152 [a]	2409±245 [b,c]	2102±154 [a,b]	2857±156 [c]
Subcutaneous Fat (mg)	597±42 [a]	1876±119 [b]	758±86 [a]	1372±141 [c]
Mesenteric Fat (mg)	623±60[a]	1189±114[b]	650±70[a]	1220±109[b]
PVAT (mg)	35±4 [a,c]	49±4 [a,b]	27±2 [c]	56±6 [b]

Values are in mean±SEM. *PVAT* perivascular adipose tissue, n=11-12/group. Statistical analysis was performed using one-way ANOVA with Tukey's post hoc test. Data with different superscript letters are significantly different ($p<0.05$).

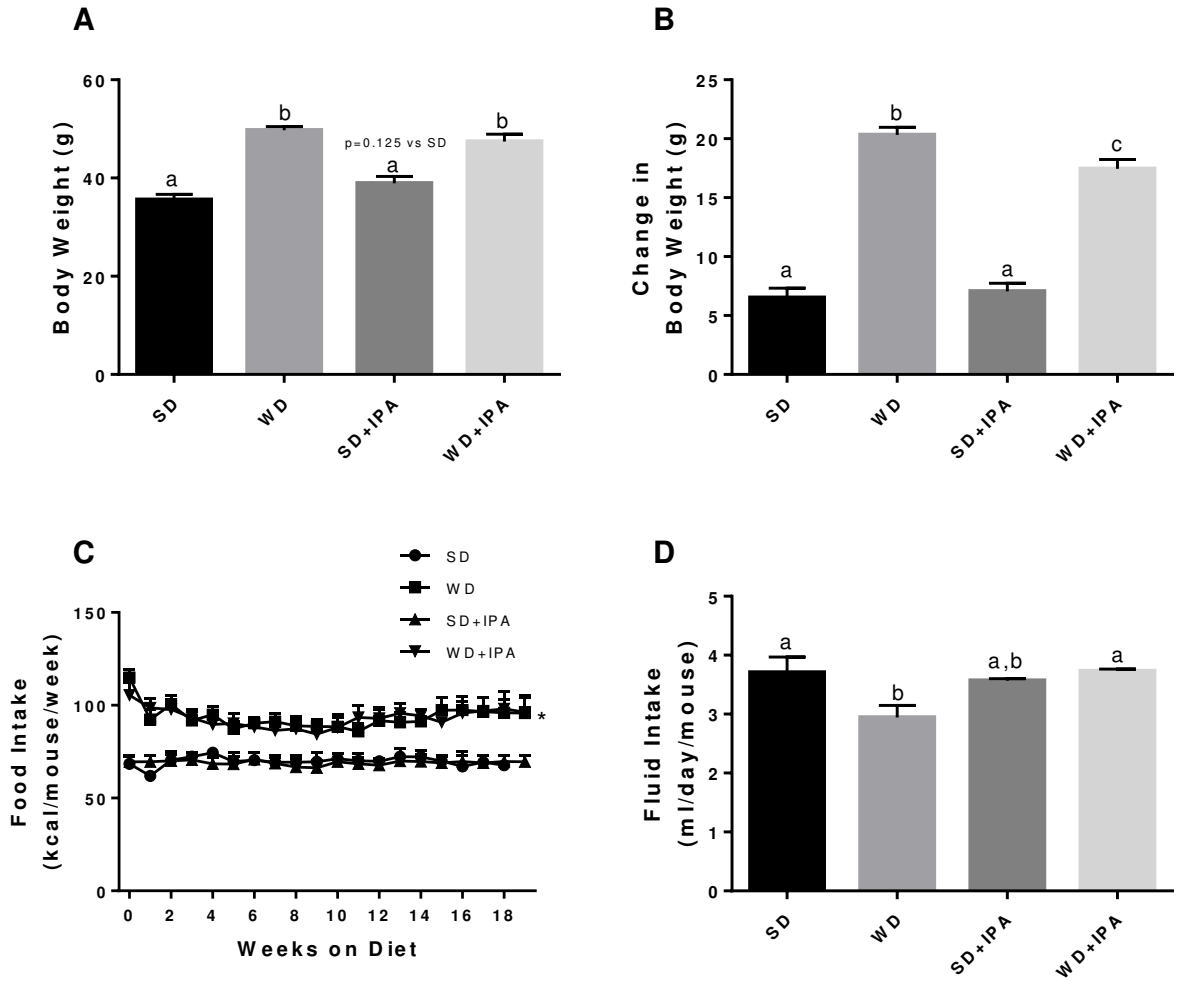

Figure 3.1. Western diet (WD) feeding increases body weight. A) body weight (in g) of animals fed a standard diet (SD) or WD with or without indole-3-propionic acid supplementation (IPA) at the 5-mo time point, B) Body weight change (in g) of animals calculated from baseline and 5-mo weights, C) food intake over the 5mo feeding and treatment period, D) average fluid intake over the course of the 5mo feeding and treatment period. Data are expressed as means ± SEM; n= 11-12/group. Statistical analysis was performed using one-way ANOVA with Tukey's post hoc test. *p<0.05 vs both SD groups.

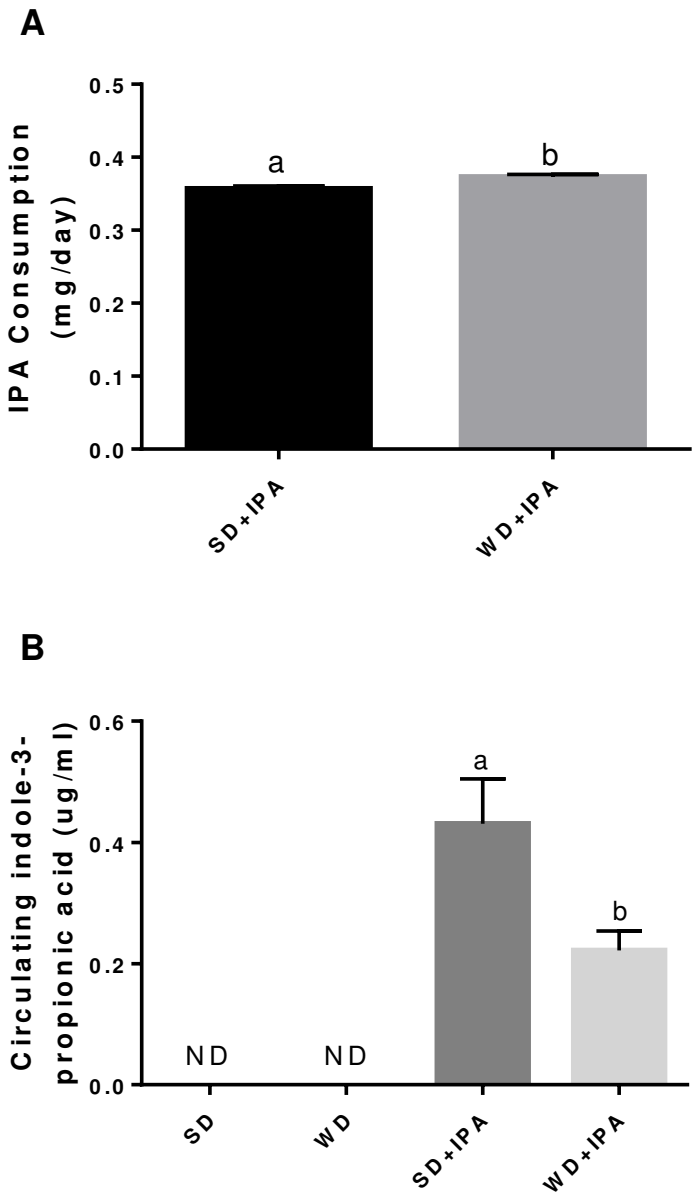

Figure 3.2. IPA consumption increases circulating levels. A) average IPA consumption over the course of the 5mo feeding and treatment period, B) circulating levels of IPA in plasma measured via HPLC. Data are expressed as means ± SEM; n= 11-12/group. Statistical analysis was performed using Student's t-test. Data with different superscript letters are significantly different ($p<0.05$).

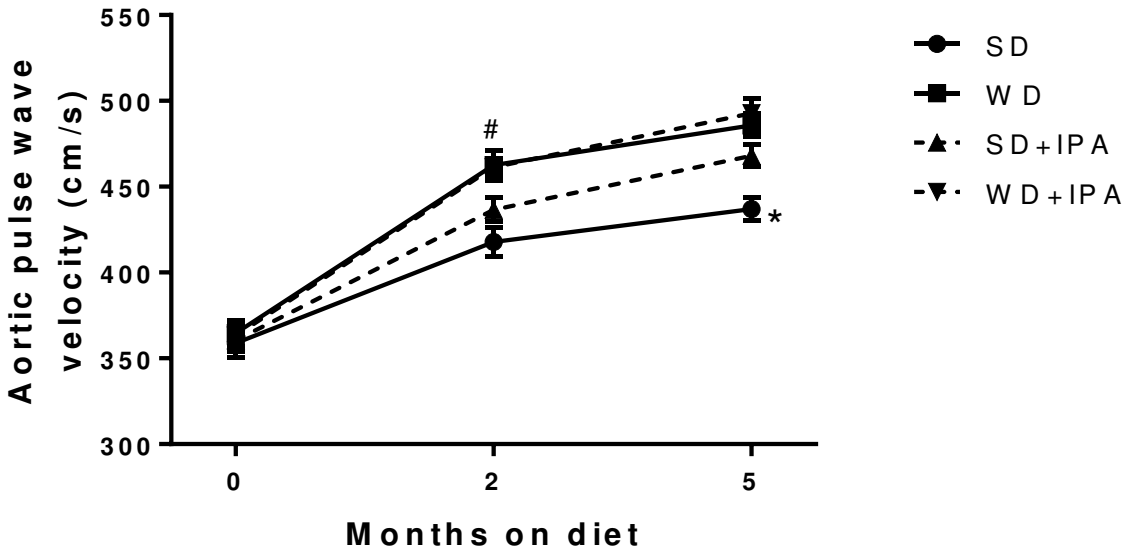

Figure 3.3. IPA does not affect western diet-induced arterial stiffness but increases stiffness in SD. Arterial stiffness measured by aPWV at baseline, 2mo, and 5mo of feeding and treatment. Data are expressed as means ± SEM; n= 11-12/group. Statistical analysis was performed using one-way ANOVA with Tukey's post hoc test. #$p<0.05$ for both WD groups vs. SD, *$p<0.05$ vs all other groups.

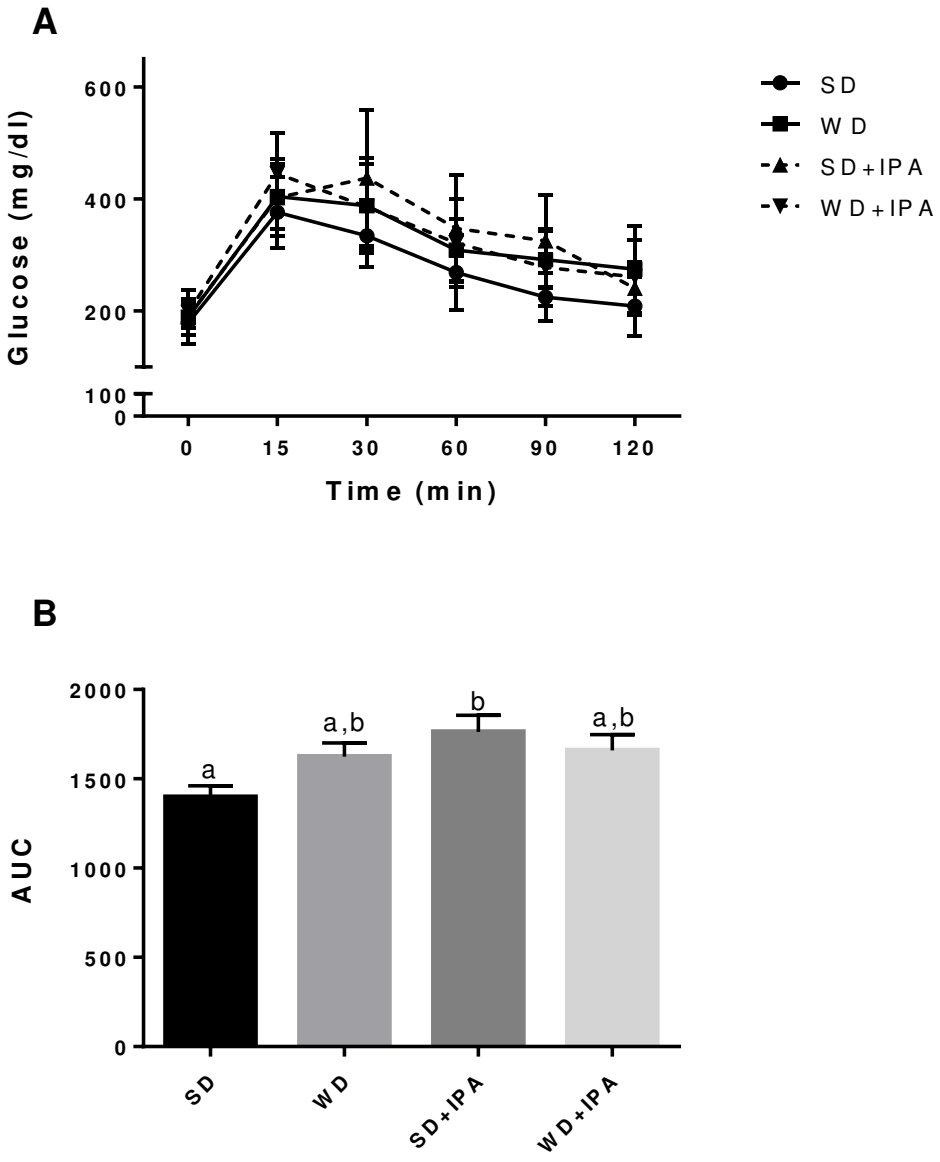

Figure 3.4. IPA supplementation worsens glucose tolerance in SD. A) Data are expressed as means ± SEM; n= 11-12/group. Statistical analysis was performed using one-way ANOVA with Tukey's post hoc test. Data with different superscript letters are significantly different ($p<0.05$).

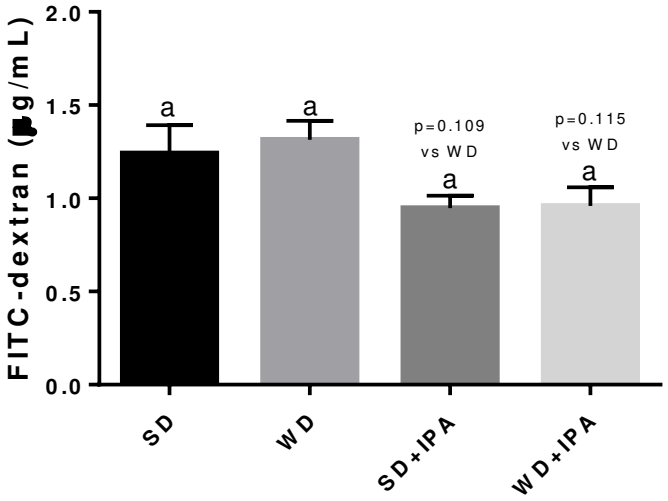

Figure 3.5. IPA does not alter gut barrier function. Intestinal permeability assessed by FITC-dextran 4hr post gavage at 5mo feeding and treatment period. Data are expressed as means ± SEM; n= 11-12/group. Statistical analysis was performed using one-way ANOVA with Tukey's post hoc test. Data with different superscript letters are significantly different ($p<0.05$).

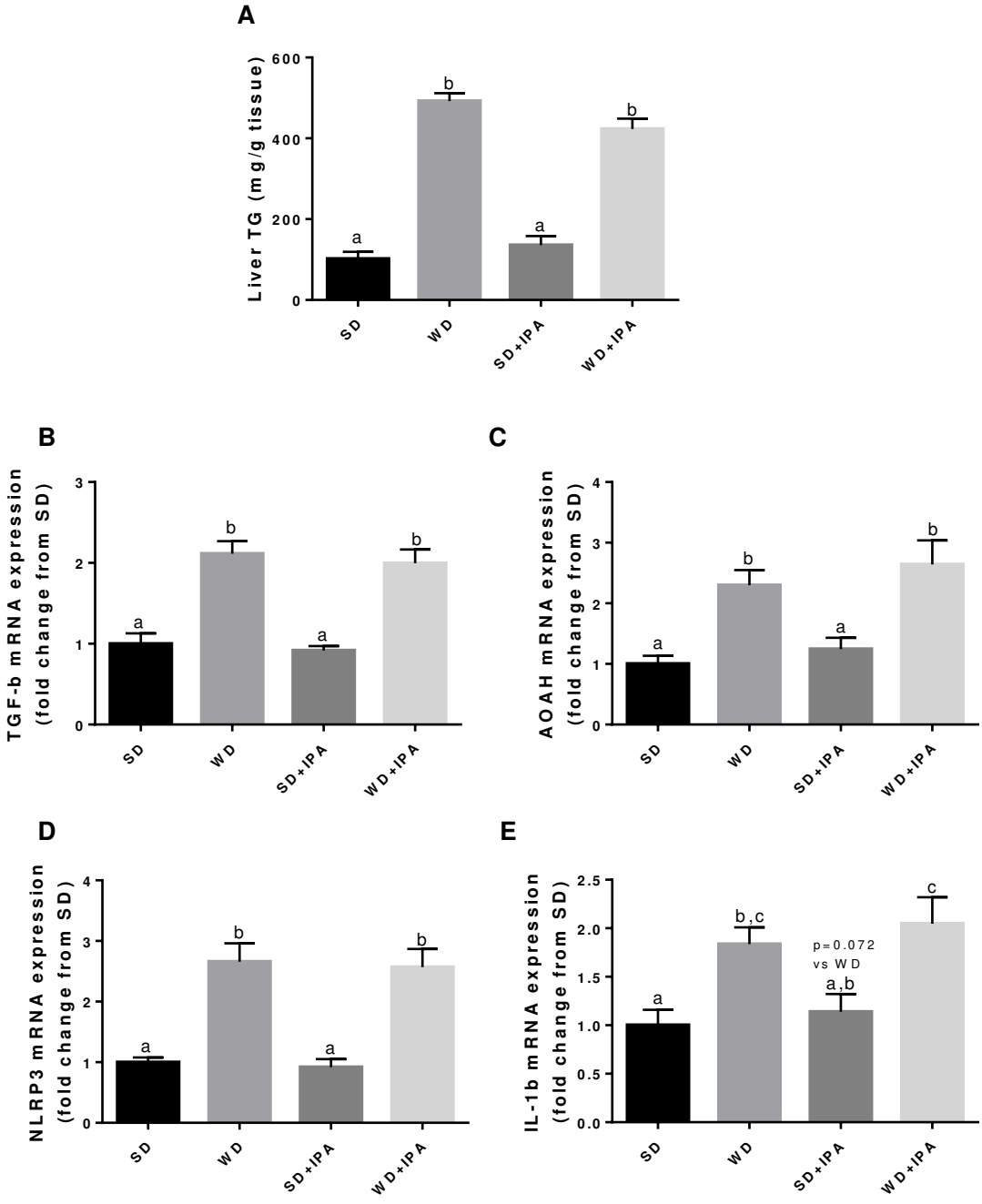

Figure 3.6. Western Diet (WD) feeding increases liver triglycerides and makers of inflammation. Liver A) triglycerides expressed as mg/g of tissue, B) expression of TGF-b, C) expression of AOAH, D) expression of NLRP3, and E) expression of IL-1b. Data are expressed as means ± SEM; n= 10-12/group. Statistical analysis was performed using one-way ANOVA with Tukey's post hoc test. Data with different superscript letters are significantly different ($p<0.05$).

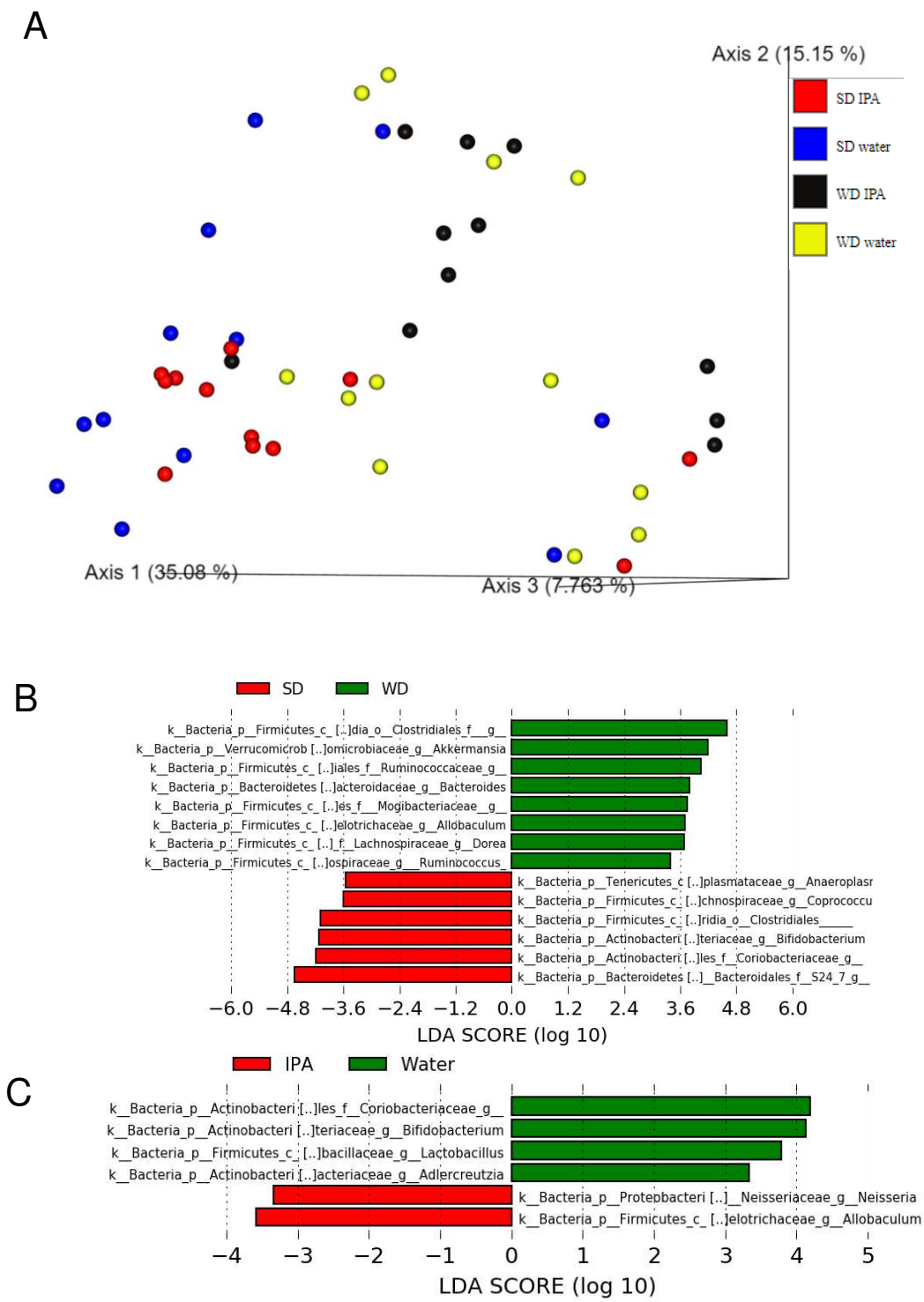

Figure 3.7. Western diet feeding drives changes in the gut microbiota. A) PCoA plot showing Bray-Curtis distances of mouse fecal microbiota species level communities colored by diet and treatment, B) LDA scores of differentially abundant taxa showing enrichment of taxa in the SD (red) and WD (green), C) LDA scores of differentially abundant taxa showing enrichment of taxa in the IPA supplemented groups (red) and non-supplemented groups (green), FDR was set to α<0.05.

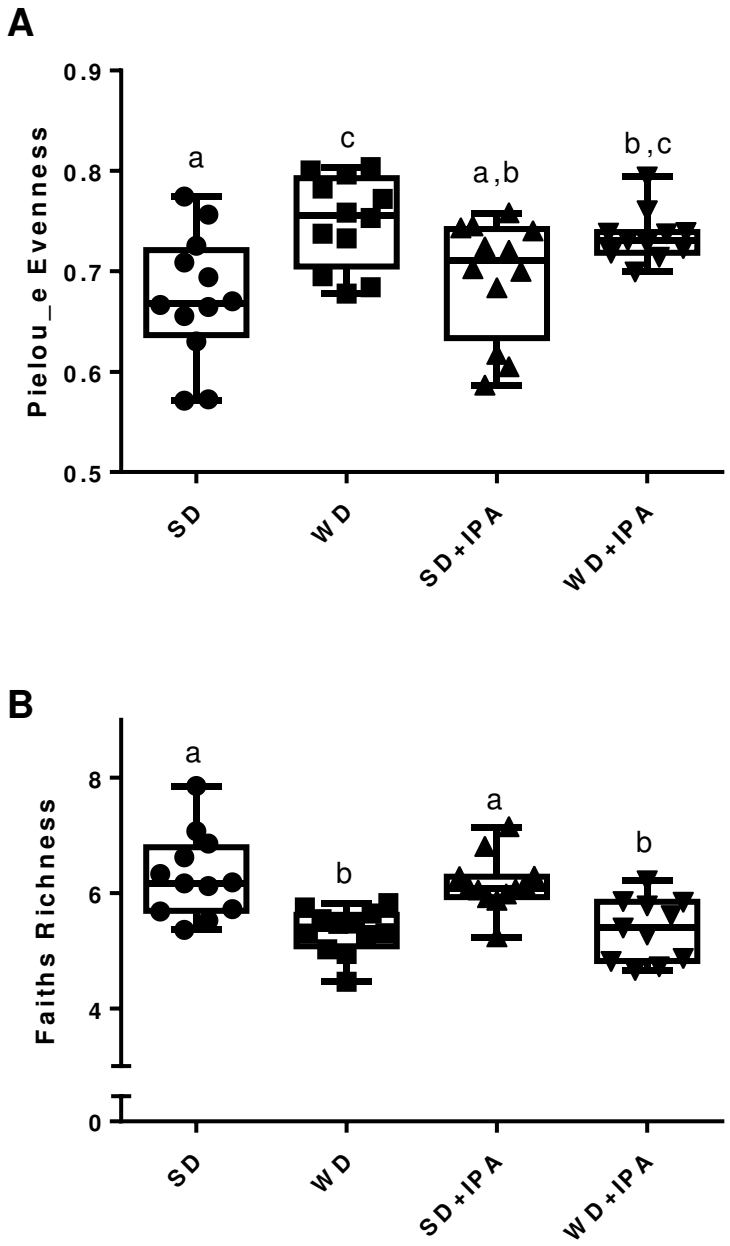

Figure 3.7. Western diet feeding drives changes in the gut microbiota alpha-diversity. A) Pielou_e plot showing evenness estimates of mouse fecal microbiota samples and B) Faiths Richness of mouse fecal microbiota samples. Box represents 25-75th percentiles, median values are represented by boxplot internal line and ranges by whiskers; n= 10-12/group. Statistical analysis was performed using Kruskal-Wallis test. Data with different superscript letters are significantly different ($p<0.05$).

CHAPTER 4: THE HUMAN GUT MICROBIOTA MODULATES VASCULAR DYSFUNCTION IN GNOTOBIOTIC MICE

Summary

Background/Aims: Obesity rates continues to rise and pose a significant health crisis in the United States. Obese individuals are at higher risk of cardiovascular disease (CVD). The gut microbiota is altered in obesity and data from our lab provides evidence for the role of the gut microbiota in the development of vascular dysfunction, which precedes CVD. The aim of the current study was to determine if the human gut microbiota can directly modulate vascular function. *Methods*: Lean and obese human subjects were recruited, measurements of vascular function obtained, and fecal samples were collected. In humans, arterial stiffness was measured via carotid-femoral pulse wave velocity (cfPWV) and endothelial function assessed via reactive hyperemia index (RHI). Two female subjects were selected to serve as donors. Male and female germfree mice were colonized for 14-18wk with the gut microbiota of a lean or obese females without and with vascular dysfunction, respectively. Both groups of mice (n=10/group) were provided with *ad libitum* access to sterile food and water. Glucose tolerance was assessed after a 6 hour fast followed by intraperitoneal injection of 2g/kg glucose solution. Prior to termination, arterial stiffness was measured via aortic pulse wave velocity (aPWV) and immediately after termination, endothelial function was assessed via pressure myography in isolated mesenteric arteries. *Results*: Obese human subjects had significantly higher blood pressure (obese: 126±4.4/76±2.0 vs lean: 114±2.2/68±2.4 mmHg, $p<0.05$), cfPWV (obese: 7.6±0.3 vs lean: 6.2±0.2 m/s, $p<0.05$), and displayed endothelial dysfunction measured by RHI (obese: 1.7±0.4 vs lean: 2.2±0.1, $p<0.05$). Transplantation of human gut microbiota to germfree mice did not alter body weight (lean: 22.5±0.8 vs obese: 23.7±0.8 g, $p>0.05$) or aPWV (lean: 400±9.1 vs obese: 413±13.8 cm/s, $p>0.05$) at the end of the study. However, the obese gut

microbiota significantly impaired endothelium-dependent dilation (lean: 324±27 vs obese: 202±37 AUC, $p<0.05$) and induced glucose intolerance (lean: 1210±72 vs obese: 1577±175 AUC, $p=0.08$). *Conclusions*: These result demonstrate that the obese human gut microbiota contributes to the development of endothelial dysfunction, independent of weight gain.

Introduction

The worldwide obesity epidemic continues to plague the health of humans. In the United States (US), over one third of the adult population is considered obese and by 2030 it is estimated that 51% of the population will be obese (58). Individuals with obesity are at heightened risk for cardiovascular disease (CVD) (119), the leading cause of death in the US and worldwide (16). This is particularly concerning given the aforementioned projected rates of obesity. Thus, identifying and understanding the mechanisms by which obesity leads to CVD continues to be a critical area of research.

One of the key features that links obesity to CVD is the development of vascular dysfunction characterized by 1) arterial stiffness and 2) endothelial dysfunction. Vascular dysfunction in obesity occurs prior to overt CVD (175) and strongly predicts future cardiovascular events and mortality (116, 185). It has been suggested that chronic low-grade inflammation observed in obese individuals contributes to the pathogenesis of vascular dysfunction (161, 179). While obese individuals display increased circulating inflammation (99), localized inflammation also occurs directly in the vascular tissue that contributes to vascular dysfunction (156, 180). A seminal study by Cani et al. posited that alterations in the gut are the initiating factor in obesity-related metabolic dysfunction (28) which may also represent a critical link in obesity-related vascular dysfunction.

The gut microbiota consists of trillions of microorganisms that reside in the intestinal tract and regulate many aspects of human physiology (120). Obese individuals display alterations in gut microbiota composition (102), termed gut dysbiosis. These alterations have been suggested to alter intestinal and metabolic homeostasis (29, 30, 146). For example, early studies linking

the gut microbiota and obesity showed a shift in favor of Firmicutes over Bacteroidetes (102) and colonization of germfree mice with the gut microbiota from obese humans resulted in greater adiposity compared to lean donors (173). Several studies have also suggested that the gut microbiota may influence cardiovascular outcomes (23) including hypertension (2), postinfarction cardiac repair (168), and thrombosis risk (198). Changes to the gut microbiota and in particular, alterations in gut tight junction proteins or barrier function precede increases in blood pressure (141), providing further evidence in support of the gut microbiota mediating cardiovascular diseases. However, limited data exists linking the gut microbiota to vascular dysfunction.

In one of the first reports to show a link between the gut microbiota and vascular function, Vikram et al. utilized gut microbiota transplantations and antibiotics to demonstrate that gut dysbiosis can induce endothelial dysfunction (178). Additionally, germfree mice lacking a commensal gut microbiota are protected against angiotensin II-induced endothelial dysfunction (83). In a proof of concept model, our lab has previously shown that suppression of gut dysbiosis in western diet-fed mice reverses vascular dysfunction, including both arterial stiffness and endothelial dysfunction (12). Unpublished data from our lab utilizing fecal transplantation from obese mice to lean mice suggests that obesity-related alterations in the gut microbiota elicit arterial stiffening.

Collectively these data suggest that the gut microbiota is a critical mediator of vascular function. A growing number of studies have started to examine the causative role of the human gut microbiota in mediating disease progression including irritable bowel disease (21), prior dietary practices (68), salivary amylase gene variations (127), or inflammation and nonalcoholic fatty liver disease (159). However, no studies have examined a causative role of the human gut microbiota in relation to vascular function. Therefore the aim of the present study was to test the hypothesis that the human gut microbiota can directly modulate vascular function, including both endothelial function and arterial stiffness. We hypothesized that colonizing germfree mice with

the gut microbiota from obese subjects with impaired vascular function, but not the microbiota from lean subjects with normal vascular function, would induce vascular dysfunction in germfree mice.

Methods

Human Studies.

Study Population. Men and women 30 to 50 years of age and with a BMI (kg/m^2) of 20-24.9 or 30-34.9 were recruited to participate in this study. Exclusion criteria included subjects that were actively trying to alter body weight, currently smoking, heavily drinking alcohol (>12 drinks/week for men and >8 drinks/week for women), pregnant or breastfeeding, taking antibiotics, commercial probiotic or prebiotic supplements, or certain prescription medications that affect cardiovascular function, and previous diagnosis of hyperlipidemia, diabetes, kidney or renal disease, or any intestinal diseases.

Participant Recruitment. Participants were recruited from the greater Fort Collins, Colorado area through Colorado State University email and flyer distribution between August 2018 and January 2019. Individuals were instructed to email or call to indicate interest, and were then pre-screened using a series of questions regarding their health and medical history to determine eligibility over the phone. Eligible participants were invited for an onsite visit at the Colorado State University Food & Nutrition Clinical Research Laboratory where they provided written informed consent, and inclusion and exclusion criteria were confirmed. After informed consent was obtained, brief self-administered health and diet history questionnaires were completed, followed by anthropometric measurements (e.g. height, weight, and waist and hip circumferences) to confirm BMI. Qualified participants then underwent a 10-minute supine rest in a quiet, dimly-lit room prior to blood pressure assessment. Supine brachial blood pressure and hemodynamics were measured in triplicate, with each measurement separated by one minute of rest, using the SphygmoCor XCEL system (AtCor Medical, Inc.). A detailed schematic

of participant recruitment and enrollment is provided in Figure 4.1**.** A total of 37 individuals responded to the advertisements, 22 of which met inclusion criteria through the phone prescreening and completed the onsite visit. Of those 22 individuals, 20 met inclusion criteria, agreed to partake in the study, and completed all protocol-specified procedures. From there, 10 individuals were from the top and bottom tertiles of vascular function were selected for the study. This trial was conducted in accordance with the Declaration of Helsinki and was approved by the Colorado State University Institutional Review Board (protocol #18-7882H).

Study Design. The study consisted of one experimental visit lasting for ~2 hours. Prior to the experimental visit, participants were instructed to refrain from exercise for 24 hours, over-the-counter and prescription medications, smoking, alcohol or caffeine-containing beverages, and food for 12 hours. Participants were allowed to consume water prior to the study visit. The primary outcome measures for this study were endothelial function measured by reactive hyperemia index (RHI) and arterial stiffness measured by carotid-femoral pulse wave velocity (cfPWV). cfPWV is a validated method and considered the gold standard for assessing arterial stiffness (35). RHI is a validated measure of microvascular endothelial function that is predictive of atherosclerosis and future cardiovascular events (17, 140). Secondary outcome measures included augmentation index [AIx] and AIx@75, hemodynamics (brachial and aortic systolic blood pressure, diastolic blood pressure, pulse pressure, heart rate, mean arterial pressure, and augmented pressure).

Anthropometrics. Height without shoes was measured using a scale-mounted stadiometer to the nearest 0.5 cm and weight was assessed using a digital scale (Health o Meter Professional, Sunbeam Products, Ibc). BMI was calculated as weight in kilograms divided by height in meters^2. Midabdominal waist circumference and hip circumference were measured using a Gulick fiberglass measuring tape with a tension handle (Creative Health Products, Inc.).

Assessment of Blood Pressure, Arterial Stiffness and Related Hemodynamics. At the beginning of the testing visit and following 10 min of supine rest, brachial and aortic blood pressure, central hemodynamics (e.g., aortic mean arterial pressure, aortic pulse pressure) and AIx were measured in the non-dominant arm using the SphygmoCor XCEL system (AtCor Medical, Inc.), and the mean value of three measurements was used for analyses. Since AIx can be significantly affected by heart rate, the index was corrected for a standard heart rate at 75 beats per minute (AIx@75). Aortic stiffness was assessed by measuring cfPWV also using the SphygmoCor XCEL and in the supine position (80, 186). Carotid waveforms were simultaneously captured using applanation tonometry of the left carotid artery, and a femoral pulse waves were captured by sphygmomanometry of the left thigh using a thigh blood pressure cuff. The tonometer was positioned at the site of the carotid pulse, while the femoral cuff was placed at mid to upper thigh. Distance between the suprasternal notch and the carotid pulse site, the suprasternal notch to the top/proximal edge of the femoral cuff, and the femoral pulse site to the top/proximal edge of the femoral cuff were measured with a nonelastic measuring tape. While remaining in the supine position, participants were asked to breathe steadily and remain relaxed to facilitate an optimal carotid pulse tonometry measurement. Once a regular carotid pulse was detected, femoral pulse waves were collected simultaneously by partially inflating the thigh cuff to 80 mmHg. cfPWV was then determined by calculating the ratio of the distance between the pulse measuring sites to the transit time between the carotid and femoral pulse waves, which is automatically determined by the SphygmoCor XCEL system and is expressed as distance over transit time (i.e. meters/second). Three measurements were obtained and averaged for analyses.

Assessment of Vascular Endothelial Function. To assess vascular endothelial function, digital artery endothelium-dependent vasodilation was used via a non-invasive, reproducible plethysmographic procedure (EndoPAT2000, Itamar Medical, Ltd) in accordance with conditions

specified by the manufacturer (20, 72, 114, 140). Participants were placed in a supine position for 10 minutes of rest, and then pneumatic finger-tip probes were placed on the index finger of each hand and a blood pressure cuff was placed on the experimental (non-dominant) upper arm in a quiet, dimly-lit, temperature-controlled room. The other arm served as a contralateral control, and both arms rested on arm rests during the procedure. Baseline recording of pulse wave amplitude from both fingers were recorded for 5 minutes. The blood pressure cuff on the experimental arm was then inflated to suprasystolic pressure (i.e., 200 mmHg or 60 mmHg higher than the participants' systolic blood pressure) for 5 minutes to occlude blood flow of the brachial artery. The cuff was then deflated to induce reactive hyperemia and post-occlusion peripheral arterial tonometry (PAT)-signals were recorded for an additional 5 minutes in both arms. RHI, an index of flow-mediated dilation, was derived as the ratio of the average pulse wave amplitude during hyperemia (60 to 120 sec of post-occlusion period) to the average pulse wave amplitude during baseline in the occluded hand, divided by the same value in the control hand and then multiplied by a baseline correction factor. An RHI of <1.67 was defined as the cutoff value for endothelial dysfunction (166).

***Blood and stool sample collection and analyses*.** Immediately after vascular testing and while participants were still in the fasted state, blood was collected from an antecubital vein using a 21G butterfly needle. Blood was collected in vacutainers with a serum clot activator (Greiner Bio-One lithium heparin tubes) for measurement of lipid and lipoprotein levels and a comprehensive metabolic panel with a blood chemistry analyzer (Piccolo Xpress, Abaxis) using manufacturer procedures. Blood was also collected into EDTA (BD Biosciences) vacutainers for separation of plasma, and then centrifuged according to the manufacturers' instructions, aliquoted, and stored at -80°C for later analysis. Hemoglobin A1c (HbA1c) levels were measured using whole blood from EDTA tube with an analyzer system (Alere Afinion Analyzer System, Abbott). Participants self-collected fresh stool, which they stored at 4°C, and brought to

the clinic within 24 hours for processing. Briefly, stool samples were suspended in reduced sterile PBS with 10% glycerol and stored at -80°C until use in animal studies.

Animal Studies.

Experimental design. Male and female C57BL/6J mice were bred and maintained in a germ free facility at the University of Colorado Anschutz Gnotobiotic Facility and given *ad libitum* access to a standard diet (SD; 2020SX, Envigo, Indianapolis, IN) as shown in Table 1. Germ free isolators were routinely tested for sterility by culturing and pan-bacterial 16S rRNA gene PCR analysis of feces. Mice were co-housed 2-4 per cage in a temperature- and humidity-controlled environment on a 12h:12h light-dark cycle. All animal procedures were reviewed and approved by the University of Colorado and Colorado State University Institutional Animal Care and Use Committee. We selected two human female donors, one from the lean and one from the obese group with the best and poorest vascular measures. Colonization of germ free mice was performed using a lean or obese single donor human fecal samples resuspended in sterile, reduced PBS. Each mouse was inoculated once by oral gavage with 200μl of the lean or obese fecal sample under sterile conditions (n=10 per group) and allowed to colonize for 14-18 weeks. Mice received normal autoclaved drinking water. Body weight and food intake were recorded weekly.

Gut Permeability. 2 weeks prior to termination, mice were water-fasted for 12 hours during the dark cycle prior to oral gavage with a 125mg/ml FITC-dextran (4,000 mol. wt.) (Sigma-Aldrich, #46944) solution diluted in sterile 1x PBS for a goal dose of 600mg/kg of FITC-dextran. Food was removed immediately after oral gavage and blood was collected 4 hours later via mandibular vein for quantification of plasma FITC-dextran concentration. Plasma samples were diluted 1:2 in 1x PBS and fluorescence was measure on a spectrophotometer at 485/20 (excitation) and 528/20 (emissions). Plasma concentrations were calculated based on a

standard curve of known FITC-dextran concentrations prepared in control plasma from untreated mice.

Glucose Tolerance Test. 1 week prior to termination, mice were food fasted for 6 hours and blood glucose was determined from tail-vein blood using AlphaTRAK 2 glucose meters (Abbott Laboratories, Chicago, IL). After baseline glucose readings (time point "0"), mice received an intraperitoneal injection of 2 g/kg glucose, and blood glucose levels were measured at 15, 30, 60, 90, and 120 min post injection.

Arterial Stiffness. Aortic pulse wave velocity (aPWV) was measured at 14-18 weeks post colonization and at least 20 minutes prior to termination. Mice were anesthetized using 2% isoflurane and oxygen at 2L per minute, placed supine on a heating board with legs secured to ECG electrodes, and maintained at a target heart rate of ~450 bpm by adjusting isoflurane concentration. Doppler probes (20MHz) (Mouse Doppler data acquisition system; Indus Instruments, Houston, TX) were placed on the transverse aortic arch and abdominal aorta and the distance between the probes was determined simultaneously with precision calipers. At least five consecutive 2-second recordings were obtained for each mouse and used to determine the time between the R-wave of the ECG and the foot of the Doppler signal for each probe site (Δtime). aPWV (in cm/s) was calculated as aPWV = (distance between the two probes) / ($\Delta time_{abdominal}$ - $\Delta time_{transverse}$).

Animal Termination and Tissue Collection. At 14-18 weeks post colonization, mice were anaesthetized with isoflurane and euthanized by exsanguination via cardiac puncture. The liver, along with the spleen, were immediately excised, weighed, and flash frozen for later analyses. Next, the intestinal tract was removed and placed on ice-cold physiologic saline solution (PSS: 0.288g NaH2PO4, 1.802g glucose, 0.44g sodium pyruvate, 20.0g BSA, 21.48g NaCl, 0.875g KCl, 0.7195g MgSO4 7H20, 13.9g MOPS sodium salt, and 0.185g EDTA per liter solution at pH 7.4). The colon and cecum were separated from the rest of the intestinal tract that remained on

ice-cold PSS during mesenteric artery isolation (see *Vascular Reactivity* section). Colon length was recorded, a 0.5cm section of the terminal colon was cut and placed in RNA-later (Qiagen, #76104), and 0.5cm section of the proximal colon was cut and fixed in 10% formalin for 24 hours then held in 70% ethanol. Next, the cecum was weighed, a portion of tissue was removed closest to the proximal colon and placed in RNA-later and the remaining colon and colon contents were flash frozen separately. The thoracic aorta was excised and cleaned of surrounding perivascular adipose tissue (PVAT) on ice-cold PSS. A 1mm segment of proximal aorta was frozen in optimal cutting temperature (OCT) media for later analysis. The remainder of the aorta and PVAT were flash frozen and stored at -80°C for biochemical analyses. The heart was weighed and flash frozen. Adipose tissue (subcutaneous, epididymal, and mesenteric depots) were isolated, weighed, and flash frozen. Lastly, the gastrocnemius and soleus muscles were isolated and flash frozen. All adipose and muscle depots that were flash frozen for later use were harvested from the right side of the animal for consistency.

Vascular Reactivity. Vascular function was determined as previously described (11, 97). Briefly, second-order mesenteric arteries were placed in pressure myograph chambers (DMT Inc., Atlanta, GA) containing warm PSS, cannulated onto glass micropipettes and secured with suture. Arteries were equilibrated for 1 hour at 37°C and an intraluminal pressure of 50 mmHg. Arteries were constricted with increasing doses of phenylephrine (PE: 10^{-9} to 10^{-5} M) followed immediately by a dose-response with endothelium-dependent dilator acetylcholine (ACh: 10^{-9} to 10^{-4} M). We have previously established that arteries maintain constriction to PE for the duration of experiments and that dilation is not spontaneous. If arteries do spontaneously dilate during the constriction period (i.e. 5-12 minutes), data are not included. After a washout period, a dose-response to endothelium-independent dilator sodium nitroprusside (SNP: 10^{-10} to 10^{-4} M) was obtained after pre-constriction to PE (10^{-5} M). Percent dilation was calculated based on the maximal luminal diameter of each artery.

Statistics. Data are expressed as mean ± SEM. Statistical analysis was performed using a Student's t-test (SPSS for Windows, Release 25.0.0.1; SPSS, Chicago, IL, USA). A p-value of <0.05 was considered statistically significant.

Results

Subjects recruited in the obese group displayed significantly higher BMI, systolic and diastolic blood pressure, arterial stiffness, and endothelial dysfunction compared to lean subjects (Table 4.2). There were no differences in age or HbA1c. We chose to take a "personalized" approach and selected two female individuals, one from the lean group with the best vascular measures and one from the obese group with the poorest vascular measures to use as fecal microbiota donors. The obese subject selected as a fecal microbiota donor displayed a BMI classified as obese, elevated systolic blood pressure, arterial stiffness, and endothelial dysfunction compared to the lean fecal microbiota donor subject (Table 4.3).

To assess whether the human gut microbiota could directly modulate host vascular function, we transferred fecal microbiota from the two human donors (Table 4.3) to germfree mice. Interestingly, we observed no differences in body weight over the duration of the inoculation period between lean and obese microbiota recipients (Figure 4.2A and B). Given the similarity in body weight, we characterized other general and metabolic features of the mice (Table 4.4). Adipose tissue mass for both epididymal and subcutaneous pads were similar between groups although the obese mice had significantly less perivascular adipose tissue surrounding the thoracic aorta. No differences in liver weight were observed but obese mice tended to have smaller heart and spleen weights. While no differences were observed in colon length, obese mice had significantly smaller cecum sizes (Table 4.4).

We next assessed vascular function of mice to determine if the gut microbiota can impact vascular function independent of body weight changes. Prior to termination, we measured arterial stiffness via aPWV and found no significant differences between the two

groups of mice (Figure 4.3). Immediately after termination we assessed vascular function in isolated mesenteric arteries via pressure myography. We observed no differences in constriction to phenylephrine (Figure 4.4A) but found that endothelium-dependent dilation (EDD) was significantly impaired in mice receiving the obese microbiota (Figure 4.4B and C). Conversely, endothelium-independent dilation (EID) was not altered by microbiota transplantation as both groups had similar smooth muscle cell responses to sodium nitroprusside (Figure 4.4D and E). To assess other metabolic effects of the gut microbiota, we subjected mice to an intraperitoneal glucose tolerance test. We found that mice receiving the obese microbiota displayed impaired glucose tolerance (Figure 4.5A and B). Collectively, these results suggest that the obese gut microbiota may directly modulate endothelial dysfunction independent of body weight changes.

Discussion

The primary findings of the current study were that germfree mice colonized with an obese human microbiota developed endothelial dysfunction and glucose intolerance independent of weight gain. In contrast to our hypothesis, we did not observe any differences in arterial stiffness between mice colonized with lean and obese microbiota. This was also in contrast to our human subjects who displayed differences in cfPWV in addition to endothelial dysfunction. Collectively, these results demonstrate and provide new evidence that the obese human gut microbiota contributes to the development of endothelial dysfunction, independent of weight gain. Our data extend the growing body of research linking the gut microbiota to the regulation of cardiovascular function and development of cardiovascular diseases (13).

Given the emerging link between the gut microbiota and host physiology (120), efforts to elucidate the upstream mechanisms of CVD have begun to focus on the contribution of the gut microbiota. Alterations in the composition of the gut microbiota, termed gut dysbiosis, have been observed in obesity (102). Early studies showed that the obese gut microbiota led to increased energy harvest and weight gain in colonized germfree mice (173). Interestingly, we did not

observe any significant changes in body weight in mice receiving the obese human microbiota. A few experimental similarities and differences should be considered between existing literature and our study design. In the first study to show transmission of the obese phenotype though the gut microbiota, Turnbaugh et al. utilized cecal microbiota from genetically obese ob/ob mice to induce weight gain in germfree mice. In the current study, we utilized human fecal microbiota. Later studies have indeed shown that fecal microbiota from twins discordant for obesity led to transmissible phenotypes whereby the obese microbiota induced increased body and fat mass in gnotobiotic mice (136). In contrast to these findings, Bruce-Keller utilized a murine obese-type gut microbiota transplantation from pooled cecal and colonic content to induce neurobehavioral changes but did not observe changes in body weight compared to control animals (24). Additionally, infant microbiota from lean or obese mothers induced liver inflammation and nonalcoholic fatty liver disease independent of body weight changes (159) and fecal microbiota transplants from obese or bariatric surgery patients to germfree mice did not alter body weight in mice after 2 weeks (171). Our lab has also previously shown from published and unpublished data that improvements in vascular function mediated by the gut microbiota occur independent of body weight changes (12). Regardless, further research is needed to address the specific mechanisms of the gut microbiota that produce an obese phenotype.

Previous studies have examined the role of the gut microbiota on endothelial function. Vikram et al. were among the first to show a link between the gut microbiota and endothelial function. Utilizing antibiotics, they demonstrated that microRNA-204 is remotely regulated by the gut microbiota and impairs aortic endothelial function by downregulating Sirtuin1 (178). Next, in a high-fat diet model, they show that elimination of gut dysbiosis with antibiotics partially restored endothelial function and rescued nitric oxide bioavailability by downregulating microRNA-204. Around the same time, Karbach et al. demonstrated the role of the gut microbiota in mediating angiotensin-II-induced endothelial dysfunction. Utilizing germfree mice, they demonstrated that the gut microbiota is required for angiotensin-II-induced endothelial

dysfunction in aortic rings, whereby germfree mice were protected from dysfunction (83). This protection was accompanied by reduced recruitment of accumulation of inflammatory myelomonocytic cells in the vasculature. In the current study we observed that the obese microbiota induced endothelial dysfunction independent of changes to smooth muscle cell function, a commonly observed observation (12, 178). Recently, our lab has also demonstrated that the gut microbiota mediates vascular function in mice. Utilizing a western-diet model, we found that suppression of gut dysbiosis with broad spectrum antibiotics reversed both endothelial dysfunction and arterial stiffness (12).

To the best of our knowledge, our lab is the first to examine the impact of the gut microbiota on arterial stiffness. Unpublished data from our lab found that the gut microbiota from genetically obese *ob/ob* mice induced arterial stiffness in control mice independent of weight changes. In the present study, we did not observe differences in arterial stiffness. While we can only speculate, it is possible that the duration of our microbiota colonization intervention was not long enough to induce changes in arterial stiffness and more specifically, structural changes to the aorta that are often associated with stiffening. Future biochemical analyses will need to be conducted to gain more insight into this observation. Regardless, our results compliment and extend previous findings liking the gut microbiota to vascular dysfunction. We demonstrated that the human gut microbiota mediates endothelial function independent of body weight changes.

In the progression of obesity, metabolic complications such as glucose intolerance develop. Therefore we also examined glucose tolerance by an intraperitoneal glucose tolerance test and found that the obese microbiota led to impaired glucose tolerance in mice. Recent data from human studies utilizing human to human microbiota transplantation also suggests that the gut microbiota can mediate glucose and insulin sensitivity (91, 183). Data utilizing human fecal transplants to germfree mice have also demonstrated a role of the gut microbiota in glucose intolerance (165). While not all studies have shown this effect (6), the observed effects of fecal

microbiota transplantation impacting glucose tolerance may be dependent on individual donors (165).

We realize the current study is not without limitations. Although germ free mice have some distinct differences in physiology (67, 101, 115), we chose to utilize germfree mice as they are a widely accepted model for studying the gut microbiota (70). We avoided the use of antibiotics given the known taste aversions that can lead to weight loss (135, 168) and potentially confound study findings. Although we utilized one diet for both groups of mice, consideration should be given to widespread use of various rodent diets with varying fiber contents when interpreting results between studies (87). Studies investigating the role of the gut microbiota utilizing microbiota transplantations have use both pooled and single donor approaches. We chose to utilize a single donor microbiota as a more “personalized” approach given that variation can exist in individual gut microbiota phenotypes (165) and controversy exits among using pooled inoculum with some data suggesting that one donor’s microbiota may outcompete another’s. Finally, we cannot exclude the factor of multiple users dissecting and harvesting tissues that may introduce unwanted variability in tissue weights. Nevertheless, the current study provides evidence that the human gut microbiota directly mediates vascular function in gnotobiotic mice. Future data collection and analyses will include data on true germfree mice, the effect of microbiota transplantation from male human donors, the effects of western diet exposure to lean and obese gut microbiota recipients, and numerous biochemical analyses to provide more mechanistic insight mediating the observed physiological outcomes.

Figures and Tables

Table 4.1. Diet composition

	Diet 2020sx
Carbohydrate (% kcal)	60
Crude Fiber (% by weight)	2.7
Neutral Detergent Fiber (% by weight)	12.3
Lipid (% kcal)	16
Protein (% kcal)	24
Energy (kcal/g)	3.1

Composition of the diet used in the duration of the experimental protocol.

Table 4.2. General and Vascular-related Characteristics in Human Subjects

Variable	**Lean**	**Obese**
Age	37±3 [a]	42±4 [a]
Male/Female	2/3	2/3
BMI	21.8±0.4 [a]	32±0.4 [b]
Systolic BP	114±2.2 [a]	126±4.4 [b]
Diastolic BP	68±2.4 [a]	76±2.0 [b]
cfPWV	6.2±0.2 [a]	7.6±0.3 [b]
RHI	2.2±0.1 [a]	1.7±0.4 [b]
HbA1c	5.1±0.1 [a]	5.1±0.1 [a]

Values are in mean±SEM. *BMI* Body Mass Index, *BP* Blood Pressure, *cfPWV* carotid to femoral pulse wave velocity, *RHI* reactive hyperemia index, n=5/group. Statistical analysis was performed using Student's t-test. Data with different superscript letters are significantly different ($p<0.05$).

Table 4.3. General and Vascular-related Characteristics of Human Donors

Variable	Lean	Obese
Age	44	48
Sex	Female	Female
BMI	23.2	32.6
Systolic BP	115	129
Diastolic BP	66	75
cfPWV	5.6	7.4
RHI	2.17	1.28
HbA1c	5.3	5.2

Values are in mean±SEM. *BMI* Body Mass Index, *BP* Blood Pressure, *cfPWV* carotid to femoral pulse wave velocity, *RHI* reactive hyperemia index, n=1/group.

Table 4.4. General and Metabolic Characteristics of Mice

Variable	Lean	Obese
Sex (M/F)	8/2	8/2
Liver (mg)	1144±50[a]	1110±36 [a]
Heart (mg)	116±5 [a]	105±2 [a] (p=0.067)
Spleen (mg)	81±3.4 [a]	74±2.4 [a] (p=0.09)
Cecum (mg)	573±39 [a]	478±19 [b]
Colon Length (cm)	6.3±0.2 [a]	6.05±0.1 [a]
Epididymal Fat (mg)	378±120 [a]	376±61 [a]
Subcutaneous Fat (mg)	211±36 [a]	221±29 [a]
PVAT (mg)	23.3±2 [a]	15.4±1.1 [b]

Values are in mean±SEM. *PVAT* perivascular adipose tissue, n=8-10/group. Statistical analysis was performed using Student's t-test. Data with different superscript letters are significantly different ($p<0.05$).

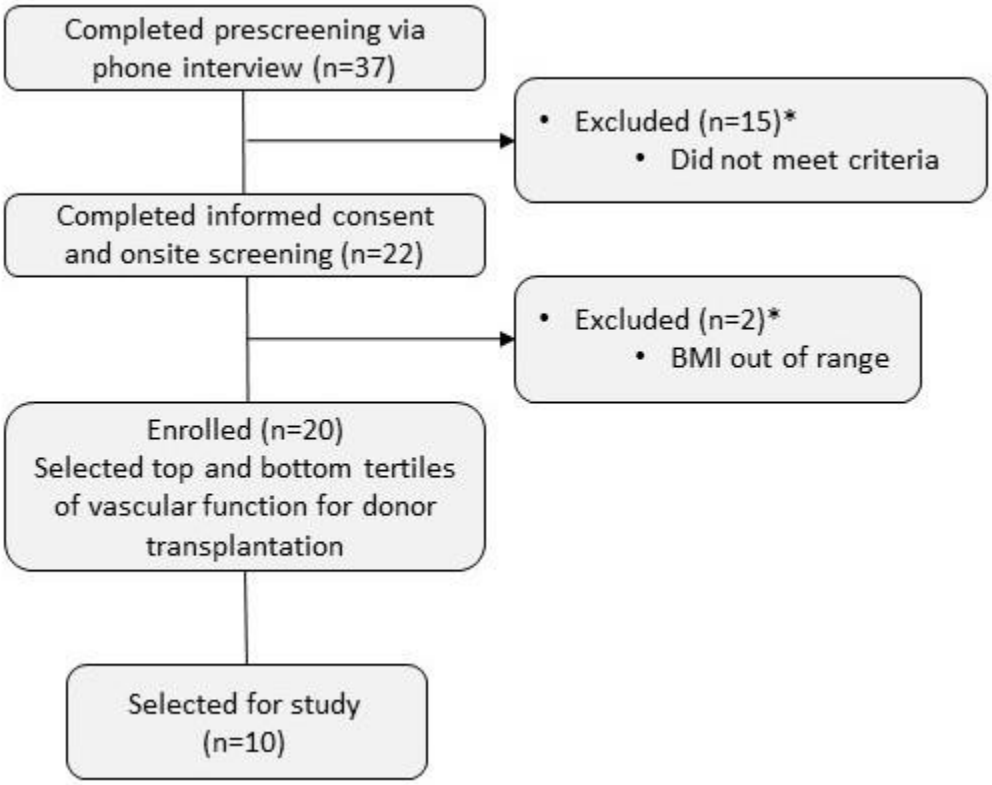

Figure 4.1. Schematic of human participant recruitment and enrollment. *BMI* body mass index.

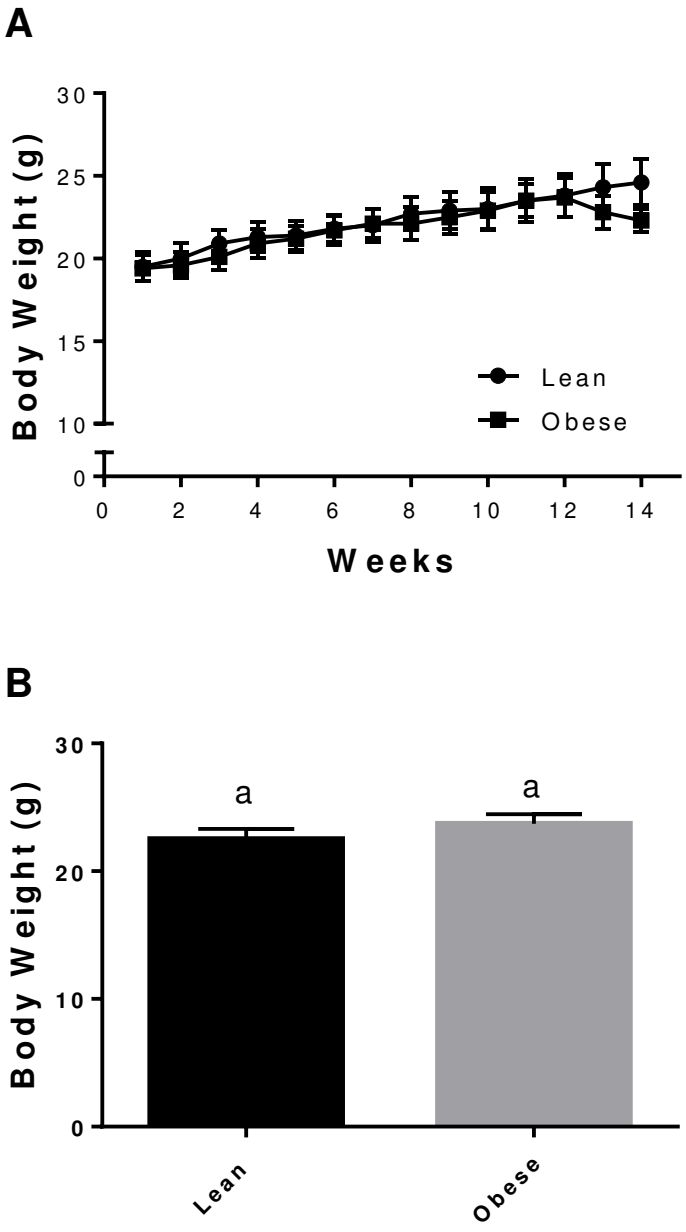

Figure 4.2. Microbiota transplantation does not affect body weight. A) body weight by week over the duration of microbiota transplantation, B) body weight at termination. Data are expressed as mean ± SEM, n=9-10/group. Statistical analysis was performed using Student's t-test. Data with different superscript letters are significantly different ($p<0.05$).

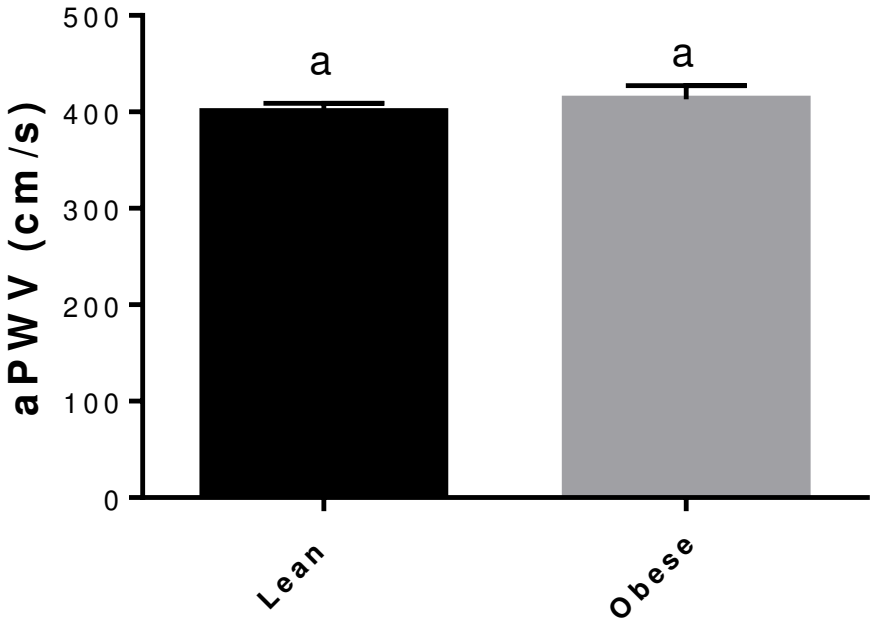

Figure 4.3. Microbiota transplantation does not affect arterial stiffness. Arterial stiffness measured by aPWV after 14-18wk of colonization and prior to termination. Data are expressed as mean ± SEM, n=10/group. Statistical analysis was performed using Student's t-test. Data with different superscript letters are significantly different ($p<0.05$).

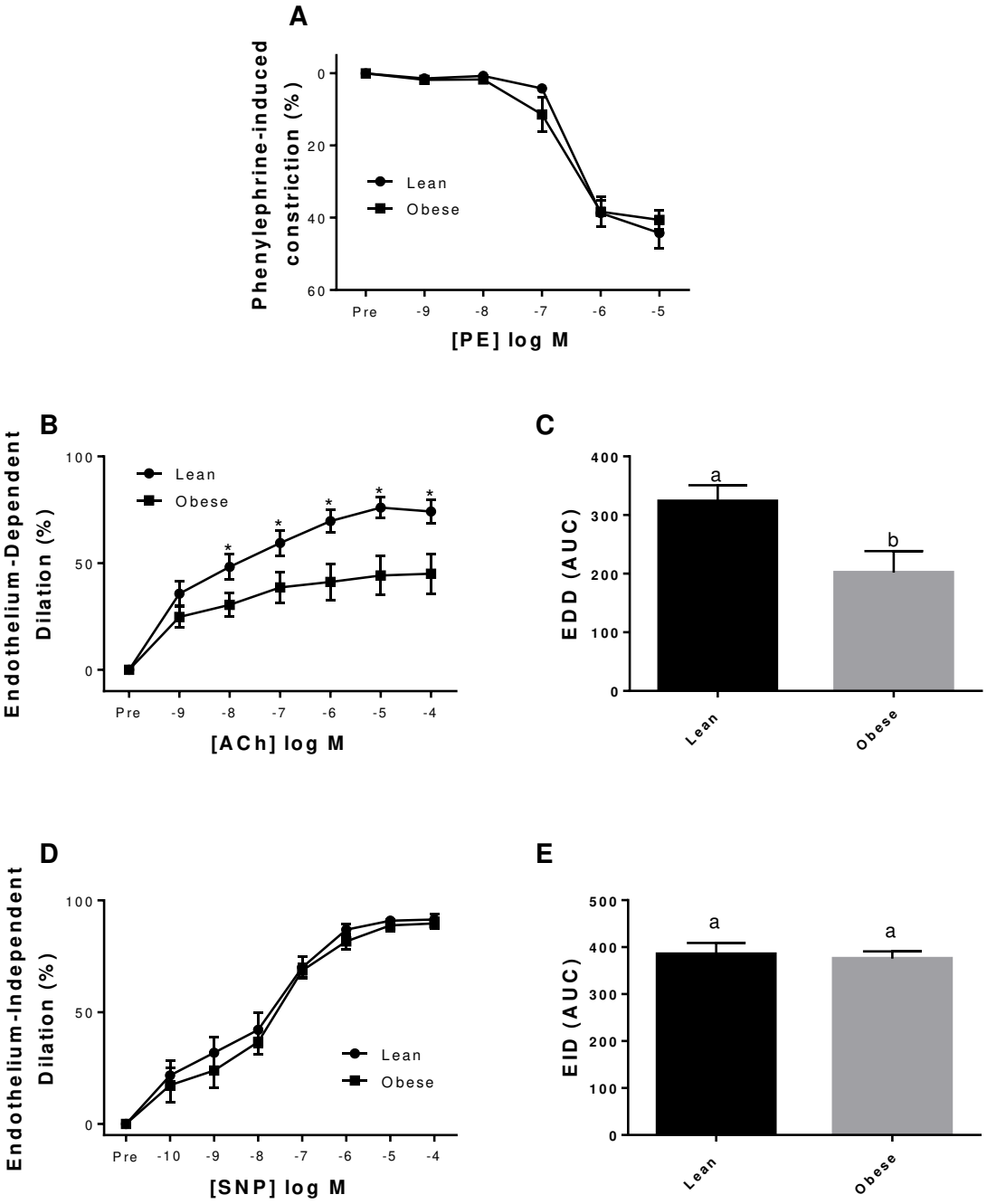

Figure 4.4. Microbiota transplantation from an obese subject leads to endothelial dysfunction. A) constriction to phenylephrine, B) endothelium-dependent dilation (EDD) to acetylcholine (ACh), C) area under the curve for EDD, D) endothelium-independent dilation (EID) to sodium nitroprusside (SNP) and E) area under the curve for EID. Data are expressed as mean ± SEM, n=7-10/group. Statistical analysis was performed using Student's t-test. Data with different superscript letters are significantly different ($p<0.05$) and *$p<0.05$.

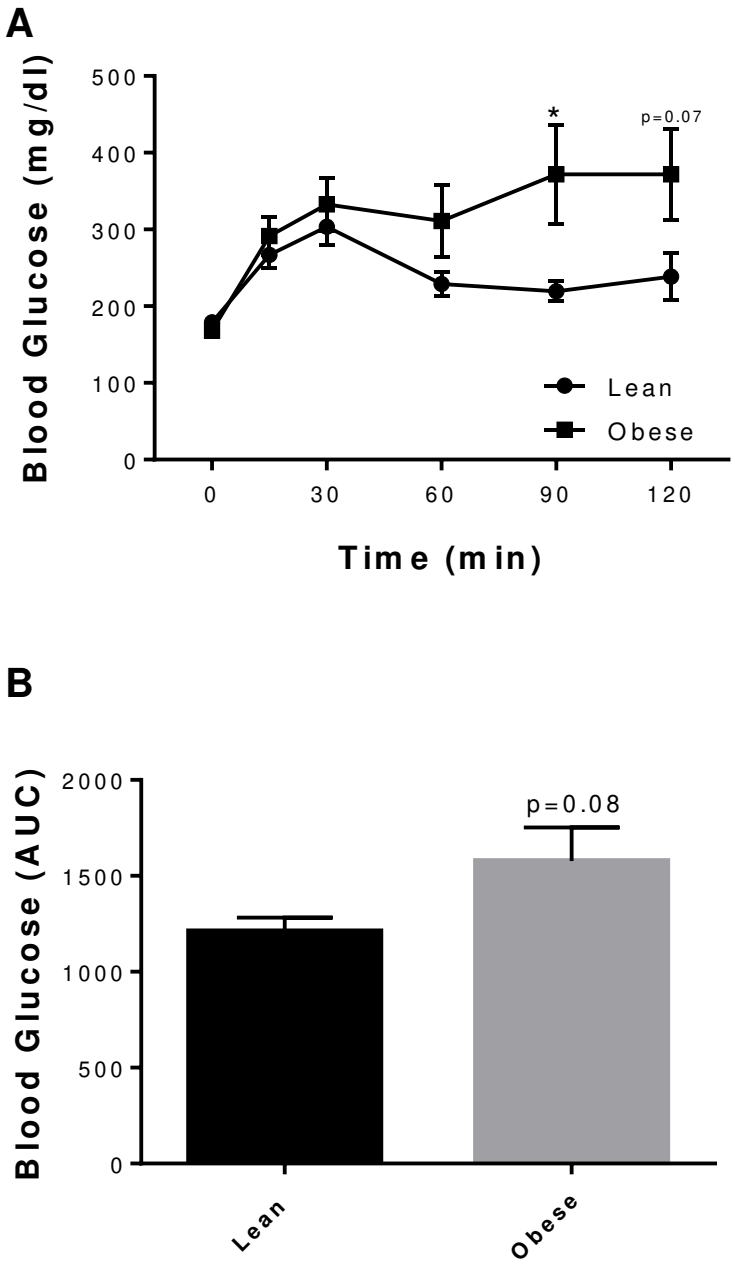

Figure 4.5. Microbiota transplantation from an obese subject leads to impaired glucose tolerance. A) intraperitoneal glucose tolerance test performed at time points 0, 15, 30, 60, 90, and 120 minutes, B) area under the curve for glucose tolerance test. Data are expressed as mean ± SEM, n=9-10/group. Statistical analysis was performed using Student's t-test, *p<0.05.

CHAPTER 5: SUMMARY AND FUTURE DIRECTIONS

The United States faces an epidemic of obesity and type 2 diabetes (T2D), both of which play a significant role in the prevalence of cardiovascular diseases (CVD). Vascular dysfunction occurs prior to overt CVD, and the development of vascular dysfunction in obesity and T2D strongly predicts future cardiovascular events and mortality. While the mechanisms of vascular dysfunction continue to be fully elucidated, an abundant body of research suggests that the gut microbiota mediate many cardiometabolic diseases. Thus, it is critical to elucidate the upstream mechanisms of vascular dysfunction and identify useful and cost effective treatments that beneficially target the gut microbiota in obesity or T2D to prevent or reverse vascular dysfunction.

The studies conducted as part of this dissertation research examined 1) the underlying causes of vascular dysfunction in models of obesity and T2D and 2) novel strategies to prevent or attenuate the development of vascular dysfunction in both obesity and T2D. First, we tested the hypothesis that the newest class of antidiabetic drugs, sodium glucose cotransporter 2 inhibitors (SGLT2i) would improve vascular function in genetically T2D mice. Results from this study show that treatment with the SGLT2i, dapagliflozin, improved mesenteric artery endothelial function and arterial stiffness in T2D mice. These changes were accompanied by a reduction in blood glucose and circulating markers of inflammation. While some alterations in the gut microbiota composition were observed in mice treated with dapagliflozin, the extent to which these alterations mediate the beneficial effects of SGLT2i on vascular function are unclear. Future studies should focus on the specific effects of SGLT2i on the gut microbiota to further examine this question.

Next, we tested the hypothesis that the gut microbial metabolite of tryptophan, indole-3-propionic acid (IPA), would improve vascular function in western diet (WD)-induced obese mice.

Utilizing a preventative approach by implementing a diet (WD) and treatment (IPA) concurrently, we found that WD-fed mice displayed increased body weight, arterial stiffness, and markers of liver inflammation, with no effect of IPA supplementation. Although some studies have shown beneficial effects of indoles, our study questions the salutary role of the specific tryptophan metabolite, IPA. Most research surrounding indoles has focused on intestinal health. More research is needed on the effects of specific indoles and their effects on cardiometabolic health outcomes.

Lastly, utilizing human microbiota transplants and germfree mice, we tested the hypothesis that colonizing germfree mice with the gut microbiota from obese female subjects with impaired vascular function, but not the microbiota from lean subjects with normal vascular function, would induce vascular dysfunction in germfree mice. Results from this study show that the obese human gut microbiota is capable of inducing endothelial dysfunction in mesenteric arteries independent of changes in body weight. We also found that the obese microbiota induced glucose intolerance. Ongoing analyses are being conducted by our lab to 1) determine to effect of gut microbiota transplantation from male human donors, 2) determine the effect of pooled samples from multiple human donors, 3) determine if a western diet can cause further deleterious changes to an obese microbiota, 4) examine intestinal permeability and 5) explore potential mechanisms underlying the changes in endothelial function and glucose intolerance.

Collectively, the studies from this dissertation research shed light on the role and contribution of the gut microbiota in vascular dysfunction. Published data from our own lab and others have demonstrated the role of the gut microbiota in mediating vascular dysfunction (12, 25, 83, 178). The last chapter of this dissertation research compliments and extends this body of knowledge by providing evidence that the human gut microbiota can regulate vascular function in gnotobiotic mice. However, the first two chapters question the role and contribution of the gut microbiota in relation to drug treatments (i.e. dapagliflozin) and specific gut microbial metabolites (i.e. IPA).

In chapter 2, we found that treatment with SGLT2i improved glucose levels and vascular function in diabetic mice. While we observed subtle changes to the gut microbiota in diabetic mice treated with SGLT2i, the exact contribution of these microbiota changes in mediating the physiologic effects remain unknown. For example, treatment with SGLT2i led to a reduction in the Firmicutes/Bacteriodetes ratio, diversity, and richness indices in diabetic mice. It was traditionally thought an increase in Firmicutes phylum over Bacteriodetes was characteristic of the obese-type gut microbiota (102) but we observed the opposite with regard to our diabetic mice having the greatest body weight and lowest F:B ratio, and others have shown no differences in F:B ratio in high-fat versus control diet groups (4, 194). Additionally, low bacterial richness has been associated with disease risk (96) but we observed decreased richness in diabetic mice treated with SGLT2i. Other studies have provided data that question the association of α-diversity and health in models of hypertension (2) and vascular dysfunction (25). These disparate findings warrant further investigation and a deeper analysis beyond the associations between microbial diversity and diseases.

These results and differences shed light on the relative contribution of the gut microbiota in mediating the effect of treatments (i.e. drugs or exogenous metabolites) and/or the effect of treatments on the gut microbiota. While we can only speculate, it is certainly possible that the majority of the beneficial effects of SGLT2i that we observed are independent of changes in the gut microbiota. It is also possible that the observed changes in the gut microbiota from SGLT2i were due to differences in host physiology (i.e. glucose levels or body fat/mass) rather than direct effects of SGLT2i on microbial composition and caution should be taken when interpreting data correlating changes in vascular function and gut microbiota composition in dapagliflozin treated diabetic mice in chapter 2. However, given that other antidiabetic drugs such as Metformin have indeed been shown to exert beneficial effects via the gut microbiota, characterizing the effects of new drugs (i.e. SGLT2i) certainly deserves scientific scrutiny.

Similar to the role of xenobiotics, the effects of bacterial metabolites garnered considerably more attention. For example, short chain fatty acids (SCFA) produced by the gut microbiota have been established as important modulators in host physiology both within the intestines and in circulation (89). Similarly, indoles have been implicated in host health but have only begun to receive attention in comparison to SCFA. In chapter 3, we investigated the cardiometabolic effects of IPA given the evidence for IPA in intestinal health. We found little effect of the gut bacterial metabolite, IPA, on cardiometabolic outcomes in WD-fed mice. Examining the effects of metabolites in isolation provides important information for the individual roles of bioactive compounds. However, it is possible that a variety of indole compounds in concert are important in mediating host physiology and that a single gut bacterial metabolite is insufficient to affect the deleterious impacts of a WD. Furthermore, the primary target for indoles, the aryl hydrocarbon receptor (AhR), has a variety of ligands beyond indole compounds adding a layer of complexity in teasing out physiologic differences in ligand specific AhR activation. For example, indoxyl sulfate (IS) is generated in the host liver from the conversion of indole and serves as an AhR agonist. In contrast to the general findings that indole compounds are beneficial, the host generated metabolite, IS, can have deleterious effects to the host. Thus, examining the downstream catabolites of indoles should be an important analysis in determining the effects of certain indole compounds beyond their direct effects.

In chapter 4, we demonstrated the role of the obese gut microbiota in mediating vascular dysfunction. However, similar to chapters 2 and 3, our data raise questions related to the role and contribution of the gut microbiota on host physiology. For example, we observed differences in endothelium-dependent dilation independent of body weight changes between the lean and obese gut microbiota recipients. These findings in regard to body weight are contrary to the findings of some labs but also supported by those who have found similar results as discussed in chapter 4. This example of conflicting findings related to weight gain sheds light on methodological differences between studies (i.e. differing diets, differing region of gut microbiota

used, etc.) and the need for identifying mechanisms by which these differences are being driven.

Prior to this dissertation research, our lab has conducted several studies examining the role of the gut microbiota in vascular dysfunction utilizing genetic and diet-induced obese models. Interestingly, a few commonalities and some differences exist between the studies in regard to gut microbiota composition. Disease state (i.e. diabetes) or diet (i.e. western diet) drives differences in gut microbiota composition in our models. In previously publish data, we found that western diet feeding led to decreases in *Bifidobacteria* and three species significantly correlated with vascular function and markers of endotoxemia (12). In chapter 3, western diet feeding also appeared to drive differences in gut microbiota composition compared to standard diet-fed mice and *Bifidobacteria* was again one of the key drivers of these differences. Future analyses will determine if *Bifidobacteria* were also correlated to physiologic outcomes observed in chapter 3. Another interesting bacteria that has arisen as a key driver in differences among our models is *Akkermansia muciniphila*. Unpublished data from our lab suggest that the obese gut microbiota leads to the development arterial stiffness and higher levels of *A. muciniphilia* were significantly correlated with lower aPWV. In chapter 2, we found that diabetic mice had decreased levels of *A. muciniphilia* and treatment with dapagliflozin increased *A. muciniphilia*. Furthermore, levels of *A. muciniphilia* were significantly correlated with vascular function whereby higher levels of *A. muciniphilia* were associated with better vascular function. Converse to these data, we found that *A. muciniphilia* was higher and drove differences in the western diet-fed group in Chapter 3 and a study by Brunt et al. examining age-related alterations to the gut microbiota and vascular dysfunction found that older mice, with vascular dysfunction, had higher levels of Verrucomicrobia compared to young mice (25). These findings are intriguing given our data suggesting that *A. muciniphilia* may be important to vascular function, as well as data from others that it protects against atherosclerosis (104) and may mediate some effects of the antidiabetic drug Metformin (153). Lastly, Proteobacteria was significantly correlated with

endothelium-dependent dilation in chapter 2 and in support of this, the same study by Brunt et al. found Proteobacteria levels to be higher in older mice with vascular dysfunction (25). Although we have not yet analyzed the gut microbiota from human donors or gnotobiotic recipient mice from chapter 4, it will certainly be interesting to compare these results with previous findings from our lab. The commonalities and differences among our studies may be intriguing, however, future analyses will need to be conducted to determine the potential of manipulating or altering these species in efforts to examine their exact role in our models of vascular dysfunction.

Collectively, the studies conducted in this dissertation research elucidate the role of the gut microbiota in various models of vascular dysfunction. This research also gives insight to the relative role and contribution that the gut microbiota plays in treatments (i.e. SGLT2i or IPA) for obesity or T2D. While studies examining the link between the gut microbiota and health or disease has risen exponentially, research is only beginning to understand the mechanisms by which this occurs and the relative contribution by which alterations in the gut microbiota contribute to disease. Initial studies have characterized differences within the gut microbiota between healthy (i.e. lean) and diseased (i.e. obese) groups and many studies continue to do so. Characterizing the microbes and differences between groups or treatments is an important and critical step but lacks insight into the specific mechanisms by which the gut microbiota drive health or disease. Research continues to provide evidence that the gut microbiota is different in "X" disease state and that the gut microbiota from "X" disease state can transfer the "X" disease phenotype. If these findings are confirmed, the next logical step is to understand more mechanistically how the gut microbiota is contributing to "X" disease and the contribution of that mechanism. While there is skepticism that microbial communities such as the gut microbiota are irreducibly complex and that science will never have satisfying answers to the above questions, a push for research beyond characterization of the gut microbiota can help to propel the scientific community to find these answers.

Future studies from our lab could utilize more mechanistic approaches to gain insight into how the gut microbiota is mediating vascular dysfunction. We have previously utilized 16s rRNA for sequencing but have not employed functional characteristics of the gut microbiota in our models which could provide useful data beyond the presence or absence of bacteria. Bacteriophages could be utilized to manipulate specific bacteria (i.e. *Bifidobacteria*) and thus host physiology. Beyond gut bacteria, the gut microbiota consists also of vira, fungi, and archea. The role of other gut microorganisms has received much less attention although it is reasonable to predict that these other components of the gut microbiota could play a critical role in host health and vascular function. Use of genetic knockout (i.e. TLR4) or overexpression models could also aid in better understanding how the gut microbiota and their components signal to impact host health. Utilizing data from our current *in vivo* work in mice, more mechanistic insight could be harnessed from conducting *in vitro* work with the use of transwell co-cultures of both intestinal and endothelial cells. Finally, causal evidence utilizing clinical trials has received less attention but would immensely compliment the wealth of preclinical data from our lab and others.

In conclusion, the studies included in this dissertation research provide strong evidence in support of the gut microbiota mediating vascular function. Future studies utilizing pre/probiotics, targeted alterations to the gut microbiota (i.e. bacteriophages), as well as identifying specific bacteria or metabolites that mediate these vascular effects will further our understanding of the relationship between the gut microbiota and vascular function.

REFERENCES

1. Guidelines (2013) for managing overweight and obesity in adults. Preface to the Expert Panel Report (comprehensive version which includes systematic evidence review, evidence statements, and recommendations). *Obesity (Silver Spring)* 22 Suppl 2: S40, 2014.

2. Adnan S, Nelson JW, Ajami NJ, Venna VR, Petrosino JF, Bryan RM, Jr., and Durgan DJ. Alterations in the gut microbiota can elicit hypertension in rats. *Physiol Genomics* 49: 96-104, 2017.

3. Agus A, Planchais J, and Sokol H. Gut Microbiota Regulation of Tryptophan Metabolism in Health and Disease. *Cell Host Microbe* 23: 716-724, 2018.

4. Al K, Sarr O, Dunlop K, Gloor GB, Reid G, Burton J, and Regnault TR. Impact of birth weight and postnatal diet on the gut microbiota of young adult guinea pigs. *PeerJ* 5: e2840, 2017.

5. Alexeev EE, Lanis JM, Kao DJ, Campbell EL, Kelly CJ, Battista KD, Gerich ME, Jenkins BR, Walk ST, Kominsky DJ, and Colgan SP. Microbiota-Derived Indole Metabolites Promote Human and Murine Intestinal Homeostasis through Regulation of Interleukin-10 Receptor. *Am J Pathol* 188: 1183-1194, 2018.

6. Allin KH, Tremaroli V, Caesar R, Jensen BAH, Damgaard MTF, Bahl MI, Licht TR, Hansen TH, Nielsen T, Dantoft TM, Linneberg A, Jorgensen T, Vestergaard H, Kristiansen K, Franks PW, consortium I-D, Hansen T, Backhed F, and Pedersen O. Aberrant intestinal microbiota in individuals with prediabetes. *Diabetologia* 61: 810-820, 2018.

7. American Diabetes A. Economic Costs of Diabetes in the U.S. in 2017. *Diabetes Care* 41: 917-928, 2018.

8. Anderson J, Burns PJ, Milroy D, Ruprecht P, Hauser T, and Siegel HJ. Deploying RMACC Summit: An HPC Resource for the Rocky Mountain Region. In: *Proceedings of the*

Practice and Experience in Advanced Research Computing 2017 on Sustainability, Success and Impact. New Orleans, LA, USA: ACM, 2017, p. 1-7.

9. Banoglu E, Jha GG, and King RS. Hepatic microsomal metabolism of indole to indoxyl, a precursor of indoxyl sulfate. *Eur J Drug Metab Pharmacokinet* 26: 235-240, 2001.

10. Bansal T, Alaniz RC, Wood TK, and Jayaraman A. The bacterial signal indole increases epithelial-cell tight-junction resistance and attenuates indicators of inflammation. *P Natl Acad Sci USA* 107: 228-233, 2010.

11. Battson ML, Lee DM, Jarrell DK, Hou S, Ecton KE, Phan AB, and Gentile CL. Tauroursodeoxycholic Acid Reduces Arterial Stiffness and Improves Endothelial Dysfunction in Type 2 Diabetic Mice. *J Vasc Res* 54: 280-287, 2017.

12. Battson ML, Lee DM, Jarrell DK, Hou S, Ecton KE, Weir TL, and Gentile CL. Suppression of gut dysbiosis reverses Western diet-induced vascular dysfunction. *Am J Physiol Endocrinol Metab* 314: E468-E477, 2018.

13. Battson ML, Lee DM, Weir TL, and Gentile CL. The gut microbiota as a novel regulator of cardiovascular function and disease. *J Nutr Biochem* 56: 1-15, 2018.

14. Beaumont M, Neyrinck AM, Olivares M, Rodriguez J, de Rocca Serra A, Roumain M, Bindels LB, Cani PD, Evenepoel P, Muccioli GG, Demoulin JB, and Delzenne NM. The gut microbiota metabolite indole alleviates liver inflammation in mice. *FASEB J* fj201800544, 2018.

15. Beckman JA, Goldfine AB, Gordon MB, Garrett LA, Keaney JF, Jr., and Creager MA. Oral antioxidant therapy improves endothelial function in Type 1 but not Type 2 diabetes mellitus. *Am J Physiol Heart Circ Physiol* 285: H2392-2398, 2003.

16. Benjamin EJ, Muntner P, Alonso A, Bittencourt MS, Callaway CW, Carson AP, Chamberlain AM, Chang AR, Cheng S, Das SR, Delling FN, Djousse L, Elkind MSV, Ferguson JF, Fornage M, Jordan LC, Khan SS, Kissela BM, Knutson KL, Kwan TW, Lackland DT, Lewis TT, Lichtman JH, Longenecker CT, Loop MS, Lutsey PL, Martin SS, Matsushita K, Moran AE, Mussolino ME, O'Flaherty M, Pandey A, Perak AM, Rosamond WD, Roth GA, Sampson UKA,

Satou GM, Schroeder EB, Shah SH, Spartano NL, Stokes A, Tirschwell DL, Tsao CW, Turakhia MP, VanWagner LB, Wilkins JT, Wong SS, Virani SS, American Heart Association Council on E, Prevention Statistics C, and Stroke Statistics S. Heart Disease and Stroke Statistics-2019 Update: A Report From the American Heart Association. *Circulation* 139: e56-e528, 2019.

17. Bonetti PO, Pumper GM, Higano ST, Holmes DR, Jr., Kuvin JT, and Lerman A. Noninvasive identification of patients with early coronary atherosclerosis by assessment of digital reactive hyperemia. *J Am Coll Cardiol* 44: 2137-2141, 2004.

18. Boron WF, and Boulpaep EL. *Medical physiology : a cellular and molecular approach*. Philadelphia, PA: Saunders/Elsevier, 2012.

19. Boulange CL, Neves AL, Chilloux J, Nicholson JK, and Dumas ME. Impact of the gut microbiota on inflammation, obesity, and metabolic disease. *Genome Med* 8: 42, 2016.

20. Brant LC, Barreto SM, Passos VM, and Ribeiro AL. Reproducibility of peripheral arterial tonometry for the assessment of endothelial function in adults. *J Hypertens* 31: 1984-1990, 2013.

21. Britton GJ, Contijoch EJ, Mogno I, Vennaro OH, Llewellyn SR, Ng R, Li Z, Mortha A, Merad M, Das A, Gevers D, McGovern DPB, Singh N, Braun J, Jacobs JP, Clemente JC, Grinspan A, Sands BE, Colombel JF, Dubinsky MC, and Faith JJ. Microbiotas from Humans with Inflammatory Bowel Disease Alter the Balance of Gut Th17 and RORgammat(+) Regulatory T Cells and Exacerbate Colitis in Mice. *Immunity* 50: 212-224 e214, 2019.

22. Brown JM, and Hazen SL. The gut microbial endocrine organ: bacterially derived signals driving cardiometabolic diseases. *Annu Rev Med* 66: 343-359, 2015.

23. Brown JM, and Hazen SL. Microbial modulation of cardiovascular disease. *Nat Rev Microbiol* 16: 171-181, 2018.

24. Bruce-Keller AJ, Salbaum JM, Luo M, Blanchard Et, Taylor CM, Welsh DA, and Berthoud HR. Obese-type gut microbiota induce neurobehavioral changes in the absence of obesity. *Biol Psychiatry* 77: 607-615, 2015.

25. Brunt VE, Gioscia-Ryan RA, Richey JJ, Zigler MC, Cuevas LM, Gonzalez A, Vazquez-Baeza Y, Battson ML, Smithson AT, Gilley AD, Ackermann G, Neilson AP, Weir T, Davy KP, Knight R, and Seals DR. Suppression of the gut microbiome ameliorates age-related arterial dysfunction and oxidative stress in mice. *J Physiol* 597: 2361-2378, 2019.

26. Busse R, Edwards G, Feletou M, Fleming I, Vanhoutte PM, and Weston AH. EDHF: bringing the concepts together. *Trends Pharmacol Sci* 23: 374-380, 2002.

27. Callahan BJ, McMurdie PJ, Rosen MJ, Han AW, Johnson AJ, and Holmes SP. DADA2: High-resolution sample inference from Illumina amplicon data. *Nat Methods* 13: 581-583, 2016.

28. Cani PD, Amar J, Iglesias MA, Poggi M, Knauf C, Bastelica D, Neyrinck AM, Fava F, Tuohy KM, Chabo C, Waget A, Delmee E, Cousin B, Sulpice T, Chamontin B, Ferrieres J, Tanti JF, Gibson GR, Casteilla L, Delzenne NM, Alessi MC, and Burcelin R. Metabolic endotoxemia initiates obesity and insulin resistance. *Diabetes* 56: 1761-1772, 2007.

29. Cani PD, Bibiloni R, Knauf C, Waget A, Neyrinck AM, Delzenne NM, and Burcelin R. Changes in gut microbiota control metabolic endotoxemia-induced inflammation in high-fat diet-induced obesity and diabetes in mice. *Diabetes* 57: 1470-1481, 2008.

30. Cani PD, Neyrinck AM, Fava F, Knauf C, Burcelin RG, Tuohy KM, Gibson GR, and Delzenne NM. Selective increases of bifidobacteria in gut microflora improve high-fat-diet-induced diabetes in mice through a mechanism associated with endotoxaemia. *Diabetologia* 50: 2374-2383, 2007.

31. Cani PD, Van Hul M, Lefort C, Depommier C, Rastelli M, and Everard A. Microbial regulation of organismal energy homeostasis. *Nature Metabolism* 1: 34-46, 2019.

32. Caparros-Martin JA, Lareu RR, Ramsay JP, Peplies J, Reen FJ, Headlam HA, Ward NC, Croft KD, Newsholme P, Hughes JD, and O'Gara F. Statin therapy causes gut dysbiosis in mice through a PXR-dependent mechanism. *Microbiome* 5: 95, 2017.

33. Caporaso JG, Lauber CL, Walters WA, Berg-Lyons D, Huntley J, Fierer N, Owens SM, Betley J, Fraser L, Bauer M, Gormley N, Gilbert JA, Smith G, and Knight R. Ultra-high-

throughput microbial community analysis on the Illumina HiSeq and MiSeq platforms. *ISME J* 6: 1621-1624, 2012.

34. Cason CA, Dolan KT, Sharma G, Tao M, Kulkarni R, Helenowski IB, Doane BM, Avram MJ, McDermott MM, Chang EB, Ozaki CK, and Ho KJ. Plasma microbiome-modulated indole- and phenyl-derived metabolites associate with advanced atherosclerosis and postoperative outcomes. *J Vasc Surg* 68: 1552-+, 2018.

35. Cavalcante JL, Lima JA, Redheuil A, and Al-Mallah MH. Aortic stiffness: current understanding and future directions. *J Am Coll Cardiol* 57: 1511-1522, 2011.

36. Chen CA, Wang TY, Varadharaj S, Reyes LA, Hemann C, Talukder MA, Chen YR, Druhan LJ, and Zweier JL. S-glutathionylation uncouples eNOS and regulates its cellular and vascular function. *Nature* 468: 1115-1118, 2010.

37. Chen JY, Tsai PJ, Tai HC, Tsai RL, Chang YT, Wang MC, Chiou YW, Yeh ML, Tang MJ, Lam CF, Shiesh SC, Li YH, Tsai WC, Chou CH, Lin LJ, Wu HL, and Tsai YS. Increased aortic stiffness and attenuated lysyl oxidase activity in obesity. *Arterioscler Thromb Vasc Biol* 33: 839-846, 2013.

38. Chilton R, Tikkanen I, Cannon CP, Crowe S, Woerle HJ, Broedl UC, and Johansen OE. Effects of empagliflozin on blood pressure and markers of arterial stiffness and vascular resistance in patients with type 2 diabetes. *Diabetes Obes Metab* 17: 1180-1193, 2015.

39. Chow B, and Rabkin SW. The relationship between arterial stiffness and heart failure with preserved ejection fraction: a systemic meta-analysis. *Heart Fail Rev* 20: 291-303, 2015.

40. Chung AW, Yang HH, Sigrist MK, Brin G, Chum E, Gourlay WA, and Levin A. Matrix metalloproteinase-2 and -9 exacerbate arterial stiffening and angiogenesis in diabetes and chronic kidney disease. *Cardiovasc Res* 84: 494-504, 2009.

41. Danaei G, Finucane MM, Lu Y, Singh GM, Cowan MJ, Paciorek CJ, Lin JK, Farzadfar F, Khang YH, Stevens GA, Rao M, Ali MK, Riley LM, Robinson CA, Ezzati M, and Global Burden of Metabolic Risk Factors of Chronic Diseases Collaborating G. National, regional, and global

trends in fasting plasma glucose and diabetes prevalence since 1980: systematic analysis of health examination surveys and epidemiological studies with 370 country-years and 2.7 million participants. *Lancet* 378: 31-40, 2011.

42. Dao MC, Everard A, Aron-Wisnewsky J, Sokolovska N, Prifti E, Verger EO, Kayser BD, Levenez F, Chilloux J, Hoyles L, Consortium MI-O, Dumas ME, Rizkalla SW, Dore J, Cani PD, and Clement K. Akkermansia muciniphila and improved metabolic health during a dietary intervention in obesity: relationship with gut microbiome richness and ecology. *Gut* 65: 426-436, 2016.

43. David LA, Maurice CF, Carmody RN, Gootenberg DB, Button JE, Wolfe BE, Ling AV, Devlin AS, Varma Y, Fischbach MA, Biddinger SB, Dutton RJ, and Turnbaugh PJ. Diet rapidly and reproducibly alters the human gut microbiome. *Nature* 505: 559-563, 2014.

44. de Jager J, Dekker JM, Kooy A, Kostense PJ, Nijpels G, Heine RJ, Bouter LM, and Stehouwer CD. Endothelial dysfunction and low-grade inflammation explain much of the excess cardiovascular mortality in individuals with type 2 diabetes: the Hoorn Study. *Arterioscler Thromb Vasc Biol* 26: 1086-1093, 2006.

45. de La Serre CB, Ellis CL, Lee J, Hartman AL, Rutledge JC, and Raybould HE. Propensity to high-fat diet-induced obesity in rats is associated with changes in the gut microbiota and gut inflammation. *Am J Physiol Gastrointest Liver Physiol* 299: G440-448, 2010.

46. Deanfield JE, Halcox JP, and Rabelink TJ. Endothelial function and dysfunction: testing and clinical relevance. *Circulation* 115: 1285-1295, 2007.

47. DeMarco VG, Habibi J, Jia G, Aroor AR, Ramirez-Perez FI, Martinez-Lemus LA, Bender SB, Garro M, Hayden MR, Sun Z, Meininger GA, Manrique C, Whaley-Connell A, and Sowers JR. Low-Dose Mineralocorticoid Receptor Blockade Prevents Western Diet-Induced Arterial Stiffening in Female Mice. *Hypertension* 66: 99-107, 2015.

48. Dhariwal A, Chong J, Habib S, King IL, Agellon LB, and Xia J. MicrobiomeAnalyst: a web-based tool for comprehensive statistical, visual and meta-analysis of microbiome data. *Nucleic Acids Res* 45: W180-W188, 2017.

49. Dodd D, Spitzer MH, Van Treuren W, Merrill BD, Hryckowian AJ, Higginbottom SK, Le A, Cowan TM, Nolan GP, Fischbach MA, and Sonnenburg JL. A gut bacterial pathway metabolizes aromatic amino acids into nine circulating metabolites. *Nature* 551: 648-652, 2017.

50. Du B, Ouyang A, Eng JS, and Fleenor BS. Aortic perivascular adipose-derived interleukin-6 contributes to arterial stiffness in low-density lipoprotein receptor deficient mice. *Am J Physiol Heart Circ Physiol* 308: H1382-1390, 2015.

51. Dziuba J, Alperin P, Racketa J, Iloeje U, Goswami D, Hardy E, Perlstein I, Grossman HL, and Cohen M. Modeling effects of SGLT-2 inhibitor dapagliflozin treatment versus standard diabetes therapy on cardiovascular and microvascular outcomes. *Diabetes Obes Metab* 16: 628-635, 2014.

52. Einarson TR, Acs A, Ludwig C, and Panton UH. Prevalence of cardiovascular disease in type 2 diabetes: a systematic literature review of scientific evidence from across the world in 2007-2017. *Cardiovasc Diabetol* 17: 83, 2018.

53. Escobedo G, Lopez-Ortiz E, and Torres-Castro I. Gut microbiota as a key player in triggering obesity, systemic inflammation and insulin resistance. *Rev Invest Clin* 66: 450-459, 2014.

54. Esser N, Paquot N, and Scheen AJ. Inflammatory markers and cardiometabolic diseases. *Acta Clin Belg* 70: 193-199, 2015.

55. Evenepoel P, Claus D, Geypens B, Hiele M, Geboes K, Rutgeerts P, and Ghoos Y. Amount and fate of egg protein escaping assimilation in the small intestine of humans. *Am J Physiol* 277: G935-943, 1999.

56. Everard A, Belzer C, Geurts L, Ouwerkerk JP, Druart C, Bindels LB, Guiot Y, Derrien M, Muccioli GG, Delzenne NM, de Vos WM, and Cani PD. Cross-talk between Akkermansia

muciniphila and intestinal epithelium controls diet-induced obesity. *Proc Natl Acad Sci U S A* 110: 9066-9071, 2013.

57. Everard A, and Cani PD. Diabetes, obesity and gut microbiota. *Best Pract Res Clin Gastroenterol* 27: 73-83, 2013.

58. Finkelstein EA, Khavjou OA, Thompson H, Trogdon JG, Pan L, Sherry B, and Dietz W. Obesity and severe obesity forecasts through 2030. *Am J Prev Med* 42: 563-570, 2012.

59. Finkelstein EA, Trogdon JG, Cohen JW, and Dietz W. Annual medical spending attributable to obesity: payer-and service-specific estimates. *Health Aff (Millwood)* 28: w822-831, 2009.

60. Fleenor BS, Seals DR, Zigler ML, and Sindler AL. Superoxide-lowering therapy with TEMPOL reverses arterial dysfunction with aging in mice. *Aging Cell* 11: 269-276, 2012.

61. Fleenor BS, Sindler AL, Marvi NK, Howell KL, Zigler ML, Yoshizawa M, and Seals DR. Curcumin ameliorates arterial dysfunction and oxidative stress with aging. *Exp Gerontol* 48: 269-276, 2013.

62. Flegal KM, Kruszon-Moran D, Carroll MD, Fryar CD, and Ogden CL. Trends in Obesity Among Adults in the United States, 2005 to 2014. *JAMA* 315: 2284-2291, 2016.

63. Fox CS, Golden SH, Anderson C, Bray GA, Burke LE, de Boer IH, Deedwania P, Eckel RH, Ershow AG, Fradkin J, Inzucchi SE, Kosiborod M, Nelson RG, Patel MJ, Pignone M, Quinn L, Schauer PR, Selvin E, Vafiadis DK, American Heart Association Diabetes Committee of the Council on L, Cardiometabolic H, Council on Clinical Cardiology CoC, Stroke Nursing CoCS, Anesthesia CoQoC, Outcomes R, and American Diabetes A. Update on Prevention of Cardiovascular Disease in Adults With Type 2 Diabetes Mellitus in Light of Recent Evidence: A Scientific Statement From the American Heart Association and the American Diabetes Association. *Diabetes Care* 38: 1777-1803, 2015.

64. Ganz ML, Wintfeld N, Li Q, Alas V, Langer J, and Hammer M. The association of body mass index with the risk of type 2 diabetes: a case-control study nested in an electronic health records system in the United States. *Diabetol Metab Syndr* 6: 50, 2014.

65. Gao J, Xu K, Liu H, Liu G, Bai M, Peng C, Li T, and Yin Y. Impact of the Gut Microbiota on Intestinal Immunity Mediated by Tryptophan Metabolism. *Front Cell Infect Microbiol* 8: 13, 2018.

66. Gerstein HC, Pogue J, Mann JF, Lonn E, Dagenais GR, McQueen M, Yusuf S, and investigators H. The relationship between dysglycaemia and cardiovascular and renal risk in diabetic and non-diabetic participants in the HOPE study: a prospective epidemiological analysis. *Diabetologia* 48: 1749-1755, 2005.

67. Greig CJ, Alper A, Goodman AL, and Cowles RA. Mucosal homeostasis is altered in the ileum of gnotobiotic mice. *J Surg Res* 231: 331-337, 2018.

68. Griffin NW, Ahern PP, Cheng J, Heath AC, Ilkayeva O, Newgard CB, Fontana L, and Gordon JI. Prior Dietary Practices and Connections to a Human Gut Microbial Metacommunity Alter Responses to Diet Interventions. *Cell Host Microbe* 21: 84-96, 2017.

69. Group AC, Patel A, MacMahon S, Chalmers J, Neal B, Billot L, Woodward M, Marre M, Cooper M, Glasziou P, Grobbee D, Hamet P, Harrap S, Heller S, Liu L, Mancia G, Mogensen CE, Pan C, Poulter N, Rodgers A, Williams B, Bompoint S, de Galan BE, Joshi R, and Travert F. Intensive blood glucose control and vascular outcomes in patients with type 2 diabetes. *N Engl J Med* 358: 2560-2572, 2008.

70. Grover M, and Kashyap PC. Germ-free mice as a model to study effect of gut microbiota on host physiology. *Neurogastroenterol Motil* 26: 745-748, 2014.

71. Guerville M, Leroy A, Sinquin A, Laugerette F, Michalski MC, and Boudry G. Western-diet consumption induces alteration of barrier function mechanisms in the ileum that correlates with metabolic endotoxemia in rats. *Am J Physiol Endocrinol Metab* 313: E107-E120, 2017.

72. Hamburg NM, Keyes MJ, Larson MG, Vasan RS, Schnabel R, Pryde MM, Mitchell GF, Sheffy J, Vita JA, and Benjamin EJ. Cross-sectional relations of digital vascular function to cardiovascular risk factors in the Framingham Heart Study. *Circulation* 117: 2467-2474, 2008.

73. Hamilton MK, Boudry G, Lemay DG, and Raybould HE. Changes in intestinal barrier function and gut microbiota in high-fat diet-fed rats are dynamic and region dependent. *Am J Physiol Gastrointest Liver Physiol* 308: G840-851, 2015.

74. Han Y, Cho YE, Ayon R, Guo R, Youssef KD, Pan M, Dai A, Yuan JX, and Makino A. SGLT inhibitors attenuate NO-dependent vascular relaxation in the pulmonary artery but not in the coronary artery. *Am J Physiol Lung Cell Mol Physiol* 309: L1027-1036, 2015.

75. Heerspink HJ, Perkins BA, Fitchett DH, Husain M, and Cherney DZ. Sodium Glucose Cotransporter 2 Inhibitors in the Treatment of Diabetes Mellitus: Cardiovascular and Kidney Effects, Potential Mechanisms, and Clinical Applications. *Circulation* 134: 752-772, 2016.

76. Heitzer T, Schlinzig T, Krohn K, Meinertz T, and Munzel T. Endothelial dysfunction, oxidative stress, and risk of cardiovascular events in patients with coronary artery disease. *Circulation* 104: 2673-2678, 2001.

77. Henry RM, Kostense PJ, Spijkerman AM, Dekker JM, Nijpels G, Heine RJ, Kamp O, Westerhof N, Bouter LM, Stehouwer CD, and Hoorn S. Arterial stiffness increases with deteriorating glucose tolerance status: the Hoorn Study. *Circulation* 107: 2089-2095, 2003.

78. Hubbard TD, Murray IA, and Perdew GH. Indole and Tryptophan Metabolism: Endogenous and Dietary Routes to Ah Receptor Activation. *Drug Metab Dispos* 43: 1522-1535, 2015.

79. Huc T, Konop M, Onyszkiewicz M, Podsadni P, Szczepanska A, Turlo J, and Ufnal M. Colonic indole, gut bacteria metabolite of tryptophan, increases portal blood pressure in rats. *Am J Physiol-Reg I* 315: R646-R655, 2018.

80. Hwang MH, Yoo JK, Kim HK, Hwang CL, Mackay K, Hemstreet O, Nichols WW, and Christou DD. Validity and reliability of aortic pulse wave velocity and augmentation index determined by the new cuff-based SphygmoCor Xcel. *J Hum Hypertens* 28: 475-481, 2014.

81. Jaglin M, Rhimi M, Philippe C, Pons N, Bruneau A, Goustard B, Dauge V, Maguin E, Naudon L, and Rabot S. Indole, a Signaling Molecule Produced by the Gut Microbiota, Negatively Impacts Emotional Behaviors in Rats. *Front Neurosci* 12: 216, 2018.

82. Kallus SJ, and Brandt LJ. The intestinal microbiota and obesity. *J Clin Gastroenterol* 46: 16-24, 2012.

83. Karbach SH, Schonfelder T, Brandao I, Wilms E, Hormann N, Jackel S, Schuler R, Finger S, Knorr M, Lagrange J, Brandt M, Waisman A, Kossmann S, Schafer K, Munzel T, Reinhardt C, and Wenzel P. Gut Microbiota Promote Angiotensin II-Induced Arterial Hypertension and Vascular Dysfunction. *J Am Heart Assoc* 5: 2016.

84. Kelly CJ, Zheng L, Campbell EL, Saeedi B, Scholz CC, Bayless AJ, Wilson KE, Glover LE, Kominsky DJ, Magnuson A, Weir TL, Ehrentraut SF, Pickel C, Kuhn KA, Lanis JM, Nguyen V, Taylor CT, and Colgan SP. Crosstalk between Microbiota-Derived Short-Chain Fatty Acids and Intestinal Epithelial HIF Augments Tissue Barrier Function. *Cell Host Microbe* 17: 662-671, 2015.

85. Khan SS, Ning H, Wilkins JT, Allen N, Carnethon M, Berry JD, Sweis RN, and Lloyd-Jones DM. Association of Body Mass Index With Lifetime Risk of Cardiovascular Disease and Compression of Morbidity. *JAMA Cardiol* 3: 280-287, 2018.

86. Kim JA, Jang HJ, and Hwang DH. Toll-like receptor 4-induced endoplasmic reticulum stress contributes to impairment of vasodilator action of insulin. *Am J Physiol Endocrinol Metab* 309: E767-776, 2015.

87. Klurfeld DM, Davis CD, Karp RW, Allen-Vercoe E, Chang EB, Chassaing B, Fahey GC, Jr., Hamaker BR, Holscher HD, Lampe JW, Marette A, Martens E, O'Keefe SJ, Rose DJ, Saarela M, Schneeman BO, Slavin JL, Sonnenburg JL, Swanson KS, Wu GD, and Lynch CJ.

Considerations for best practices in studies of fiber or other dietary components and the intestinal microbiome. *Am J Physiol Endocrinol Metab* 315: E1087-E1097, 2018.

88. Koeth RA, Wang Z, Levison BS, Buffa JA, Org E, Sheehy BT, Britt EB, Fu X, Wu Y, Li L, Smith JD, DiDonato JA, Chen J, Li H, Wu GD, Lewis JD, Warrier M, Brown JM, Krauss RM, Tang WH, Bushman FD, Lusis AJ, and Hazen SL. Intestinal microbiota metabolism of L-carnitine, a nutrient in red meat, promotes atherosclerosis. *Nat Med* 19: 576-585, 2013.

89. Koh A, De Vadder F, Kovatcheva-Datchary P, and Backhed F. From Dietary Fiber to Host Physiology: Short-Chain Fatty Acids as Key Bacterial Metabolites. *Cell* 165: 1332-1345, 2016.

90. Koide CL, Collier AC, Berry MJ, and Panee J. The effect of bamboo extract on hepatic biotransforming enzymes--findings from an obese-diabetic mouse model. *J Ethnopharmacol* 133: 37-45, 2011.

91. Kootte RS, Levin E, Salojarvi J, Smits LP, Hartstra AV, Udayappan SD, Hermes G, Bouter KE, Koopen AM, Holst JJ, Knop FK, Blaak EE, Zhao J, Smidt H, Harms AC, Hankemeijer T, Bergman J, Romijn HA, Schaap FG, Olde Damink SWM, Ackermans MT, Dallinga-Thie GM, Zoetendal E, de Vos WM, Serlie MJ, Stroes ESG, Groen AK, and Nieuwdorp M. Improvement of Insulin Sensitivity after Lean Donor Feces in Metabolic Syndrome Is Driven by Baseline Intestinal Microbiota Composition. *Cell Metab* 26: 611-619 e616, 2017.

92. Krishnan S, Ding Y, Saedi N, Choi M, Sridharan GV, Sherr DH, Yarmush ML, Alaniz RC, Jayaraman A, and Lee K. Gut Microbiota-Derived Tryptophan Metabolites Modulate Inflammatory Response in Hepatocytes and Macrophages. *Cell reports* 23: 1099-1111, 2018.

93. Laakso M, Edelman SV, Brechtel G, and Baron AD. Decreased effect of insulin to stimulate skeletal muscle blood flow in obese man. A novel mechanism for insulin resistance. *J Clin Invest* 85: 1844-1852, 1990.

94. Laakso M, Edelman SV, Brechtel G, and Baron AD. Impaired insulin-mediated skeletal muscle blood flow in patients with NIDDM. *Diabetes* 41: 1076-1083, 1992.

95. Lamas B, Natividad JM, and Sokol H. Aryl hydrocarbon receptor and intestinal immunity. *Mucosal Immunol* 11: 1024-1038, 2018.

96. Le Chatelier E, Nielsen T, Qin J, Prifti E, Hildebrand F, Falony G, Almeida M, Arumugam M, Batto JM, Kennedy S, Leonard P, Li J, Burgdorf K, Grarup N, Jorgensen T, Brandslund I, Nielsen HB, Juncker AS, Bertalan M, Levenez F, Pons N, Rasmussen S, Sunagawa S, Tap J, Tims S, Zoetendal EG, Brunak S, Clement K, Dore J, Kleerebezem M, Kristiansen K, Renault P, Sicheritz-Ponten T, de Vos WM, Zucker JD, Raes J, Hansen T, Meta HITc, Bork P, Wang J, Ehrlich SD, and Pedersen O. Richness of human gut microbiome correlates with metabolic markers. *Nature* 500: 541-546, 2013.

97. Lee DM, Battson ML, Jarrell DK, Cox-York K, Foster MT, Weir TL, and Gentile CL. Fuzhuan tea reverses arterial stiffening after modest weight gain in mice. *Nutrition* 2016.

98. Lee H, and Ko G. Effect of metformin on metabolic improvement and gut microbiota. *Appl Environ Microbiol* 80: 5935-5943, 2014.

99. Lee YH, and Pratley RE. The evolving role of inflammation in obesity and the metabolic syndrome. *Curr Diab Rep* 5: 70-75, 2005.

100. Leng W, Ouyang X, Lei X, Wu M, Chen L, Wu Q, Deng W, and Liang Z. The SGLT-2 Inhibitor Dapagliflozin Has a Therapeutic Effect on Atherosclerosis in Diabetic ApoE(-/-) Mice. *Mediators Inflamm* 2016: 6305735, 2016.

101. Leone V, Gibbons SM, Martinez K, Hutchison AL, Huang EY, Cham CM, Pierre JF, Heneghan AF, Nadimpalli A, Hubert N, Zale E, Wang Y, Huang Y, Theriault B, Dinner AR, Musch MW, Kudsk KA, Prendergast BJ, Gilbert JA, and Chang EB. Effects of diurnal variation of gut microbes and high-fat feeding on host circadian clock function and metabolism. *Cell Host Microbe* 17: 681-689, 2015.

102. Ley RE, Backhed F, Turnbaugh P, Lozupone CA, Knight RD, and Gordon JI. Obesity alters gut microbial ecology. *Proc Natl Acad Sci U S A* 102: 11070-11075, 2005.

103. Li CY, Wang LX, Dong SS, Hong Y, Zhou XH, Zheng WW, and Zheng C. Phlorizin Exerts Direct Protective Effects on Palmitic Acid (PA)-Induced Endothelial Dysfunction by Activating the PI3K/AKT/eNOS Signaling Pathway and Increasing the Levels of Nitric Oxide (NO). *Med Sci Monit Basic Res* 24: 1-9, 2018.

104. Li J, Lin S, Vanhoutte PM, Woo CW, and Xu A. Akkermansia Muciniphila Protects Against Atherosclerosis by Preventing Metabolic Endotoxemia-Induced Inflammation in Apoe-/- Mice. *Circulation* 133: 2434-2446, 2016.

105. Lin B, Koibuchi N, Hasegawa Y, Sueta D, Toyama K, Uekawa K, Ma M, Nakagawa T, Kusaka H, and Kim-Mitsuyama S. Glycemic control with empagliflozin, a novel selective SGLT2 inhibitor, ameliorates cardiovascular injury and cognitive dysfunction in obese and type 2 diabetic mice. *Cardiovasc Diabetol* 13: 148, 2014.

106. Liu L, Simon B, Shi J, Mallhi AK, and Eisen HJ. Impact of diabetes mellitus on risk of cardiovascular disease and all-cause mortality: Evidence on health outcomes and antidiabetic treatment in United States adults. *World J Diabetes* 7: 449-461, 2016.

107. Lorber D. Importance of cardiovascular disease risk management in patients with type 2 diabetes mellitus. *Diabetes Metab Syndr Obes* 7: 169-183, 2014.

108. Luckey TD. Introduction to intestinal microecology. *Am J Clin Nutr* 25: 1292-1294, 1972.

109. Maier L, Pruteanu M, Kuhn M, Zeller G, Telzerow A, Anderson EE, Brochado AR, Fernandez KC, Dose H, Mori H, Patil KR, Bork P, and Typas A. Extensive impact of non-antibiotic drugs on human gut bacteria. *Nature* 555: 623-628, 2018.

110. Maki JM, Rasanen J, Tikkanen H, Sormunen R, Makikallio K, Kivirikko KI, and Soininen R. Inactivation of the lysyl oxidase gene Lox leads to aortic aneurysms, cardiovascular dysfunction, and perinatal death in mice. *Circulation* 106: 2503-2509, 2002.

111. Malik RA, Schofield IJ, Izzard A, Austin C, Bermann G, and Heagerty AM. Effects of angiotensin type-1 receptor antagonism on small artery function in patients with type 2 diabetes mellitus. *Hypertension* 45: 264-269, 2005.

112. Manter DK, Korsa M, Tebbe C, and Delgado JA. myPhyloDB: a local web server for the storage and analysis of metagenomic data. *Database (Oxford)* 2016: 2016.

113. Martin M. Cutadapt removes adapter sequences from high-throughput sequencing reads. *EMBnetjournal* 17: 10-12, 2011.

114. McCrea CE, Skulas-Ray AC, Chow M, and West SG. Test-retest reliability of pulse amplitude tonometry measures of vascular endothelial function: implications for clinical trial design. *Vasc Med* 17: 29-36, 2012.

115. Mistry RH, Verkade HJ, and Tietge UJ. Reverse Cholesterol Transport Is Increased in Germ-Free Mice-Brief Report. *Arterioscler Thromb Vasc Biol* 37: 419-422, 2017.

116. Mitchell GF, Hwang SJ, Vasan RS, Larson MG, Pencina MJ, Hamburg NM, Vita JA, Levy D, and Benjamin EJ. Arterial stiffness and cardiovascular events: the Framingham Heart Study. *Circulation* 121: 505-511, 2010.

117. Montandon SA, and Jornayvaz FR. Effects of Antidiabetic Drugs on Gut Microbiota Composition. *Genes (Basel)* 8: 2017.

118. Natividad JM, Agus A, Planchais J, Lamas B, Jarry AC, Martin R, Michel ML, Chong-Nguyen C, Roussel R, Straube M, Jegou S, McQuitty C, Le Gall M, da Costa G, Lecornet E, Michaudel C, Modoux M, Glodt J, Bridonneau C, Sovran B, Dupraz L, Bado A, Richard ML, Langella P, Hansel B, Launay JM, Xavier RJ, Duboc H, and Sokol H. Impaired Aryl Hydrocarbon Receptor Ligand Production by the Gut Microbiota Is a Key Factor in Metabolic Syndrome. *Cell Metab* 28: 737-749 e734, 2018.

119. Ndumele CE, Matsushita K, Lazo M, Bello N, Blumenthal RS, Gerstenblith G, Nambi V, Ballantyne CM, Solomon SD, Selvin E, Folsom AR, and Coresh J. Obesity and Subtypes of Incident Cardiovascular Disease. *J Am Heart Assoc* 5: 2016.

120. Nicholson JK, Holmes E, Kinross J, Burcelin R, Gibson G, Jia W, and Pettersson S. Host-gut microbiota metabolic interactions. *Science* 336: 1262-1267, 2012.

121. Ning M, and Jeong H. High-Fat Diet Feeding Alters Expression of Hepatic Drug-Metabolizing Enzymes in Mice. *Drug Metab Dispos* 45: 707-711, 2017.

122. Nowak KL, Rossman MJ, Chonchol M, and Seals DR. Strategies for Achieving Healthy Vascular Aging. *Hypertension* 71: 389-402, 2018.

123. Nyangale EP, Mottram DS, and Gibson GR. Gut microbial activity, implications for health and disease: the potential role of metabolite analysis. *J Proteome Res* 11: 5573-5585, 2012.

124. Peters BA, Shapiro JA, Church TR, Miller G, Trinh-Shevrin C, Yuen E, Friedlander C, Hayes RB, and Ahn J. A taxonomic signature of obesity in a large study of American adults. *Sci Rep* 8: 9749, 2018.

125. Pfeifer M, Townsend RR, Davies MJ, Vijapurkar U, and Ren J. Effects of canagliflozin, a sodium glucose co-transporter 2 inhibitor, on blood pressure and markers of arterial stiffness in patients with type 2 diabetes mellitus: a post hoc analysis. *Cardiovasc Diabetol* 16: 29, 2017.

126. Pi X, Xie L, and Patterson C. Emerging Roles of Vascular Endothelium in Metabolic Homeostasis. *Circ Res* 123: 477-494, 2018.

127. Poole AC, Goodrich JK, Youngblut ND, Luque GG, Ruaud A, Sutter JL, Waters JL, Shi Q, El-Hadidi M, Johnson LM, Bar HY, Huson DH, Booth JG, and Ley RE. Human Salivary Amylase Gene Copy Number Impacts Oral and Gut Microbiomes. *Cell Host Microbe* 25: 553-564 e557, 2019.

128. Promotion NCfCDPaH. National Diabetes Statistics Report, 2017: Estimates of Diabetes and Its Burden in the United States. 2017.

129. Qin J, Li R, Raes J, Arumugam M, Burgdorf KS, Manichanh C, Nielsen T, Pons N, Levenez F, Yamada T, Mende DR, Li J, Xu J, Li S, Li D, Cao J, Wang B, Liang H, Zheng H, Xie Y, Tap J, Lepage P, Bertalan M, Batto JM, Hansen T, Le Paslier D, Linneberg A, Nielsen HB, Pelletier E, Renault P, Sicheritz-Ponten T, Turner K, Zhu H, Yu C, Li S, Jian M, Zhou Y, Li Y, Zhang X, Li S, Qin N, Yang H, Wang J, Brunak S, Dore J, Guarner F, Kristiansen K, Pedersen

O, Parkhill J, Weissenbach J, Meta HITC, Bork P, Ehrlich SD, and Wang J. A human gut microbial gene catalogue established by metagenomic sequencing. *Nature* 464: 59-65, 2010.

130. Qin J, Li Y, Cai Z, Li S, Zhu J, Zhang F, Liang S, Zhang W, Guan Y, Shen D, Peng Y, Zhang D, Jie Z, Wu W, Qin Y, Xue W, Li J, Han L, Lu D, Wu P, Dai Y, Sun X, Li Z, Tang A, Zhong S, Li X, Chen W, Xu R, Wang M, Feng Q, Gong M, Yu J, Zhang Y, Zhang M, Hansen T, Sanchez G, Raes J, Falony G, Okuda S, Almeida M, LeChatelier E, Renault P, Pons N, Batto JM, Zhang Z, Chen H, Yang R, Zheng W, Li S, Yang H, Wang J, Ehrlich SD, Nielsen R, Pedersen O, Kristiansen K, and Wang J. A metagenome-wide association study of gut microbiota in type 2 diabetes. *Nature* 490: 55-60, 2012.

131. Raaz U, Schellinger IN, Chernogubova E, Warnecke C, Kayama Y, Penov K, Hennigs JK, Salomons F, Eken S, Emrich FC, Zheng WH, Adam M, Jagger A, Nakagami F, Toh R, Toyama K, Deng A, Buerke M, Maegdefessel L, Hasenfuss G, Spin JM, and Tsao PS. Transcription Factor Runx2 Promotes Aortic Fibrosis and Stiffness in Type 2 Diabetes Mellitus. *Circ Res* 117: 513-524, 2015.

132. Rafikov R, Fonseca FV, Kumar S, Pardo D, Darragh C, Elms S, Fulton D, and Black SM. eNOS activation and NO function: structural motifs responsible for the posttranslational control of endothelial nitric oxide synthase activity. *J Endocrinol* 210: 271-284, 2011.

133. Rajagopalan S, Meng XP, Ramasamy S, Harrison DG, and Galis ZS. Reactive oxygen species produced by macrophage-derived foam cells regulate the activity of vascular matrix metalloproteinases in vitro. Implications for atherosclerotic plaque stability. *J Clin Invest* 98: 2572-2579, 1996.

134. Redan BW, Buhman KK, Novotny JA, and Ferruzzi MG. Altered Transport and Metabolism of Phenolic Compounds in Obesity and Diabetes: Implications for Functional Food Development and Assessment. *Adv Nutr* 7: 1090-1104, 2016.

135. Reikvam DH, Erofeev A, Sandvik A, Grcic V, Jahnsen FL, Gaustad P, McCoy KD, Macpherson AJ, Meza-Zepeda LA, and Johansen FE. Depletion of murine intestinal microbiota: effects on gut mucosa and epithelial gene expression. *PloS one* 6: e17996, 2011.

136. Ridaura VK, Faith JJ, Rey FE, Cheng J, Duncan AE, Kau AL, Griffin NW, Lombard V, Henrissat B, Bain JR, Muehlbauer MJ, Ilkayeva O, Semenkovich CF, Funai K, Hayashi DK, Lyle BJ, Martini MC, Ursell LK, Clemente JC, Van Treuren W, Walters WA, Knight R, Newgard CB, Heath AC, and Gordon JI. Gut microbiota from twins discordant for obesity modulate metabolism in mice. *Science* 341: 1241214, 2013.

137. Roager HM, and Licht TR. Microbial tryptophan catabolites in health and disease. *Nature communications* 9: 3294, 2018.

138. Rognes T, Flouri T, Nichols B, Quince C, and Mahe F. VSEARCH: a versatile open source tool for metagenomics. *PeerJ* 4: e2584, 2016.

139. Rowley WR, Bezold C, Arikan Y, Byrne E, and Krohe S. Diabetes 2030: Insights from Yesterday, Today, and Future Trends. *Popul Health Manag* 20: 6-12, 2017.

140. Rubinshtein R, Kuvin JT, Soffler M, Lennon RJ, Lavi S, Nelson RE, Pumper GM, Lerman LO, and Lerman A. Assessment of endothelial function by non-invasive peripheral arterial tonometry predicts late cardiovascular adverse events. *Eur Heart J* 31: 1142-1148, 2010.

141. Santisteban MM, Qi Y, Zubcevic J, Kim S, Yang T, Shenoy V, Cole-Jeffrey CT, Lobaton GO, Stewart DC, Rubiano A, Simmons CS, Garcia-Pereira F, Johnson RD, Pepine CJ, and Raizada MK. Hypertension-Linked Pathophysiological Alterations in the Gut. *Circ Res* 120: 312-323, 2017.

142. Sattar N, McLaren J, Kristensen SL, Preiss D, and McMurray JJ. SGLT2 Inhibition and cardiovascular events: why did EMPA-REG Outcomes surprise and what were the likely mechanisms? *Diabetologia* 59: 1333-1339, 2016.

143. Schachinger V, Britten MB, and Zeiher AM. Prognostic impact of coronary vasodilator dysfunction on adverse long-term outcome of coronary heart disease. *Circulation* 101: 1899-1906, 2000.

144. Schiering C, Wincent E, Metidji A, Iseppon A, Li Y, Potocnik AJ, Omenetti S, Henderson CJ, Wolf CR, Nebert DW, and Stockinger B. Feedback control of AHR signalling regulates intestinal immunity. *Nature* 542: 242-245, 2017.

145. Schram MT, Henry RM, van Dijk RA, Kostense PJ, Dekker JM, Nijpels G, Heine RJ, Bouter LM, Westerhof N, and Stehouwer CD. Increased central artery stiffness in impaired glucose metabolism and type 2 diabetes: the Hoorn Study. *Hypertension* 43: 176-181, 2004.

146. Schroeder BO, Birchenough GMH, Stahlman M, Arike L, Johansson MEV, Hansson GC, and Backhed F. Bifidobacteria or Fiber Protects against Diet-Induced Microbiota-Mediated Colonic Mucus Deterioration. *Cell Host Microbe* 23: 27-40 e27, 2018.

147. Scuteri A, Orru M, Morrell CH, Tarasov K, Schlessinger D, Uda M, and Lakatta EG. Associations of large artery structure and function with adiposity: effects of age, gender, and hypertension. The SardiNIA Study. *Atherosclerosis* 221: 189-197, 2012.

148. Sedeek M, Gutsol A, Montezano AC, Burger D, Nguyen Dinh Cat A, Kennedy CR, Burns KD, Cooper ME, Jandeleit-Dahm K, Page P, Szyndralewiez C, Heitz F, Hebert RL, and Touyz RM. Renoprotective effects of a novel Nox1/4 inhibitor in a mouse model of Type 2 diabetes. *Clin Sci (Lond)* 124: 191-202, 2013.

149. Segata N, Izard J, Waldron L, Gevers D, Miropolsky L, Garrett WS, and Huttenhower C. Metagenomic biomarker discovery and explanation. *Genome Biol* 12: R60, 2011.

150. Sender R, Fuchs S, and Milo R. Revised Estimates for the Number of Human and Bacteria Cells in the Body. *PLoS Biol* 14: e1002533, 2016.

151. Shigiyama F, Kumashiro N, Miyagi M, Ikehara K, Kanda E, Uchino H, and Hirose T. Effectiveness of dapagliflozin on vascular endothelial function and glycemic control in patients with early-stage type 2 diabetes mellitus: DEFENCE study. *Cardiovasc Diabetol* 16: 84, 2017.

152. Shimada Y, Kinoshita M, Harada K, Mizutani M, Masahata K, Kayama H, and Takeda K. Commensal bacteria-dependent indole production enhances epithelial barrier function in the colon. *PloS one* 8: e80604, 2013.

153. Shin NR, Lee JC, Lee HY, Kim MS, Whon TW, Lee MS, and Bae JW. An increase in the Akkermansia spp. population induced by metformin treatment improves glucose homeostasis in diet-induced obese mice. *Gut* 63: 727-735, 2014.

154. Shreiner AB, Kao JY, and Young VB. The gut microbiome in health and in disease. *Curr Opin Gastroenterol* 31: 69-75, 2015.

155. Siasos G, Gouliopoulos N, Moschos MM, Oikonomou E, Kollia C, Konsola T, Athanasiou D, Siasou G, Mourouzis K, Zisimos K, Papavassiliou AG, Stefanadis C, and Tousoulis D. Role of endothelial dysfunction and arterial stiffness in the development of diabetic retinopathy. *Diabetes Care* 38: e9-e10, 2015.

156. Singer G, and Granger DN. Inflammatory responses underlying the microvascular dysfunction associated with obesity and insulin resistance. *Microcirculation* 14: 375-387, 2007.

157. Singh A, Donnino R, Weintraub H, and Schwartzbard A. Effect of strict glycemic control in patients with diabetes mellitus on frequency of macrovascular events. *Am J Cardiol* 112: 1033-1038, 2013.

158. Skyler JS, Bergenstal R, Bonow RO, Buse J, Deedwania P, Gale EA, Howard BV, Kirkman MS, Kosiborod M, Reaven P, Sherwin RS, American Diabetes A, American College of Cardiology F, and American Heart A. Intensive glycemic control and the prevention of cardiovascular events: implications of the ACCORD, ADVANCE, and VA diabetes trials: a position statement of the American Diabetes Association and a scientific statement of the American College of Cardiology Foundation and the American Heart Association. *Circulation* 119: 351-357, 2009.

159. Soderborg TK, Clark SE, Mulligan CE, Janssen RC, Babcock L, Ir D, Lemas DJ, Johnson LK, Weir T, Lenz LL, Frank DN, Hernandez TL, Kuhn KA, D'Alessandro A, Barbour LA,

El Kasmi KC, and Friedman JE. The gut microbiota in infants of obese mothers increases inflammation and susceptibility to NAFLD. *Nature communications* 9: 4462, 2018.

160. Solini A, Giannini L, Seghieri M, Vitolo E, Taddei S, Ghiadoni L, and Bruno RM. Dapagliflozin acutely improves endothelial dysfunction, reduces aortic stiffness and renal resistive index in type 2 diabetic patients: a pilot study. *Cardiovasc Diabetol* 16: 138, 2017.

161. Sprague AH, and Khalil RA. Inflammatory cytokines in vascular dysfunction and vascular disease. *Biochem Pharmacol* 78: 539-552, 2009.

162. Staley C, Weingarden AR, Khoruts A, and Sadowsky MJ. Interaction of gut microbiota with bile acid metabolism and its influence on disease states. *Appl Microbiol Biotechnol* 101: 47-64, 2017.

163. Stehouwer CD, Henry RM, and Ferreira I. Arterial stiffness in diabetes and the metabolic syndrome: a pathway to cardiovascular disease. *Diabetologia* 51: 527-539, 2008.

164. Stepensky D, Friedman M, Raz I, and Hoffman A. Pharmacokinetic-pharmacodynamic analysis of the glucose-lowering effect of metformin in diabetic rats reveals first-pass pharmacodynamic effect. *Drug Metab Dispos* 30: 861-868, 2002.

165. Suez J, Korem T, Zeevi D, Zilberman-Schapira G, Thaiss CA, Maza O, Israeli D, Zmora N, Gilad S, Weinberger A, Kuperman Y, Harmelin A, Kolodkin-Gal I, Shapiro H, Halpern Z, Segal E, and Elinav E. Artificial sweeteners induce glucose intolerance by altering the gut microbiota. *Nature* 514: 181-186, 2014.

166. Syvanen K, Korhonen P, Partanen A, and Aarnio P. Endothelial function in a cardiovascular risk population with borderline ankle-brachial index. *Vasc Health Risk Manag* 7: 97-101, 2011.

167. Tahara A, Kurosaki E, Yokono M, Yamajuku D, Kihara R, Hayashizaki Y, Takasu T, Imamura M, Li Q, Tomiyama H, Kobayashi Y, Noda A, Sasamata M, and Shibasaki M. Effects of SGLT2 selective inhibitor ipragliflozin on hyperglycemia, hyperlipidemia, hepatic steatosis,

oxidative stress, inflammation, and obesity in type 2 diabetic mice. *Eur J Pharmacol* 715: 246-255, 2013.

168. Tang TWH, Chen HC, Chen CY, Yen CYT, Lin CJ, Prajnamitra RP, Chen LL, Ruan SC, Lin JH, Lin PJ, Lu HH, Kuo CW, Chang CM, Hall AD, Vivas EI, Shui JW, Chen P, Hacker TA, Rey FE, Kamp TJ, and Hsieh PCH. Loss of Gut Microbiota Alters Immune System Composition and Cripples Postinfarction Cardiac Repair. *Circulation* 139: 647-659, 2019.

169. Tang WH, and Hazen SL. Microbiome, trimethylamine N-oxide, and cardiometabolic disease. *Transl Res* 179: 108-115, 2017.

170. Tejada-Simon MV, Ustunol Z, and Pestka JJ. Ex vivo effects of lactobacilli, streptococci, and bifidobacteria ingestion on cytokine and nitric oxide production in a murine model. *J Food Prot* 62: 162-169, 1999.

171. Tremaroli V, Karlsson F, Werling M, Stahlman M, Kovatcheva-Datchary P, Olbers T, Fandriks L, le Roux CW, Nielsen J, and Backhed F. Roux-en-Y Gastric Bypass and Vertical Banded Gastroplasty Induce Long-Term Changes on the Human Gut Microbiome Contributing to Fat Mass Regulation. *Cell Metab* 22: 228-238, 2015.

172. Tuomainen M, Lindstrom J, Lehtonen M, Auriola S, Pihlajamaki J, Peltonen M, Tuomilehto J, Uusitupa M, de Mello VD, and Hanhineva K. Associations of serum indolepropionic acid, a gut microbiota metabolite, with type 2 diabetes and low-grade inflammation in high-risk individuals. *Nutr Diabetes* 8: 2018.

173. Turnbaugh PJ, Ley RE, Mahowald MA, Magrini V, Mardis ER, and Gordon JI. An obesity-associated gut microbiome with increased capacity for energy harvest. *Nature* 444: 1027-1031, 2006.

174. Ussar S, Fujisaka S, and Kahn CR. Interactions between host genetics and gut microbiome in diabetes and metabolic syndrome. *Mol Metab* 5: 795-803, 2016.

175. Van Guilder GP, Hoetzer GL, Dengel DR, Stauffer BL, and DeSouza CA. Impaired endothelium-dependent vasodilation in normotensive and normoglycemic obese adult humans. *J Cardiovasc Pharmacol* 47: 310-313, 2006.

176. van Sloten TT, Henry RM, Dekker JM, Nijpels G, Unger T, Schram MT, and Stehouwer CD. Endothelial dysfunction plays a key role in increasing cardiovascular risk in type 2 diabetes: the Hoorn study. *Hypertension* 64: 1299-1305, 2014.

177. Vanhoutte PM, Zhao Y, Xu A, and Leung SW. Thirty Years of Saying NO: Sources, Fate, Actions, and Misfortunes of the Endothelium-Derived Vasodilator Mediator. *Circ Res* 119: 375-396, 2016.

178. Vikram A, Kim YR, Kumar S, Li Q, Kassan M, Jacobs JS, and Irani K. Vascular microRNA-204 is remotely governed by the microbiome and impairs endothelium-dependent vasorelaxation by downregulating Sirtuin1. *Nature communications* 7: 12565, 2016.

179. Virdis A. Endothelial Dysfunction in Obesity: Role of Inflammation. *High Blood Press Cardiovasc Prev* 23: 83-85, 2016.

180. Virdis A, Santini F, Colucci R, Duranti E, Salvetti G, Rugani I, Segnani C, Anselmino M, Bernardini N, Blandizzi C, Salvetti A, Pinchera A, and Taddei S. Vascular generation of tumor necrosis factor-alpha reduces nitric oxide availability in small arteries from visceral fat of obese patients. *J Am Coll Cardiol* 58: 238-247, 2011.

181. Visse R, and Nagase H. Matrix metalloproteinases and tissue inhibitors of metalloproteinases: structure, function, and biochemistry. *Circ Res* 92: 827-839, 2003.

182. Vlachopoulos C, Aznaouridis K, and Stefanadis C. Prediction of cardiovascular events and all-cause mortality with arterial stiffness: a systematic review and meta-analysis. *J Am Coll Cardiol* 55: 1318-1327, 2010.

183. Vrieze A, Van Nood E, Holleman F, Salojarvi J, Kootte RS, Bartelsman JF, Dallinga-Thie GM, Ackermans MT, Serlie MJ, Oozeer R, Derrien M, Druesne A, Van Hylckama Vlieg JE, Bloks VW, Groen AK, Heilig HG, Zoetendal EG, Stroes ES, de Vos WM, Hoekstra JB, and

Nieuwdorp M. Transfer of intestinal microbiota from lean donors increases insulin sensitivity in individuals with metabolic syndrome. *Gastroenterology* 143: 913-916 e917, 2012.

184. Wang TJ, Larson MG, Vasan RS, Cheng S, Rhee EP, McCabe E, Lewis GD, Fox CS, Jacques PF, Fernandez C, O'Donnell CJ, Carr SA, Mootha VK, Florez JC, Souza A, Melander O, Clish CB, and Gerszten RE. Metabolite profiles and the risk of developing diabetes. *Nat Med* 17: 448-453, 2011.

185. Widlansky ME, Gokce N, Keaney JF, Jr., and Vita JA. The clinical implications of endothelial dysfunction. *J Am Coll Cardiol* 42: 1149-1160, 2003.

186. Wilkinson IM, CM; Schillaci, G; Boutouyrie, P; Segers, P; Donald, A; Chowienczyk PJ. ARTERY Society guidelines for validation of non-invasive haemodynamic measurement devices: Part 1, arterial pulse wave velocity. *Artery Research* 4: 34-40, 2010.

187. Wlodarska M, Luo C, Kolde R, d'Hennezel E, Annand JW, Heim CE, Krastel P, Schmitt EK, Omar AS, Creasey EA, Garner AL, Mohammadi S, O'Connell DJ, Abubucker S, Arthur TD, Franzosa EA, Huttenhower C, Murphy LO, Haiser HJ, Vlamakis H, Porter JA, and Xavier RJ. Indoleacrylic Acid Produced by Commensal Peptostreptococcus Species Suppresses Inflammation. *Cell Host Microbe* 22: 25-37 e26, 2017.

188. Wu H, Esteve E, Tremaroli V, Khan MT, Caesar R, Manneras-Holm L, Stahlman M, Olsson LM, Serino M, Planas-Felix M, Xifra G, Mercader JM, Torrents D, Burcelin R, Ricart W, Perkins R, Fernandez-Real JM, and Backhed F. Metformin alters the gut microbiome of individuals with treatment-naive type 2 diabetes, contributing to the therapeutic effects of the drug. *Nat Med* 23: 850-858, 2017.

189. Xu J, Kulkarni SR, Li L, and Slitt AL. UDP-glucuronosyltransferase expression in mouse liver is increased in obesity- and fasting-induced steatosis. *Drug Metab Dispos* 40: 259-266, 2012.

190. Yokoyama MT, and Carlson JR. Microbial metabolites of tryptophan in the intestinal tract with special reference to skatole. *Am J Clin Nutr* 32: 173-178, 1979.

191. Zelante T, Iannitti RG, Cunha C, De Luca A, Giovannini G, Pieraccini G, Zecchi R, D'Angelo C, Massi-Benedetti C, Fallarino F, Carvalho A, Puccetti P, and Romani L. Tryptophan catabolites from microbiota engage aryl hydrocarbon receptor and balance mucosal reactivity via interleukin-22. *Immunity* 39: 372-385, 2013.

192. Zhang J, Xia L, Zhang F, Zhu D, Xin C, Wang H, Zhang F, Guo X, Lee Y, Zhang L, Wang S, Guo X, Huang C, Gao F, Liu Y, and Tao L. A novel mechanism of diabetic vascular endothelial dysfunction: Hypoadiponectinemia-induced NLRP3 inflammasome activation. *Biochim Biophys Acta Mol Basis Dis* 1863: 1556-1567, 2017.

193. Zhang J, Zhao X, Vatner DE, McNulty T, Bishop S, Sun Z, Shen YT, Chen L, Meininger GA, and Vatner SF. Extracellular Matrix Disarray as a Mechanism for Greater Abdominal Versus Thoracic Aortic Stiffness With Aging in Primates. *Arterioscler Thromb Vasc Biol* 36: 700-706, 2016.

194. Zhang X, Zhao Y, Zhang M, Pang X, Xu J, Kang C, Li M, Zhang C, Zhang Z, Zhang Y, Li X, Ning G, and Zhao L. Structural changes of gut microbiota during berberine-mediated prevention of obesity and insulin resistance in high-fat diet-fed rats. *PloS one* 7: e42529, 2012.

195. Zheng J, Yuan X, Cheng G, Jiao S, Feng C, Zhao X, Yin H, Du Y, and Liu H. Chitosan oligosaccharides improve the disturbance in glucose metabolism and reverse the dysbiosis of gut microbiota in diabetic mice. *Carbohydr Polym* 190: 77-86, 2018.

196. Zhou H, Wang S, Zhu P, Hu S, Chen Y, and Ren J. Empagliflozin rescues diabetic myocardial microvascular injury via AMPK-mediated inhibition of mitochondrial fission. *Redox Biol* 15: 335-346, 2018.

197. Zhou RH, Vendrov AE, Tchivilev I, Niu XL, Molnar KC, Rojas M, Carter JD, Tong H, Stouffer GA, Madamanchi NR, and Runge MS. Mitochondrial oxidative stress in aortic stiffening with age: the role of smooth muscle cell function. *Arterioscler Thromb Vasc Biol* 32: 745-755, 2012.

198. Zhu W, Gregory JC, Org E, Buffa JA, Gupta N, Wang Z, Li L, Fu X, Wu Y, Mehrabian M, Sartor RB, McIntyre TM, Silverstein RL, Tang WH, DiDonato JA, Brown JM, Lusis AJ, and Hazen SL. Gut Microbial Metabolite TMAO Enhances Platelet Hyperreactivity and Thrombosis Risk. *Cell* 165: 111-124, 2016.

199. Zinman B, Wanner C, Lachin JM, Fitchett D, Bluhmki E, Hantel S, Mattheus M, Devins T, Johansen OE, Woerle HJ, Broedl UC, Inzucchi SE, and Investigators E-RO. Empagliflozin, Cardiovascular Outcomes, and Mortality in Type 2 Diabetes. *N Engl J Med* 373: 2117-2128, 2015.